MIT-CTP/6114

Emergent classicality and wavefunction branching in an isolated quantum many-body system

Saúl Pilatowsky-Cameo,[1,*] Jordan Cotler,[2,†] Daniel Ranard,[3,‡] and C. Jess Riedel[4,§]

[1] *Center for Theoretical Physics — a Leinweber Institute, Massachusetts Institute of Technology, Cambridge, MA 02139, USA*
[2] *Department of Physics, Harvard University, Cambridge, MA 02138, USA*
[3] *Department of Physics, California Institute of Technology, Pasadena, CA 91125, USA*
[4] *NTT Research, Inc., Physics & Informatics Laboratories, Sunnyvale, CA 94085, USA*

arXiv:2609.19254v1 [quant-ph] 16 Sep 2026

Decoherence in quantum systems is conventionally modeled as the effect of interactions with an external environment. However, such a prescription excludes isolated many-body systems, which are also expected to display classical behavior at macroscopic scales. In isolated systems, decoherence must emerge internally from microscopic degrees of freedom that are invisible to the macroscopic description. Here we explicitly show that classicality can emerge in such a fashion. We consider a weakly disordered, 3-local chaotic kicked top of N qubits, where the collective spin sector serves as the macroscopic description, while the microscopic permutation sector acts as an internal bath, decohering the collective spin sector. Starting from closed unitary dynamics, we derive and numerically confirm an effective Lindblad equation for the collective spin variables. In the thermodynamic limit these reduced dynamics converge to a classical chaotic Fokker–Planck equation with vanishingly small diffusion on the spherical phase space, producing a quantum-classical correspondence beyond the Ehrenfest time. The chaotic dynamics evolve the pure many-body wavefunction into continuously branching components associated with distinct classical trajectories. These branches acquire nearly orthogonal microscopic records in the permutation sector, preventing quantum interferences and ensuring the corresponding histories remain consistent.

The theory of decoherence [1–4] explains why quantum effects do not manifest at macroscopic scales. A large quantum system inevitably entangles with its environment, which delocalizes phase information, suppresses interferences, and enables effectively classical behavior. Decoherence has been studied from many complementary viewpoints, including idealized bath models in Lindblad dynamics [5–7] with analyses of the threshold system-bath coupling necessary for quantum-classical correspondence [8–12], a purified closed-system perspective where the system and environment branch into superpositions of macroscopically distinct states [13–17], and the proliferation of redundant information in the environment via quantum Darwinism [18–20]. Despite their conceptual differences, these approaches share the same basic premise: decoherence arises because the system couples to a distinct, external environment.

This premise is not fully satisfactory, since it excludes isolated systems, which exist not only as a matter of principle (e.g., a closed universe), but also in practice as enabled by modern experimental capabilities [21–23]. A complete account of the emergence of classicality should explain how an isolated system can decohere absent an external environment. While one may treat an explicit system and bath as a jointly "isolated system", nature does not always equip us with explicit system-bath decompositions; instead, one hopes to identify bath variables that emerge from the local interactions within the system. A natural parallel exists in quantum thermalization [24–29], where an isolated system can reach thermal equilibrium by acting as *its own bath*: even though the global state remains pure, subsystems effectively thermalize by becoming highly entangled with their complements. We ask if classicality may arise through a similarly intrinsic mechanism, where internal, perhaps hidden degrees of freedom play the role of a decohering environment.

In this work, we present a simple many-body model that exhibits decoherence from its internal degrees of freedom, giving rise to classical behavior without coupling to any external environment. Going beyond previous works in few-body systems [30, 31], we study a system of N qubits evolving under a chaotic (kicked-top) Hamiltonian [32–38], perturbed by weak disorder. The permutation degrees of freedom act as an intrinsic bath, decohering the collective spin sector, and we analytically obtain, and numerically confirm, an effective Lindblad equation for the spin sector in the thermodynamic limit. In contrast with previous work deriving reduced dynamics in isolated discrete systems [39–45], here the classical variables have extensive support (many-body), are continuous, and possess a classical limit governed by a chaotic Hamiltonian. This enables us to leverage recent techniques on the classical-quantum correspondence in open systems [10–12] to derive the emergence of classical behavior in the isolated model. We remark that, while there is an extensive body of work studying the quantum-classical correspondence in isolated quantum systems [35] where classicality is maintained up to the *Ehrenfest time* [46], the Ehrenfest time is prohibitively short (scaling only logarithmically with $\hbar_{\text{eff}}^{-1} \sim N$). The emergent classicality we describe here is maintained beyond the Ehrenfest time.

Having established quasiclassical dynamics for the collective spin variable, we describe the branching of the overall wavefunction with the consistent histories formal-

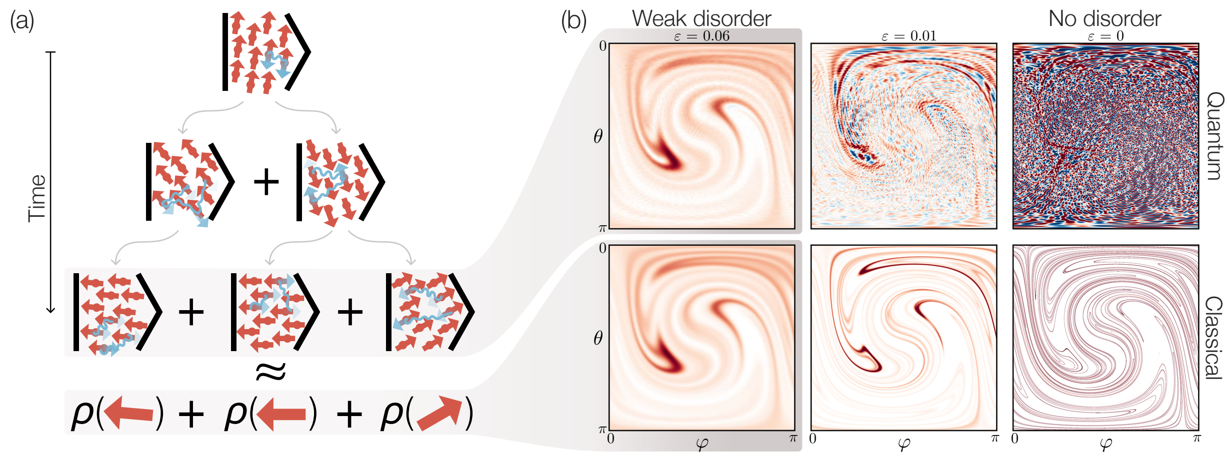

FIG. 1. (a) *Emergence of decoherence in an isolated many-body system of spins.* The system is initialized with all spins pointing in the same direction, with the exception of a few particles coupled in singlets (blue). The disorder in the Hamiltonian scrambles the singlets throughout, leading to microscopically distinct branches that cannot interfere in collective observables, so their superposition is indistinguishable from a classical mixture. (b) *Emergence of classicality.* Wigner function of the quantum evolution in the collective spin sector (top) and classical evolution according to the classical dissipative equation (7) (bottom). In the presence of a single realization of a small amount of disorder ε, the quantum and classical evolutions are identical, with no regions of negative probability (blue) ($k = 4$, $N = 200$, $\kappa = 4.2$, $p = \pi/2$, $\theta_0 = 0.5$, $\varphi_0 = 1.1$, $t = 8$).

ism [47–53]. *Histories* are sequences of projections, forming discrete-time trajectories of the collective variable, to which one would like to assign well-behaved classical probabilities. Histories are *consistent* when their associated conditional states, called branches [54–58], are orthogonal, and therefore admit probabilities obeying the Kolmogorov axioms. We explicitly construct the branches in this disordered kicked-top model and numerically verify that the associated histories are indeed consistent. This is enabled by the strong distinguishability of the microscopic arrangement of spins in each branch, which is invisible to collective measurements (see Fig. 1).

Decoherence from microscopic degrees of freedom.— The Hilbert space of N qubits has dimension 2^N, but a macroscopic description typically involves only coarse-grained observables. In spin systems, natural examples are collective spin observables, such as the total magnetization in different directions. By Schur–Weyl duality [59, 60], the total Hilbert space splits into a direct sum of subspaces $\mathcal{H}_S = \mathcal{S} \otimes \mathcal{P}$, where $\mathcal{S} = \mathcal{S}(S)$ is the collective spin sector (an irreducible representation of SU(2) of dimension $d_\mathcal{S} = 2S+1$) on which collective spin operators $(\hat{S}_x, \hat{S}_y, \hat{S}_z) = \frac{1}{2}\sum_{i=1}^N (\hat{X}_i, \hat{Y}_i, \hat{Z}_i)$ [61] act, and $\mathcal{P} = \mathcal{P}(S)$ is the SU(2)-invariant permutation space of dimension $d_\mathcal{P} = \binom{N}{N/2-S} - \binom{N}{N/2-S-1}$. Crucially, outside the fully symmetric sector $S_{\max} = N/2$, the multiplicity space can become large. For example, if $S = N/2-j$, then $d_\mathcal{P} \sim N^j$ while $d_\mathcal{S} \sim N$, so the overwhelming majority of the degrees of freedom are invisible to collective measurements. We will show that these internal degrees of freedom can serve as an effective environment for the collective sector, leading to decoherence. This system-bath decomposition is emergent in the sense that it is not a partition of locally interacting subsystems, but rather arises due to symmetry and hence is delocalized with respect to the microscopic interactions.

For simplicity, we consider an initial state contained entirely in one of the spin subspaces $\mathcal{H}_S$: $N-k$ qubits pointing in the same direction $|\theta_0, \varphi_0\rangle = \cos\left(\frac{\theta_0}{2}\right)|0\rangle + e^{i\varphi_0}\sin\left(\frac{\theta_0}{2}\right)|1\rangle$, while the remaining k spins are paired in singlets (for even $k \geq 2$):

$$|\psi(0)\rangle = |\theta_0, \varphi_0\rangle^{\otimes(N-k)} \otimes \left[\tfrac{1}{\sqrt{2}}(|01\rangle - |10\rangle)\right]^{\otimes k/2}. \quad (1)$$

If we choose k to be small compared to N, then $S = (N-k)/2$ is close to the total spin of the top sector $S_{\max} = N/2$, and the permutation sector has dimension $d_\mathcal{P} \sim N^{k/2}/(k/2)!$, which is polynomially larger than $d_\mathcal{S} \sim N$.

Weakly disordered kicked top.— We consider a chaotic Hamiltonian describing the dynamics of the spins. For simplicity, we consider the paradigmatic kicked top

$$\hat{H}_{\mathrm{KT}}(t) = \frac{\kappa}{2S+1}\hat{S}_x^2 + \sum_{n=1}^{\infty} p\,\delta(t-n)\hat{S}_z\,, \quad (2)$$

but we expect our results to apply to a broader class of chaotic systems. Since $\hat{H}_{\mathrm{KT}}$ is permutation symmetric, it only acts on the spin sector $\mathcal{S}$. To observe decoherence, we will break the permutation symmetry.

A simple way to break this symmetry would be to introduce weak on-site disorder of the form $\varepsilon \sum_i c_i \hat{Z}_i$, with random coefficients c_i. This form of disorder couples $\mathcal{S}$ and $\mathcal{P}$, as it is neither permutation symmetric nor SU(2) invariant, but it also couples different total spin subspaces, since it does not commute with the total spin.

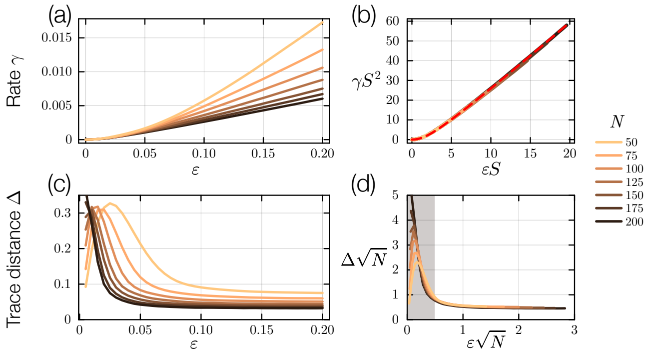

FIG. 2. Effective Lindblad dynamics. (a) Optimized rate γ, obtained by minimizing the average trace distance Δ to the exact quantum dynamics. (b) $S^2\gamma$ against εS: empirical rates γ collapse to the predicted $S^2\gamma = \varepsilon S J_*(\varepsilon S)$ (dashed). (c) Time-averaged trace distance for optimal γ, for time $t \in [2, 8]$. (d) Collapse of the trace-distance curves obtained by multiplying ε and Δ by $\sqrt{N}$. Gray: Non-Lindblad regime (large Δ). All plots are averaged over 20 disorder realizations; the fitting procedure is described in the SM [62] (Fig. S3) ($k = 4$, $\kappa = 4.2$, $p = \pi/2$, $\theta_0 = 0.5$, $\varphi_0 = 1.1$).

For simplicity of the analysis and to greatly decrease the computational cost of simulation, we instead consider the following form of disorder that commutes with the total spin:

$$\hat{H}_{\mathrm{dis}} = \hat{K}_x \hat{S}_x + \hat{K}_y \hat{S}_y + \hat{K}_z \hat{S}_z \,, \tag{3}$$

from which we define the weakly disordered kicked top:

$$\hat{H}(t) = \hat{H}_{\mathrm{KT}}(t) + \varepsilon \hat{H}_{\mathrm{dis}}. \tag{4}$$

For each $\mu = x, y, z$, we take $\hat{K}_\mu$ to be an independent random all-to-all Heisenberg coupling, $\hat{K}_\mu = \sum_{i<j} c_{ij}^{(\mu)} \hat{h}_{ij}$, where $\hat{h}_{ij} := \hat{X}_i\hat{X}_j + \hat{Y}_i\hat{Y}_j + \hat{Z}_i\hat{Z}_j$. The coefficients $c_{ij}^{(\mu)}$ are Gaussian with variance $\sim (4Nk)^{-1}$, with their mean component subtracted so that $\sum_{i<j} c_{ij}^{(\mu)} = 0$ for each μ. This normalization keeps the spectral width of each $\hat{K}_\mu$ bounded [62]. Because the Heisenberg couplings are SU(2) invariant, the operators $\hat{K}_\mu$ act only in $\mathcal{P}$, while the spin operators $\hat{S}_\mu$ act only in $\mathcal{S}$, so $\hat{H}_{\mathrm{dis}}$ naturally couples $\mathcal{S}$ and $\mathcal{P}$ within the subspace of total spin S. The ensemble of random disorder terms $\hat{H}_{\mathrm{dis}}$ is invariant under physical rotations (isotropic).

Effective Lindblad dynamics.— We begin by showing that $\mathcal{P}$ acts as an effective Markovian bath for the dynamics in $\mathcal{S}$. We first show numerically that the evolution of the reduced density matrix $\psi_{\mathcal{S}}(t) := \mathrm{tr}_{\mathcal{P}} |\psi(t)\rangle\langle\psi(t)|$ is well described by a Lindblad equation

$$\frac{\partial \rho}{\partial t} = -i[\hat{H}_{\mathrm{KT}}(t), \rho] + \gamma \sum_{\mu=x,y,z} \hat{\mathcal{D}}_\mu[\rho] \,, \tag{5}$$

with dissipator $\hat{\mathcal{D}}_\mu[\rho] = -\frac{1}{2}[\hat{S}_\mu, [\hat{S}_\mu, \rho]]$ [63].

In Fig. 2 we show an empirical value of γ obtained numerically, by minimizing the finite-time-averaged trace distance $\Delta = \frac{1}{2}\,\mathbb{E}_t \left\| \psi_{\mathcal{S}}(t) - \rho(t) \right\|_1$ between the actual evolution $\psi_{\mathcal{S}}(t)$ and the Lindblad approximation $\rho(t)$. For disorder strength $\varepsilon \gtrsim 1/\sqrt{N}$, the reduced dynamics agree well with the Lindblad approximation: the error Δ decays as $\sim 1/\sqrt{N}$, and the fitted rate satisfies the empirical scaling $\gamma \propto \varepsilon/N$. Via a heuristic derivation of γ and obtain [62]

$$\gamma = \frac{\varepsilon}{S} J_*(\varepsilon S) \sim \frac{\varepsilon}{S} O(\log(\varepsilon S)^\alpha) \,, \tag{6}$$

where J_* is the finite-time integral of a disorder-averaged effective bath correlation function at infinite temperature, evaluated up to a time proportional to εS. Fig. 2(b) shows excellent agreement between the empirical rate γ and our derived Eq. (6).

For large $\tau := \varepsilon S$, we numerically see that the correlator has a logarithmic-type divergence $J_*(\tau) = O(\log(\tau)^\alpha)$ for a certain $0 < \alpha \leq 1$. This logarithmic factor is characteristic of choosing the bath operators $\hat{K}_\mu$ to be random 2-local Heisenberg couplings; in this construction, $\hat{H}_{\mathrm{dis}}$ is then 3-local in the microscopic spins. The logarithm is absent for analogous disorder ensembles built from higher-locality operators, such as 4-local disorder or GOE random matrices [62]. Nevertheless, this logarithmic growth does not obstruct Markovian behavior, since τ is independent of the physical evolution time t.

Emergent classicality.— The effective Lindblad dynamics lead to the emergence of classical equations of motion for the collective spin observables. Specifically, consider the classical diffusion equation obtained by treating the collective spin operators as if they were continuous commuting variables on the sphere, $\hat{\boldsymbol{S}} = (\hat{S}_x, \hat{S}_y, \hat{S}_z) \to \boldsymbol{S} = (S_x, S_y, S_z) \in \mathbb{R}^3$, and replacing the commutator with a Poisson bracket, $-i[\,\cdot\,,\,\cdot\,] \longrightarrow \{\,\cdot\,,\,\cdot\,\}$ [64], namely

$$\frac{\partial f}{\partial t} = \{H_{\mathrm{KT}}(t), f\} + \gamma \sum_{\mu=x,y,z} \mathcal{D}_\mu[f] \,. \tag{7}$$

Here, $f(t, \boldsymbol{S}) \geq 0$ represents a classical distribution on the sphere, while the classical Hamiltonian is given by [65]

$$H_{\mathrm{KT}}(t) = \frac{\kappa}{2S} S_x^2 \; + \; \sum_{n=1}^{\infty} p\, S_z \delta(t-n) \tag{8}$$

and the classical dissipator by $\mathcal{D}_\mu[f] = \frac{1}{2}\{S_\mu, \{S_\mu, f\}\}$.

In Fig. 1(b), we compare the classical dynamics of Eq. (7) with the Wigner function of $|\psi\rangle_{\mathcal{S}}$ [66]. In the absence of disorder the quantum dynamics develop regions of negative probability, a signature of non-classicality [67]. However, introducing only a small amount of disorder [$\varepsilon = 0.06$ in Fig. 1(b)] in Eq. (4) leads to a positive Wigner function, with perfect quantum-classical correspondence. See the Supplemental Material (SM) [62] for additional figures.

This emergence of classicality can be asymptotically established rigorously, starting from the Lindblad dynamics. Under sufficiently strong diffusion (but still vanishing in the thermodynamic limit), the dynamics remain in a mixture of coherent states in $\mathcal{S}$, associated with an asymptotically positive phase-space distribution.

Theorem 1. *If $\gamma \geq \gamma_* := \frac{|\kappa|}{2S+1}$, under the Lindblad equation* (5)*, starting in a spin coherent state, the dynamics remain a positive mixture of coherent states,*

$$\rho(t) = \int \mathrm{d}\Omega\, P(\Omega, t)\, |\Omega\rangle\!\langle\Omega|\,, \qquad P(\Omega, t) \geq 0, \tag{9}$$

where the integral is taken over the sphere. Furthermore, the differential equation governing the evolution of P matches Eq. (7) *up to a relative error $O(1/S)$ in the Hamiltonian terms and $O(\gamma_*/\gamma)$ in the dissipator.*

Proof. The function $P(\Omega, t)$ is simply the Glauber–Sudarshan quasiprobability distribution for the spin [68]. Any state can be represented in this form, but P in general might not be positive. We show that, under sufficient diffusion, positivity is guaranteed.

The evolution of ρ can be described by the evolution of P via the substitutions [62]

$$\begin{aligned} -i[\hat{S}_z, \rho] &\to \{S_z, P\}, \qquad -[\hat{S}_\mu, [\hat{S}_\mu, \rho]] \to \{S_\mu, \{S_\mu, P\}\} \\ -i[\hat{S}_x^2, \rho] &\to \{S_x^2, P\} + \frac{1}{S}\sum_{\nu,\lambda} \epsilon_{x\nu\lambda}\{S_x, \{S_\nu, S_\lambda P\}\}, \end{aligned} \tag{10}$$

where $\epsilon_{x\nu\lambda}$ is the Levi-Civita symbol. Equation (5) is recast into a differential equation resembling Eq. (7),

$$\frac{\partial P}{\partial t} = \{\widetilde{H}_{\mathrm{KT}}(t), P\} + \frac{1}{2}\sum_{\mu,\nu} \Lambda_{\mu\nu}\{S_\mu, \{S_\nu, P\}\}, \tag{11}$$

but with a slightly modified classical Hamiltonian $\widetilde{H}_{\mathrm{KT}}(t) = H_{\mathrm{KT}}(t) + \frac{3c}{4}S_x^2$ and diffusion matrix $\Lambda_{\mu\nu} = \gamma\delta_{\mu\nu} + c\sum_\lambda(\delta_{x\mu}\epsilon_{x\nu\lambda} + \delta_{x\nu}\epsilon_{x\mu\lambda})S_\lambda$, where $c = \frac{\kappa}{S(2S+1)}$. Equation (11) exactly describes the quantum evolution, where the distribution P might become negative and singular due to the negative eigenvalues of the diffusion matrix $\Lambda_{\mu\nu}$. However, if $\gamma \geq |c|S = \gamma_*$, then $\Lambda_{\mu\nu}$ is positive semidefinite, turning Eq. (11) into a classical diffusive equation which evolves P into a positive and nonsingular distribution. Furthermore, the relative error in the coefficients for S_x^2 in Eqs. (7) and (11) is $(3c/4)/(\kappa/2S) = O(1/S)$ and the relative error between $\Lambda_{\mu\nu}$ and the isotropic diffusion matrix is $O(\|(\Lambda_{\mu\nu} - \gamma\delta_{\mu\nu})_{\mu\nu}\|/\gamma) = O(\gamma_*/\gamma)$. □

Theorem 1 guarantees classical evolution whenever $\gamma \gg O(S^{-1})$. Furthermore, in the SM [62] we present an improved theorem (which also holds for general Hamiltonians) where the threshold for classicality is $\gamma \gg O(S^{-4/3})$. This improved threshold is enabled by allowing slightly

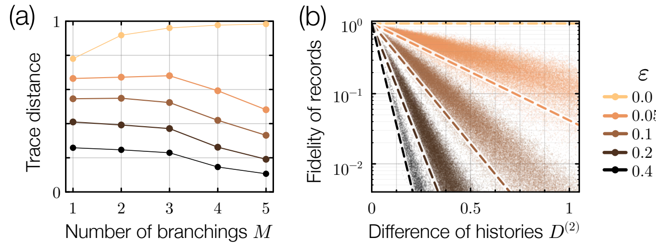

FIG. 3. (a) *Quantum branching.* Trace distance between the reduced state of the global unitary dynamics and the mixture of branches [left and right sides of Eq. (14), respectively], for different values of disorder ε and number of branchings M. (b) *Consistent histories.* Fidelity of records vs cumulative squared distance between histories $D^{(2)}$ after $M = 5$ branchings. Each dot is a pair of independently sampled branches. Dashed lines mark the decay $e^{-\Gamma D^{(2)}}$. ($N = 100$, $k = 4$, $\kappa = 4.2$, $p = \pi/2$, $\theta_0 = 0.5$, $\varphi_0 = 1.1$, $\Delta t = 1$)

squeezed states in the decomposition of ρ [10, 11], and is expected to be optimal [12]. Combined with Eq. (6), it implies that, for sufficiently large S, our disordered kicked-top model displays classical behavior as long as $\varepsilon \geq O(N^{-1/3+\delta})$ for any constant $\delta > 0$.

Quantum branching.— The emergence of classicality in closed systems is believed to be described via the theory of wavefunction branching [16] and consistent histories [47–50], which we introduce next. We then numerically confirm that these phenomena indeed arise in our model.

We may describe the state of the system as a superposition of different *branches*,

$$|\psi(t_M)\rangle = \int \mathrm{d}\boldsymbol{\Omega}\, c_{\boldsymbol{\Omega}}\, |\phi_{\boldsymbol{\Omega}}\rangle\,. \tag{12}$$

Each branch is labeled by a *history*, $\boldsymbol{\Omega} = (\Omega_0, \ldots, \Omega_M)$, a sequence of points on the sphere $\Omega_m = (\theta_m, \varphi_m)$, at times $t_0 = 0, t_1, \ldots, t_M$, where the integral is taken with respect to the measure $\mathrm{d}\boldsymbol{\Omega} = \mathrm{d}\Omega_1 \cdots \mathrm{d}\Omega_M$, with $\mathrm{d}\Omega_m = \frac{2S+1}{4\pi}\sin\theta_m\, \mathrm{d}\theta_m\, \mathrm{d}\varphi_m$. These branches are defined by inserting spin coherent-state projectors $\hat{\Omega}_m = |\Omega_m\rangle\!\langle\Omega_m|_{\mathcal{S}} \otimes \mathbb{1}_{\mathcal{P}}$ at the corresponding times:

$$c_{\boldsymbol{\Omega}}\, |\phi_{\boldsymbol{\Omega}}\rangle = \hat{\Omega}_M U_M \cdots \hat{\Omega}_2 U_2 \hat{\Omega}_1 U_1\, |\psi(0)\rangle\,, \tag{13}$$

where the initial state is given by Eq. (1), with $\Omega_0 = (\theta_0, \varphi_0)$. The coefficient $c_{\boldsymbol{\Omega}}$ is chosen so that $|\phi_{\boldsymbol{\Omega}}\rangle$ is normalized, and $U_m = \mathcal{T}\exp\!\left(-i\int_{t_{m-1}}^{t_m} \mathrm{d}t\, \hat{H}(t)\right)$ is the unitary generated by Eq. (4) between times t_{m-1} and t_m. Equation (12) follows formally from the coherent-state resolution of the identity $\int \mathrm{d}\Omega_m \hat{\Omega}_m = \mathbb{1}$. In general, however, these branches may interfere, so the decomposition alone does not yet define classical alternatives.

The emergence of decoherence is a manifestation of the noninterference of branches in the collective observables. The reduced state in $\mathcal{S}$ becomes indistinguishable from a classical mixture over all branches:

$$\mathrm{tr}_{\mathcal{P}}(\psi(t_M)) \approx \int \mathrm{d}\mathbf{\Omega}\, |c_{\mathbf{\Omega}}|^2\, \mathrm{tr}_{\mathcal{P}}(|\phi_{\mathbf{\Omega}}\rangle\langle\phi_{\mathbf{\Omega}}|), \tag{14}$$

where $\mathrm{tr}_{\mathcal{P}}(|\phi_{\mathbf{\Omega}}\rangle\langle\phi_{\mathbf{\Omega}}|) = |\Omega_M\rangle\langle\Omega_M|$ is a coherent state. Indeed, numerics shown in Fig. 3(a) confirm that the trace distance between the two sides of Eq. (14) decreases with increasing ε. In fact, a stronger notion of noninterference is satisfied in our model, namely consistency of histories.

Each branch has the form $|\phi_{\mathbf{\Omega}}\rangle = |\Omega_M\rangle_{\mathcal{S}} \otimes |R_{\mathbf{\Omega}}\rangle_{\mathcal{P}}$, and the state $|R_{\mathbf{\Omega}}\rangle$ is known as a *record*. In the presence of disorder, separated histories imprint distinguishable records in the permutation sector. Specifically, we estimate via a semiclassical Lindblad approximation [62] that the fidelity of records for two histories $\mathbf{\Omega}$ and $\mathbf{\Theta}$ should decay exponentially in $D^{(2)}_{\mathbf{\Omega},\mathbf{\Theta}} \approx \frac{1}{2}\sum_{m=1}^{M}\big[d(\Omega_{m-1},\Theta_{m-1})^2 + d(\Omega_m,\Theta_m)^2\big]$ [69]. Namely,

$$|\langle R_{\mathbf{\Theta}}|R_{\mathbf{\Omega}}\rangle|^2 \sim \exp\Big(-\Gamma D^{(2)}_{\mathbf{\Omega},\mathbf{\Theta}}\Big), \tag{15}$$

with a coefficient $\Gamma = \gamma S^2\Delta t/(1+\gamma S\Delta t)$, where $\Delta t = t_m - t_{m-1}$. This is supported by the numerics shown in Fig. 3(b). In the SM [62] we present additional numerical verifications for random-matrix couplings. We remark that we can study these overlaps because our system is closed, so we can canonically identify the record states of the bath. Such an identification would not be possible if one instead had postulated an open model governed by a Lindblad equation as the starting point.

The decay in the fidelity of distinct records prevents distinct branches from interfering in any collective observable $O_{\mathcal{S}}$. Interferences are controlled by the off-diagonal terms

$$\langle\phi_{\mathbf{\Theta}}|\, O_{\mathcal{S}} \otimes \mathbb{1}_{\mathcal{P}}\, |\phi_{\mathbf{\Omega}}\rangle = \langle\Theta_M|\, O_{\mathcal{S}}\, |\Omega_M\rangle\, \langle R_{\mathbf{\Omega}}|R_{\mathbf{\Theta}}\rangle\,. \tag{16}$$

In the absence of disorder, $\gamma = 0$ and hence $\langle R_{\mathbf{\Theta}}|R_{\mathbf{\Omega}}\rangle = 1$ regardless of the histories, thus allowing interference even when $\mathbf{\Omega}$ and $\mathbf{\Theta}$ are distinct. As γ increases, the off-diagonal matrix element in Eq. (16) is suppressed exponentially in $D^{(2)}_{\mathbf{\Theta},\mathbf{\Omega}}$. This effect is analogous to the recording of which-path information in the double-slit experiment. If no degree of freedom records which slit the particle passed through, the two branches remain coherent and can interfere at the detector. If such a record is created, their coherence is suppressed and the interference disappears. In our model, the permutation sector creates the analogous record by becoming correlated with the collective-spin history due to the disordered interaction.

Discussion and outlook.— We have exhibited a concrete, numerically tractable isolated many-body model in which internal degrees of freedom act as an effective bath. For an emergent collective spin variable with chaotic classical dynamics, this leads to Lindblad dynamics, classical Fokker–Planck evolution, and consistent branching. This model is deliberately idealized. Both the kicked-top dynamics and the disorder are 3-local but all-to-all, whereas physical interactions are expected to be geometrically local. A natural next step is therefore to understand whether the same mechanism persists in geometrically local systems, where the quasiclassical variables are likely to be spatially coarse-grained densities rather than global collective spins, and whose classical equations of motion are not simply obtained by removing the hats from the quantum operators.

Additionally, our model exploits Schur–Weyl duality by having a disorder term that preserves total spin, constraining the dynamics to take place within a fixed spin sector, and ensuring a simple tensor-product decomposition $\mathcal{H}_S = \mathcal{S} \otimes \mathcal{P}$ between collective spin variables $\mathcal{S}$ and microscopic permutation variables $\mathcal{P}$. This enabled numerical simulation of a system with an otherwise inaccessibly large total spin. In contrast, a generic local perturbation would mix sectors, so that the quasiclassical variable (whether or not a collective spin) could take the form of a more general subalgebra $\mathcal{A} = \bigoplus_i \mathcal{S}_i \otimes \mathcal{P}_i$ [70]. Understanding this sector-wise form of emergent system-bath structure is an important step toward extending the present mechanism to more general and realistic settings, such as fermionic models, bosonic systems with unbounded local Hilbert spaces, and quantum field theories. A broader goal is to find a general framework describing the universal emergence of classical behavior in isolated quantum many-body systems, where wavefunction branches emerge naturally from the underlying quantum dynamics [54–58].

Acknowledgements.— We thank Curt von Keyserlingk for extensive insightful conversations and Soonwon Choi for a suggestion that informed our choice of the disorder term in Eq. (3). We acknowledge the MIT SuperCloud and Lincoln Laboratory Supercomputing Center for providing computational resources utilized for our numerical analysis. We also acknowledge the use of GPT 5.5-6 for aid in generating code and analytical derivations, in particular the identification of Eqs. (S12) and (S29) in the SM [62]. This work is supported by the U.S. Department of Energy, Office of Science, under Award Number DE-SC0021013 titled 'Emergent Phenomena in Quantum Dynamics: From Chaos to Spacetime'. JC is supported by a fellowship from the Alfred P. Sloan Foundation.

* saulpila@mit.edu
† jcotler@fas.harvard.edu
‡ dranard@caltech.edu
§ jessriedel@gmail.com

[1] W. H. Zurek, Decoherence, einselection, and the quantum origins of the classical, Reviews of Modern Physics **75**,

715–775 (2003).

[2] E. Joos and H. D. Zeh, The emergence of classical properties through interaction with the environment, Zeitschrift für Physik B Condensed Matter **59**, 223 (1985).

[3] M. Schlosshauer, Decoherence, the measurement problem, and interpretations of quantum mechanics, Reviews of Modern Physics **76**, 1267 (2005).

[4] M. Schlosshauer, Quantum decoherence, Physics Reports **831**, 1 (2019).

[5] G. Lindblad, On the generators of quantum dynamical semigroups, Communications in Mathematical Physics **48**, 119 (1976).

[6] V. Gorini, A. Kossakowski, and E. C. G. Sudarshan, Completely positive dynamical semigroups of N-level systems, Journal of Mathematical Physics **17**, 821 (1976).

[7] H.-P. Breuer and F. Petruccione, *The theory of Open Quantum Systems* (Oxford University Press, Oxford, 2002).

[8] F. Toscano, R. L. de Matos Filho, and L. Davidovich, Decoherence and the quantum-classical limit in the presence of chaos, Physical Review A **71**, 010101 (2005).

[9] D. A. Wisniacki and F. Toscano, Scaling laws in the quantum-to-classical transition in chaotic systems, Physical Review E **79**, 025203 (2009).

[10] F. Hernández, D. Ranard, and C. J. Riedel, Ehrenfest's theorem beyond the Ehrenfest time (2025), arXiv:2306.13717.

[11] F. Hernández, D. Ranard, and C. J. Riedel, Classical correspondence beyond the Ehrenfest time for open quantum systems with general Lindbladians, Communications in Mathematical Physics **406**, 4 (2024).

[12] F. Hernández, D. Ranard, and C. J. Riedel, The threshold for quantum-classical correspondence is $D \sim \hbar^{4/3}$ (2025), arXiv:2512.17623 [quant-ph].

[13] H. Everett, "Relative state" formulation of quantum mechanics, Reviews of Modern Physics **29**, 454 (1957).

[14] H. D. Zeh, On the interpretation of measurement in quantum theory, Foundations of Physics **1**, 69–76 (1970).

[15] R. Blume-Kohout and W. H. Zurek, Quantum Darwinism: Entanglement, branches, and the emergent classicality of redundantly stored quantum information, Physical Review A **73**, 062310 (2006).

[16] D. Wallace, *The Emergent Multiverse: Quantum Theory according to the Everett Interpretation* (Oxford University Press, 2012).

[17] S. Saunders, J. Barrett, A. Kent, and D. Wallace, eds., *Many Worlds? Everett, Quantum Theory, and Reality* (Oxford University Press, Oxford, 2010).

[18] W. H. Zurek, Quantum Darwinism, Nature Physics **5**, 181 (2009).

[19] H. Ollivier, D. Poulin, and W. H. Zurek, Objective properties from subjective quantum states: Environment as a witness, Physical Review Letters **93**, 220401 (2004).

[20] F. G. S. L. Brandão, M. Piani, and P. Horodecki, Generic emergence of objective observables in quantum Darwinism, Nature Communications **6**, 7908 (2015).

[21] S. Trotzky, Y.-A. Chen, A. Flesch, I. P. McCulloch, U. Schollwöck, J. Eisert, and I. Bloch, Probing the relaxation towards equilibrium in an isolated strongly correlated one-dimensional Bose gas, Nature Physics **8**, 325 (2012).

[22] A. M. Kaufman, M. E. Tai, A. Lukin, M. Rispoli, R. Schittko, P. M. Preiss, and M. Greiner, Quantum thermalization through entanglement in an isolated many-body system, Science **353**, 794 (2016).

[23] H. Bernien, S. Schwartz, A. Keesling, H. Levine, A. Omran, H. Pichler, S. Choi, A. S. Zibrov, M. Endres, M. Greiner, V. Vuletić, and M. D. Lukin, Probing many-body dynamics on a 51-atom quantum simulator, Nature **551**, 579 (2017).

[24] J. M. Deutsch, Quantum statistical mechanics in a closed system, Physical Review A **43**, 2046 (1991).

[25] M. Srednicki, Chaos and quantum thermalization, Physical Review E **50**, 888 (1994).

[26] M. Rigol, V. Dunjko, and M. Olshanii, Thermalization and its mechanism for generic isolated quantum systems, Nature **452**, 854 (2008).

[27] A. Polkovnikov, K. Sengupta, A. Silva, and M. Vengalattore, Colloquium: Nonequilibrium dynamics of closed interacting quantum systems, Rev. Mod. Phys. **83**, 863 (2011).

[28] C. Gogolin and J. Eisert, Equilibration, thermalisation, and the emergence of statistical mechanics in closed quantum systems, Rep. Prog. Phys. **79**, 056001 (2016).

[29] F. Borgonovi, F. Izrailev, L. Santos, and V. Zelevinsky, Quantum chaos and thermalization in isolated systems of interacting particles, Physics Reports **626**, 1–58 (2016).

[30] M. Hillery, L. Mlodinow, and V. Buzek, Quantum interference with molecules: The role of internal states, Physical Review A **71**, 062103 (2005).

[31] T. A. Brun and L. Mlodinow, Decoherence by coupling to internal vibrational modes, Physical Review A **94**, 052123 (2016).

[32] F. Haake, M. Kuś, and R. Scharf, Classical and quantum chaos for a kicked top, Zeitschrift für Physik B Condensed Matter **65**, 381 (1987).

[33] R. F. Fox and T. C. Elston, Chaos and a quantum-classical correspondence in the kicked top, Physical Review E **50**, 2553 (1994).

[34] S. Chaudhury, A. Smith, B. E. Anderson, S. Ghose, and P. S. Jessen, Quantum signatures of chaos in a kicked top, Nature **461**, 768 (2009).

[35] F. Haake, *Quantum Signatures of Chaos*, 3rd ed. (Springer, Berlin, 2010).

[36] A. Anand, J. Davis, and S. Ghose, Quantum recurrences in the kicked top, Phys. Rev. Res. **6**, 023120 (2024).

[37] J. A. Segura-Landa, D. A. Wisniacki, S. Lerma-Hernández, and J. G. Hirsch, Resonance assisted tunneling in Floquet spin-J systems, Physical Review E **113**, 034209 (2026).

[38] A. A. Galindo Duque, M. A. Prado Reynoso, M. Gonzalez, and J. G. Hirsch, Participation ratio as a quantum probe of hierarchical stickiness, Chaos: An Interdisciplinary Journal of Nonlinear Science **36**, 073151 (2026).

[39] C. Ates, J. P. Garrahan, and I. Lesanovsky, Thermalization of a strongly interacting closed spin system: From coherent many-body dynamics to a Fokker-Planck equation, Physical Review Letters **108**, 110603 (2012).

[40] S. Ji, C. Ates, J. P. Garrahan, and I. Lesanovsky, Equilibration of quantum hard rods in one dimension, Journal of Statistical Mechanics: Theory and Experiment **2013**, P02005 (2013).

[41] C. Nation and D. Porras, Taking snapshots of a quantum thermalization process: Emergent classicality in quantum jump trajectories, Physical Review E **102**, 042115 (2020).

[42] P. P. Mazza, D. Zietlow, F. Carollo, S. Andergassen, G. Martius, and I. Lesanovsky, Machine learning time-local generators of open quantum dynamics, Physical

Review Research **3**, 023084 (2021).
[43] F. Carnazza, F. Carollo, D. Zietlow, S. Andergassen, G. Martius, and I. Lesanovsky, Inferring Markovian quantum master equations of few-body observables in interacting spin chains, New Journal of Physics **24**, 073033 (2022).
[44] G. Cemin, F. Carnazza, S. Andergassen, G. Martius, F. Carollo, and I. Lesanovsky, Inferring interpretable dynamical generators of local quantum observables from projective measurements through machine learning, Physical Review Applied **21**, L041001 (2024).
[45] P. O'Donovan, P. Strasberg, K. Modi, J. Goold, and M. T. Mitchison, Quantum master equation from the eigenstate thermalization hypothesis, Phys. Rev. B **112**, 014312 (2025).
[46] B. V. Chirikov, F. M. Izrailev, and D. L. Shepelyansky, Quantum chaos: Localization vs. ergodicity, Physica D: Nonlinear Phenomena **33**, 77 (1988).
[47] R. B. Griffiths, Consistent histories and the interpretation of quantum mechanics, Journal of Statistical Physics **36**, 219 (1984).
[48] R. Omnès, Consistent interpretations of quantum mechanics, Reviews of Modern Physics **64**, 339 (1992).
[49] M. Gell-Mann and J. B. Hartle, Quantum mechanics in the light of quantum cosmology, in *Complexity, Entropy, and the Physics of Information*, Santa Fe Institute Studies in the Sciences of Complexity, Vol. 8, edited by W. H. Zurek (Addison-Wesley, Redwood City, CA, 1990) pp. 425–458.
[50] J. J. Halliwell, A review of the decoherent histories approach to quantum mechanics, Annals of the New York Academy of Sciences **755**, 726–740 (1995).
[51] P. Strasberg, Classicality with(out) decoherence: Concepts, relation to Markovianity, and a random matrix theory approach, SciPost Physics **15**, 024 (2023).
[52] P. Strasberg, T. E. Reinhard, and J. Schindler, First principles numerical demonstration of emergent decoherent histories, Phys. Rev. X **14**, 041027 (2024).
[53] J. Wang and P. Strasberg, Decoherence of histories: Chaotic versus integrable systems, Phys. Rev. Lett. **134**, 220401 (2025).
[54] C. J. Riedel, Classical Branch Structure from Spatial Redundancy in a Many-Body Wave Function, Physical Review Letters **118**, 120402 (2017).
[55] D. Weingarten, Macroscopic Reality from Quantum Complexity, Foundations of Physics **52**, 45 (2022).
[56] D. Weingarten, Vacuum Branching, Dark Energy, Dark Matter, Foundations of Physics **55**, 55 (2025).
[57] J. K. Taylor and I. P. McCulloch, Wavefunction branching: When you can't tell pure states from mixed states, Quantum **9**, 1670 (2025).
[58] C. J. Riedel, Wavefunction branches demand a definition!, Quantum Views **9**, 85 (2025).
[59] R. Goodman and N. R. Wallach, *Symmetry, Representations, and Invariants*, Graduate Texts in Mathematics, Vol. 255 (Springer, New York, 2009).
[60] D. Bacon, I. L. Chuang, and A. W. Harrow, Efficient quantum circuits for Schur and Clebsch-Gordan transforms, Physical Review Letters **97**, 170502 (2006).
[61] $\hat{X}_i$, $\hat{Y}_i$, and $\hat{Z}_i$ are the Pauli operators acting on spin i.
[62] See the Supplemental Material below for a characterization of features of our model in relation to prior work, numerical methods, microscopic derivation of the effective Lindblad equation and its rate, the detailed proof of Theorem 1, its extension to general Hamiltonians via not-too-squeezed states, and the estimate of the fidelity of records. The SM includes Refs. [71–82].
[63] Using that the $\hat{S}_\mu$ are Hermitian, the dissipator can be brought to the more familiar form $\hat{\mathcal{D}}_\mu[\rho] = \hat{S}_\mu \rho \hat{S}_\mu^\dagger - \frac{1}{2}(\hat{S}_\mu^\dagger \hat{S}_\mu \rho + \rho \hat{S}_\mu^\dagger \hat{S}_\mu)$.
[64] For spherical variables, the Poisson bracket is defined via the triple product $\{f, g\} = \mathbf{S} \cdot \left(\frac{\partial f}{\partial \mathbf{S}} \times \frac{\partial g}{\partial \mathbf{S}}\right)$.
[65] The replacement $(2S+1) \to 2S$ provides more accurate classical correspondence. The underlying technical reason is the non-multiplicativity of the Weyl transform for spin variables: $\mathcal{W}(\hat{S}_x^2)/(2S+1) \approx \mathcal{W}(\hat{S}_x)^2/2S$ [66].
[66] J. C. Várilly and J. M. Gracia-Bondía, The Moyal representation for spin, Annals of Physics **190**, 107 (1989).
[67] A. Kenfack and K. Życzkowski, Negativity of the Wigner function as an indicator of non-classicality, Journal of Optics B: Quantum and Semiclassical Optics **6**, 396–404 (2004).
[68] F. T. Arecchi, E. Courtens, R. Gilmore, and H. Thomas, Atomic coherent states in quantum optics, Phys. Rev. A **6**, 2211 (1972).
[69] At $m = 1$, the term $d(\Omega_{m-1}, \Theta_{m-1})$ vanishes since $\Omega_0 = \Theta_0$ corresponds to the initial state.
[70] P. Zanardi, D. A. Lidar, and S. Lloyd, Quantum Tensor Product Structures are Observable Induced, Physical Review Letters **92**, 060402 (2004).
[71] L. Li, M. J. W. Hall, and H. M. Wiseman, Concepts of quantum non-Markovianity: A hierarchy, Physics Reports **759**, 1 (2018).
[72] S. Milz, M. S. Kim, F. A. Pollock, and K. Modi, Completely positive divisibility does not mean Markovianity, Physical Review Letters **123**, 040401 (2019).
[73] W. H. Zurek, Decoherence, chaos, quantum-classical correspondence, and the algorithmic arrow of time, Physica Scripta **T76**, 186 (1998).
[74] D. Villaseñor, S. Pilatowsky-Cameo, M. A. Bastarrachea-Magnani, S. Lerma-Hernández, L. F. Santos, and J. G. Hirsch, Quantum vs classical dynamics in a spin-boson system: manifestations of spectral correlations and scarring, New Journal of Physics **22**, 063036 (2020).
[75] R. E. Ingram, Some characters of the symmetric group, Proceedings of the American Mathematical Society **1**, 358–369 (1950).
[76] D. Voiculescu, Limit laws for random matrices and free products, Inventiones mathematicae **104**, 201–220 (1991).
[77] K. Hepp, Quantum theory of measurement and macroscopic observables, Helv. Phys. Acta **45**, 237 (1972).
[78] L. Viola, E. Knill, and S. Lloyd, Dynamical decoupling of open quantum systems, Physical Review Letters **82**, 2417–2421 (1999).
[79] P. Facchi, D. A. Lidar, and S. Pascazio, Unification of dynamical decoupling and the quantum Zeno effect, Physical Review A **69**, 032314 (2004).
[80] K. E. Rönnburg, E. Mohler, H. G. Roskos, K. Ortner, C. R. Becker, and L. W. Molenkamp, Motional-narrowing-type dephasing of electron and hole spins of itinerant excitons in magnetically doped II-VI bulk semiconductors, Physical Review Letters **96**, 117203 (2006).
[81] M. Kitagawa and M. Ueda, Squeezed spin states, Phys. Rev. A **47**, 5138 (1993).
[82] S. Friedland and L.-H. Lim, Nuclear norm of higher-order tensors, Mathematics of Computation **87**, 1255 (2018).

Supplemental Material: Emergent classicality and wavefunction branching in an isolated quantum many-body system

Saúl Pilatowsky-Cameo,[1,*] Jordan Cotler,[2,†] Daniel Ranard,[3,‡] and C. Jess Riedel[4,§]

[1] *Center for Theoretical Physics — a Leinweber Institute, Massachusetts Institute of Technology, Cambridge, MA 02139, USA*
[2] *Department of Physics, Harvard University, Cambridge, MA 02138, USA*
[3] *Department of Physics, California Institute of Technology, Pasadena, CA 91125, USA*
[4] *NTT Research, Inc., Physics & Informatics Laboratories, Sunnyvale, CA 94085, USA*

In this Supplemental Material, we provide details supporting the derivations, rigorous statements, and numerical results of the main text. In Sec. I, we identify some key features of the emergence of classicality in our model, contrast it with related prior work, and present future directions. In Sec. II, we describe the numerical techniques used to simulate the unitary dynamics and present a time-resolved comparison between the reduced Wigner function and the corresponding classical dissipative evolution. In Sec. III, we compute normalization factors and moment estimates for the random coupling ensembles appearing in the disordered Hamiltonian. In Sec. IV, we give a microscopic derivation of the effective Lindblad equation for the collective spin sector and of the corresponding diffusion rate. In Sec. V, we present the detailed proof of Theorem 1, relating the spin Lindblad dynamics to a classical Fokker–Planck equation. In Sec. VI, we extend the classicality criterion using not-too-squeezed states, obtaining an improved threshold over Theorem 1, which holds for general Hamiltonians. Finally, in Sec. VII, we estimate the fidelity of records associated with different branches and compare this prediction with numerical simulations.

CONTENTS

* saulpila@mit.edu
† jcotler@fas.harvard.edu
‡ dranard@caltech.edu
§ jessriedel@gmail.com

I. MODEL FEATURES AND COMPARISON TO PRIOR WORKS

In this section, we introduce some terminology and then use it to characterize the main features of our work and compare our approach with related work in the literature.

A. General terminology

We take as given a notion of locality defined by a preferred tensor-product decomposition of a finite-dimensional Hilbert space into microscopic subsystems: $\mathcal{H} \equiv \bigotimes_j \mathcal{H}_j$. We say an observable is *k-local* when it is supported on at most k subsystems, while a family of observables is *many-body* if its support diverges in the thermodynamic limit. Likewise, the dynamics are k-local when the Hamiltonian is a sum of k-local observables.

A set of observables induces an algebra through operator multiplication and complex linear combinations. Generalizing from the identification between subsystems (in the sense of a tensor-product decomposition of Hilbert space) and the algebra of operators defined on them [S1], we can think of any algebra as a *generalized subsystem*. Unlike the microscopic subsystems defining locality, a generalized subsystem need not correspond to a tensor-product factor of $\mathcal{H}$. Its algebra $\mathcal{A}$ may have a nontrivial center and, more generally, takes the Artin-Wedderburn form $\mathcal{A} = \bigoplus_i \mathcal{A}_i \otimes \mathcal{I}_i \subset \mathcal{B}(\mathcal{H})$.

The *environment* of a generalized subsystem is the commutant (i.e., centralizer) of its algebra. We say the environment is *internal* when the degrees of freedom in the commutant are supported on the same microscopic subsystems as the generalized subsystem itself. If the environment is instead supported on the complementary microscopic subsystems, we say it is *external*. The former occurs, for instance, when the generalized subsystem has support on all microscopic subsystems but its algebra is a proper subalgebra of the full operator algebra, while the latter is the familiar case in which the generalized subsystem is the complete operator algebra on a proper subset of microscopic subsystems.

We now turn to concepts that become applicable in the thermodynamic limit $N \to \infty$, which with appropriate scaling coincides with the classical limit $\hbar_{\text{eff}} \to 0$. The reduced density matrix $\rho(t)$ of a generalized subsystem at a given time t is *localized* in a set of observables $\hat{\mathbf{A}} = (\hat{A}_r)$ when it is a mixture, with some distribution $P(\mathbf{A}, \mu; t)$, of states $|\mathbf{A}, \mu\rangle$ that are each spectrally localized[1] around the eigenvalue A_r for each of the observables $\hat{\mathbf{A}} = (\hat{A}_r)$. Marginalizing over the auxiliary[2] parameter μ yields a classical distribution $P(\mathbf{A}, t) = \int \mathrm{d}\mu\, P(\mathbf{A}, \mu; t)$ for the localized variable $\mathbf{A}$.

Due to the spectral localization of the $|\mathbf{A}, \mu\rangle$, the marginals of $P(\mathbf{A}, t)$ converge in the thermodynamic limit to the corresponding single-time measurement distributions of the observables $\hat{\mathbf{A}} = (\hat{A}_r)$. This, however, is only a statement about single-time statistics. It does not guarantee that measurements at different times have classical joint statistics; the underlying quantum dynamics need not be Markovian even when the classical distribution $P(\mathbf{A}, t)$ of localization obeys a Markovian equation. Defining quantum Markovianity is challenging [S2, S3], even within the restricted context of the quantum-classical transition [S4]. Nonetheless, the consistent histories framework can provide a stronger characterization of classicality than the behavior of $P(\mathbf{A}, t)$ alone.

Given a set of exhaustive histories defined through time-ordered sequences of Heisenberg-picture projectors, $C_\alpha = Q_{\alpha_M}(t_M) \cdots Q_{\alpha_1}(t_1)$, the histories are *consistent* (precisely, *medium decoherent*) when $\langle\psi|C_\alpha^\dagger C_\beta|\psi\rangle = 0$ for $\alpha \neq \beta$. This implies the probabilities $p(\alpha) = \langle\psi|C_\alpha^\dagger C_\alpha|\psi\rangle$ satisfy the Kolmogorov probability sum rules under coarse-graining. In the thermodynamic limit, we say that the histories are *trajectories* for a set of observables $\hat{\mathbf{A}}$ when (i) the time intervals between successive projectors vanish, and (ii) each projector is supported on a vanishing-width interval of eigenvalues of the observables $\hat{\mathbf{A}}$. A consistent set of trajectory histories for $\hat{\mathbf{A}}$ is *quasiclassical* when the probabilities satisfy the Markovian condition $p(\alpha_1, \ldots, \alpha_M)p(\alpha_m) = p(\alpha_1, \ldots, \alpha_m)p(\alpha_m, \ldots, \alpha_M)$. This stronger notion of Markovianity guarantees, for instance, that multiple hypothetical measurements of the observables $\hat{\mathbf{A}}$ at different times by an external observer would have the expected classical correlations (with the single-time measurements as a special case converging to the distribution $P(\mathbf{A}; t)$ associated with localization).

When the Heisenberg-picture conditional state associated with each history at one time overlaps only a single conditional state associated with a history at an earlier time, the conditional states form a directed tree, with edges corresponding to nonzero overlap. We refer to the conditional states as *branches* and say that the histories *branch forward in time*.

---

[1] Although we do not commit to a precise quantification of approximate localization for use in a limit, for concreteness one could require that $\|\rho - \tilde{\rho}\|_{\text{Tr}}$ is vanishing, where $\tilde{\rho} = \int \mathrm{d}\mathbf{A}\, \mathrm{d}\mu\, P(\mathbf{A}, \mu)|\mathbf{A}, \mu\rangle\langle\mathbf{A}, \mu|$ and where each state $|(A_r), \mu\rangle$ is supported strictly on an interval of eigenvalues (for each A_r) whose width is vanishing.

[2] In our main model, we can take μ to be trivial, but in our more general theorem about spin decoherence its role is played by the approximate tangent covariance matrix σ of the spin-squeezed states, which controls the squeezing strength and orientation.

B. Model characterization and future directions

With the preceding definitions, we can now compactly characterize our primary model at appropriate disorder strength. We heuristically derive a Lindblad equation for a generalized subsystem of a many-qubit system in the thermodynamic limit. Our model has these features:

A. The dynamics are unitary and the Hamiltonian is 3-local.

B. There is a preferred variable (a set of observables, $\hat{\boldsymbol{S}}/S$) that generates the algebra of the generalized subsystem, whose environment is internal.

C. In the thermodynamic limit,

   i) the preferred variable is many-body and continuous;

   ii) the preferred variable is localized by the environment, and its classical distribution obeys a Kolmogorov forward equation, specifically a Fokker-Planck equation;

   iii) the drift terms in the Fokker-Planck equation produce chaotic Hamiltonian flow;

   iv) the dissipative terms in the Fokker-Planck equation are negligible[3] compared with the drift terms; and

   v) trajectory histories of the preferred variable are consistent, quasiclassical, branch forward in time, and marginalize to the same classical distribution as in (ii).

Because we can numerically simulate the full unitary dynamics, rather than only simulating the reduced dynamics under an assumed Lindblad equation, we can *confirm* the accuracy of the Lindblad description and directly check the consistency of the histories.

At the same time, our model has three simplifying features that leave important challenges for future work:

1. The Hamiltonian is 3-local and thus contains genuine interactions, but it is not geometrically local.

2. Our model constrains the dynamics within fixed total-spin subspaces, although these spaces are still exponentially large in the number of qubits when $k = \Theta(N)$. Within each subspace the coupling takes the familiar finite-rank bilinear form, although the mapping to the k-local representation of the Hamiltonian is still nontrivial.

3. The dynamics of the quasiclassical variable can be read off rather directly from the Hamiltonian $\hat{H}$. In the thermodynamic limit, the coupling $\epsilon\hat{H}_{\mathrm{dis}}$ becomes small relative to $\hat{H}_{KT}$, so that both $\hat{H}$ and $i[\hat{H}, \hat{\mathbf{S}}]$ approach low-order polynomials in the quasiclassical variables $\hat{\mathbf{S}} = (\hat{S}_x, \hat{S}_y, \hat{S}_z)$. Thus the natural representation of the microscopic Hamiltonian already exposes the effective classical variables and their dynamics.

A corresponding challenge for future work is to find a model that can be shown to have properties B and C above, but for which

1. the Hamiltonian $\hat{H}$ is geometrically local,

2. the dynamics are not artificially constrained to a subspace of the Hilbert space, and/or

3. neither the Hamiltonian $\hat{H}$, nor its commutator $[\hat{H}, \hat{\mathbf{A}}]$ with the preferred observables $\hat{\mathbf{A}} = (\hat{A}_r)$, is a bounded-order polynomial in $\hat{\mathbf{A}}$, even in the thermodynamic limit.

Although the conditions above fall short of a general definition of wavefunction branching [S7], we expect that identifying additional models exhibiting these phenomena, especially models without the simplifying features just described, will help clarify what such a definition should be.

[3] See Refs. [S5, S6].

C. Relationship to prior work

We now briefly comment on a selection of prior work and note how it differs from the results we present.

O'Donovan et al. carry out a traditional microscopic derivation of a Lindblad equation in the weak-coupling limit for a general system coupled to an external ETH-obeying bath through local operators [S8]. They numerically compare an ETH-obeying mixed-field Ising bath with an integrable version, finding that the former is well described by the derived Lindblad equation while the latter shows strong discrepancies at the finite sizes studied. The generality of the arguments is suggestive for identifying which general many-body variables could be expected to decohere.

Nation & Porras [S9] also consider systems coupled to an external bath where the Hamiltonian eigenstates are taken to have the chaotic wavefunction form and the system-bath coupling is a random matrix. To describe the emergence of classical statistical mechanics, they obtain dynamics corresponding to an Ornstein–Uhlenbeck process for a solvable random-matrix model, and they extend the underlying thermalization and Markovian analysis numerically to several local observables on the spin chain and one global observable (the mean spin). They further consider sequences of measurements at multiple times and note that the outcomes satisfy a non-disturbance condition that they identify with consistency of histories.

Working on a spin chain, Mazza et al. [S10] use machine-learning methods to find general linear generators that accurately produce the evolution of 1-local subsystems. Carnazza et al. [S11] and Cemin et al. [S12] extend this to 2-spin subsystems and constrain the generators to be Lindbladian. These discrete variables are not many-body, and their environment is external rather than internal. The Lindblad dynamics are fit rather than derived, and they govern variables with no classical limit.

Also on a spin chain, Ates et al. [S13] derive a classical Fokker–Planck equation describing non-chaotic relaxation for a continuous excitation density, a many-body variable. In related work, Ji et al. [S14] derive an analogous master equation for the discrete number of hard rods. They do not investigate classical correlations between multiple times.

Wang and Strasberg [S15] study a closed many-body model of multi-time correlations: they consider histories of a variable with divergent support in a geometrically local XXZ Heisenberg spin chain and show that they generally become consistent in the thermodynamic limit. However, they restrict their attention to histories over a binary state space (whether the magnetization imbalance is positive or negative). They also only investigate the decoherence functional of histories for Haar-random initial states, and thus do not provide a special low-entropy initial condition that would define the forward branching arrow of time.

II. NUMERICAL TECHNIQUES FOR UNITARY EVOLUTION

In this section we describe the numerical methods used to simulate the unitary dynamics under the disordered kicked-top model. Our simulations are performed directly in the fixed-total-spin subspace with

$$S = \frac{N-k}{2}, \qquad \mathcal{H}_S = \mathcal{S} \otimes \mathcal{P},$$

where $\dim(\mathcal{S}) = 2S+1$ and $\dim(\mathcal{P}) = \binom{N}{k/2} - \binom{N}{k/2-1}$. This avoids working in the full 2^N-dimensional Hilbert space.

We first construct an orthonormal basis for the multiplicity space $\mathcal{P}$. In the computational basis, the highest-weight states of total spin $S = (N-k)/2$ lie in the sector with $k/2$ spins down. We enumerate this sector and form the rectangular matrix representing the collective raising operator $\hat{S}^+$ from the $k/2$-down sector to the $(k/2-1)$-down sector. The multiplicity space $\mathcal{P}$ is the nullspace of this matrix. We numerically compute an orthonormal basis for the nullspace and collect its vectors as the columns of an isometry V, so that $V^\dagger V = \mathbb{1}_{\mathcal{P}}$.

The collective sector $\mathcal{S}$ is represented by the usual spin-S matrices. In the $\hat{S}_z$ eigenbasis,

$$\hat{S}_z \left|m\right\rangle = m \left|m\right\rangle, \qquad \hat{S}_\pm \left|m\right\rangle = \sqrt{S(S+1) - m(m\pm 1)}\, \left|m \pm 1\right\rangle,$$

with $\hat{S}_x = (\hat{S}_+ + \hat{S}_-)/2$ and $\hat{S}_y = (\hat{S}_+ - \hat{S}_-)/(2i)$. A pure state is then stored as the coefficient matrix

$$\left|\psi(t)\right\rangle = \sum_{a=1}^{d_{\mathcal{P}}} \sum_{m=-S}^{S} C_{am}(t)\, \left|a\right\rangle_{\mathcal{P}} \left|m\right\rangle_{\mathcal{S}}, \tag{S1}$$

so the reduced density matrix on the collective sector is obtained by tracing out $\mathcal{P}$, $[\rho_{\mathcal{S}}(t)]_{mn} = \sum_{a=1}^{d_{\mathcal{P}}} C_{am}(t) C_{an}(t)^*$.

The random Heisenberg couplings (RHCs) $\hat{K}_\mu$ are constructed in the same multiplicity basis. We draw independent Gaussian coefficients $c_{ij}^{(\mu)}$, subtract their mean so that $\sum_{i<j} c_{ij}^{(\mu)} = 0$, and form

$$\hat{K}_\mu = V^\dagger \left(\sum_{i<j} c_{ij}^{(\mu)} \hat{h}_{ij} \right) V, \qquad \hat{h}_{ij} = \hat{X}_i \hat{X}_j + \hat{Y}_i \hat{Y}_j + \hat{Z}_i \hat{Z}_j.$$

The coefficients are normalized so that $d_{\mathcal{P}}^{-1} \operatorname{tr}_{\mathcal{P}}(\hat{K}_\mu^2) = 1$ on average, following Lemma S1.

Between kicks we evolve using a fixed-time Trotter step δt (we use 0.005 or smaller in all simulations, and have verified that our results are independent of this number). We numerically apply

$$|\psi(t+\delta t)\rangle \approx e^{-i\frac{\kappa \delta t}{2S+1}\hat{S}_x^2} e^{-i\varepsilon \delta t \hat{K}_x \hat{S}_x} e^{-i\varepsilon \delta t \hat{K}_y \hat{S}_y} e^{-i\varepsilon \delta t \hat{K}_z \hat{S}_z} \tag{S2}$$

by diagonalizing each $\hat{K}_\mu$ and $\hat{S}_\mu$ separately, since the eigenbasis of $\hat{K}_\mu \otimes \hat{S}_\mu$ is just the tensor product of the eigenbases.

As a time-resolved complement to Fig. 1(b) of the main text, Fig. S1 compares the Wigner function of the collective-spin state obtained from the full unitary dynamics with the corresponding classical dissipative evolution. The agreement illustrates the emergence of quantum–classical correspondence for the random Heisenberg couplings.

III. MOMENTS OF RANDOM HEISENBERG COUPLINGS

In this section we compute ensemble averages for the random Heisenberg interaction

$$\hat{K} = \sum_{i<j} c_{ij} \hat{h}_{ij}, \qquad \hat{h}_{ij} \coloneqq \hat{X}_i \hat{X}_j + \hat{Y}_i \hat{Y}_j + \hat{Z}_i \hat{Z}_j. \tag{S3}$$

The coefficients c_{ij} are Gaussian, with their mean subtracted so that $\operatorname{tr}_{\mathcal{P}}(\hat{K}) \propto \sum_{i<j} c_{ij} = 0$. We choose their standard deviation σ so that $\mathbb{E}[\langle \hat{K}^2 \rangle] = 1$, where $\langle \cdot \rangle \coloneqq \operatorname{tr}_{\mathcal{P}}(\,\cdot\,)/d_{\mathcal{P}}$. The following lemma gives this standard deviation explicitly.

A. Standard deviation

Lemma S1. *The condition $\mathbb{E}[\langle \hat{K}^2 \rangle] = 1$ holds if and only if the standard deviation of the coefficients is*

$$\sigma^{-2} = 8N(N-1)\eta(1-\eta), \qquad \eta = \frac{k(2N-k+2)}{4N(N-1)}. \tag{S4}$$

In the limit $N \gg k$, the expression simplifies to $\sigma^{-2} \approx 4Nk$.

Proof. Let us compute the expected variance $\mathbb{E}[\langle \hat{K}^2 \rangle]$ explicitly and set it equal to 1. We can write

$$\hat{K} = \sum_{i<j} c_{ij}(2F_{ij} - \mathbb{I}),$$

where F_{ij} is the swap operator between qubits i and j. By the constraint $\sum_{i<j} c_{ij} = 0$, the identity term vanishes, yielding

$$\hat{K} = 2 \sum_{\alpha=1}^{N_p} c_\alpha F_\alpha,$$

where α indexes the $N_p = N(N-1)/2$ distinct pairs of sites. The coefficients c_α are Gaussian random variables subject to the sum constraint, which implies the covariance matrix:

$$\mathbb{E}[c_\alpha c_\beta] = \sigma^2 \left(\delta_{\alpha\beta} - \frac{1}{N_p} \right).$$

We calculate the expected variance:

$$\mathbb{E}\Big[\langle \hat{K}^2 \rangle\Big] = 4 \sum_{\alpha,\beta} \mathbb{E}[c_\alpha c_\beta] \langle F_\alpha F_\beta \rangle.$$

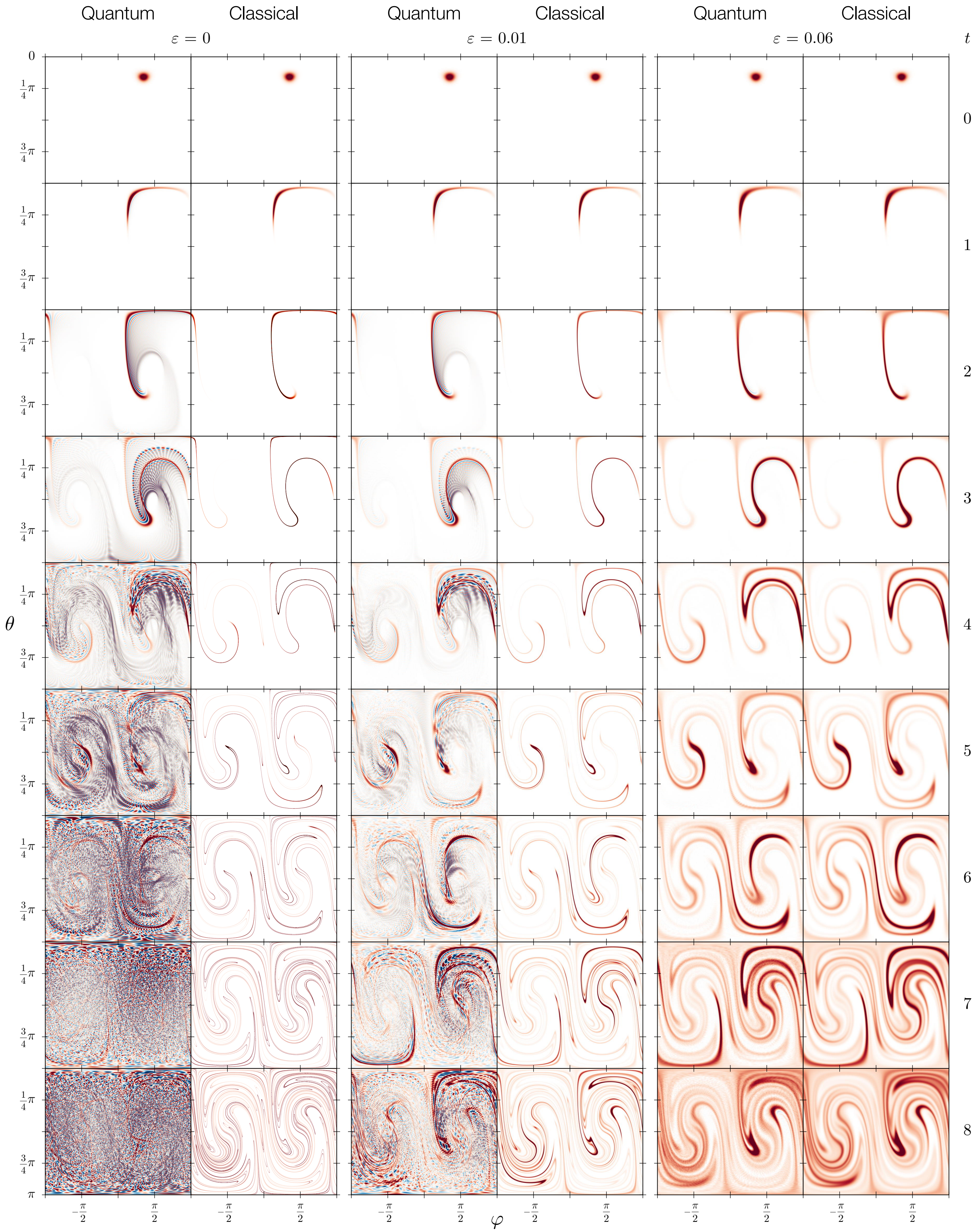

FIG. S1. Quantum vs classical dynamics in the collective sector (time from top to bottom). Odd columns: Wigner function of $\mathrm{tr}_{\mathcal{P}}(\psi(t))$, where $|\psi(t)\rangle$ undergoes unitary evolution under the disordered kicked-top Hamiltonian, with random Heisenberg couplings. Even columns: dissipative classical evolution, starting from a Gaussian distribution with variance equal to that of the spin coherent state (truncated Wigner approximation) [S16]. ($k = 4$, $N = 200$, $\kappa = 4.2$, $p = \pi/2$, $\theta_0 = 0.5$, $\varphi_0 = 1.1$.)

Substituting the covariance matrix splits the sum into diagonal and off-diagonal parts:

$$1 = \mathbb{E}[\langle \hat{K}^2 \rangle] = 4\sigma^2 \left(\sum_\alpha \langle F_\alpha^2 \rangle - \frac{1}{N_p} \sum_{\alpha,\beta} \langle F_\alpha F_\beta \rangle \right).$$

Since transpositions square to identity, the first term sums to N_p. The second term involves the square of the sum of all transpositions $\mathcal{C}_2 = \sum_\alpha F_\alpha$. Since the operator $\mathcal{C}_2$ is permutation invariant, it acts as a scalar within the space $\mathcal{P}$. Using the identity $\mathcal{C}_2 = \mathbf{S}_{\text{tot}}^2 + \frac{N(N-4)}{4}$, this scalar must be $z = S(S+1) + N(N-4)/4$, and hence

$$\sigma^{-2} = 4 \left(N_p - \frac{z^2}{N_p} \right).$$

Using $S = (N-k)/2$ one can simplify this equation to Eq. (S4). □

B. Variance of a commutator

The next result gives the variance of a commutator between two independent random Heisenberg couplings.

Lemma S2. *Let $\hat{K}_0$ and $\hat{K}_1$ be independent random Heisenberg couplings. Then*

$$\mathbb{E}\left[\langle [\hat{K}_0, \hat{K}_1]^\dagger [\hat{K}_0, \hat{K}_1] \rangle \right] = \sigma^4 \, 32 N(N-1)(N-2)(1-\phi_3), \tag{S5}$$

where σ is given by Lemma S1, and ϕ_3 is the normalized character of the 3-cycle in the representation with total spin S, given by [S17, Eq. (5.2)]

$$\phi_3 = \frac{(N-3)!}{N!} \left(\frac{M_3}{2} - \frac{3}{2} N(N-1) \right), \tag{S6}$$

$$M_3 = \sum_{j=1}^{2} \left[(\lambda_j - j)(\lambda_j - j + 1)(2\lambda_j - 2j + 1) + j(j-1)(2j-1) \right], \qquad \lambda_1 = N - k/2, \qquad \lambda_2 = k/2.$$

Proof. Let us write $\mathcal{K} = [\hat{K}_0, \hat{K}_1]$, and $\hat{K}_0 = 2\sum_\alpha c_\alpha F_\alpha$ and $\hat{K}_1 = 2\sum_\beta c'_\beta F_\beta$ as sums over transpositions F_{ij} (with α, β indexing unordered pairs), with independent Gaussian coefficients satisfying $\mathbb{E}[c'_\alpha c'_\beta] = \mathbb{E}[c_\alpha c_\beta] = \sigma^2(\delta_{\alpha\beta} - 1/N_p)$ and $\mathbb{E}[c_\alpha c'_\beta] = 0$. Then

$$\mathcal{K} = [\hat{K}_0, \hat{K}_1] = \left[2\sum_\alpha c_\alpha F_\alpha, \, 2\sum_\beta c'_\beta F_\beta \right] = 4 \sum_{\alpha,\beta} c_\alpha c'_\beta [F_\alpha, F_\beta]. \tag{S7}$$

Only non-disjoint pairs contribute: for transpositions, $[F_{ij}, F_{kl}] = 0$ unless the pairs share exactly one site. There are $N(N-1)(N-2)$ such ordered choices: choose the repeated site in N ways and the other two sites in $(N-1)(N-2)$ ways. The constraints $i < j$ and $k < l$ then fix the internal order within each pair. For such shared-site pairs, we have

$$[F_{ij}, F_{jk}] = F_{ij} F_{jk} - F_{jk} F_{ij} = F_{(ijk)} - F_{(ikj)},$$

so that

$$[F_{ij}, F_{jk}]^\dagger [F_{ij}, F_{jk}] = \left(F_{(ikj)} - F_{(ijk)} \right) \left(F_{(ijk)} - F_{(ikj)} \right) = 2\mathbb{I} - F_{(ijk)} - F_{(ikj)},$$

where $F_{(ijk)} := F_{ij} F_{jk}$ denotes the operator representing the 3-cycle (ijk) in $\mathcal{P}$ (and $F_{(ikj)} := F_{jk} F_{ij} = F_{(ijk)}^\dagger$). Taking the trace over $\mathcal{P}$ and using $\mathrm{tr}_\mathcal{P}(F_{(ijk)}) = \mathrm{tr}_\mathcal{P}(F_{(ikj)}) = d_\mathcal{P} \phi_3$ yields

$$\langle [F_{ij}, F_{jk}]^\dagger [F_{ij}, F_{jk}] \rangle = 2(1 - \phi_3).$$

We now perform an average over disorder. Since the disorder is Gaussian, we evaluate the fourth moments using Wick's theorem,

$$\mathbb{E}[c_\alpha c_{\alpha'} c_\gamma c_{\gamma'}] = \mathbb{E}[c_\alpha c_{\alpha'}] \, \mathbb{E}[c_\gamma c_{\gamma'}] + \mathbb{E}[c_\alpha c_\gamma] \, \mathbb{E}[c_{\alpha'} c_{\gamma'}] + \mathbb{E}[c_\alpha c_{\gamma'}] \, \mathbb{E}[c_{\alpha'} c_\gamma],$$

and similarly for the c''s. Mixed contractions vanish since the two disorder families are independent: $\mathbb{E}[c_\alpha c'_\beta] = 0$. Moreover $\mathbb{E}[c_\alpha c_{\alpha'}] = \sigma^2(\delta_{\alpha\alpha'} - 1/N_p)$ (and similarly for c'). Using Eq. (S7),

$$\mathbb{E}\big[\langle \mathcal{K}^\dagger \mathcal{K}\rangle\big] = 16 \sum_{\alpha,\beta} \sum_{\alpha',\beta'} \mathbb{E}[c_\alpha c_{\alpha'}]\, \mathbb{E}\big[c'_\beta c'_{\beta'}\big]\ \langle [F_\alpha, F_\beta]^\dagger [F_{\alpha'}, F_{\beta'}]\rangle. \tag{S8}$$

Using $\sum_\alpha F_\alpha = \mathcal{C}_2 \propto \mathbb{I}$ on $\mathcal{P}$, the $-1/N_p$ pieces in the covariances only contribute permutation-invariant terms (proportional to $\mathcal{C}_2$) which commute with all F_α. Therefore these contributions vanish inside the commutators and make no contribution to $\mathbb{E}[\langle \mathcal{K}^\dagger \mathcal{K}\rangle]$. Consequently, we may replace $\mathbb{E}[c_\alpha c_{\alpha'}] \to \sigma^2 \delta_{\alpha\alpha'}$ and $\mathbb{E}[c'_\beta c'_{\beta'}] \to \sigma^2 \delta_{\beta\beta'}$ in Eq. (S8), yielding

$$\mathbb{E}\big[\langle \mathcal{K}^\dagger \mathcal{K}\rangle\big] = 16\sigma^4 \sum_{\alpha,\beta} \langle [F_\alpha, F_\beta]^\dagger [F_\alpha, F_\beta]\rangle = \sigma^4\, 32N(N-1)(N-2)(1-\phi_3). \qquad \square$$

In the limit $N \gg k$ the expression above simplifies greatly. In particular, using $1-\phi_3 \approx 3k/(2N)$ and $\sigma^{-2} \approx 4Nk$, Eq. (S5) becomes

$$\mathbb{E}\left[\langle [\hat{K}_0, \hat{K}_1]^\dagger [\hat{K}_0, \hat{K}_1]\rangle\right] \approx \frac{3}{k}. \tag{S9}$$

This simple formula admits a higher-order generalization.

C. Higher-order moments of commutators

For two operators A and B, define the iterated commutators $[A,B]_0 = B$, and $[A,B]_{n+1} = [A,[A,B]_n]$. The leading fixed-$k$ moments of these commutators can be expressed in terms of constants C_n, defined as follows. Let $G(y) = \sum_{n\geq 0} g_n y^n$ starting at $g_0 = 1$ be the formal power series satisfying

$$\left(1 + yG(y) + 2y^2 G'(y)\right)\left(2 - G(y) + yG(y)^2\right) = 1. \tag{S10}$$

Define the formal power series:

$$H(y,z) = \sum_{n\geq 0}\sum_{p=0}^{2n} g_n z^p y^n, \qquad P(y,z) = \frac{H(y,z)}{1+zyH(y,z)} = \sum_{n\geq 0}\sum_{p=0}^{2n} P_{n,p} z^p y^n. \tag{S11}$$

Then we set

$$C_n = \frac{1}{2}\left[\sum_{r=0}^{n} \binom{2n}{2r} g_r g_{n-r} + \sum_{p=0}^{2n} (-1)^p \binom{2n}{p} P_{n,p}\right]. \tag{S12}$$

Lemma S3. *Let $\hat{K}_0$ and $\hat{K}_1$ be independent random Heisenberg couplings, normalized as in Lemma S1. For each fixed n and fixed k,*

$$\mathbb{E}\left[\left\langle [\hat{K}_0, \hat{K}_1]_n^\dagger [\hat{K}_0, \hat{K}_1]_n \right\rangle\right] = \frac{C_n}{k^n} + O(N^{-1}), \tag{S13}$$

where C_n is defined in Eq. (S12).

The first values are $C_0 = 1$ and $C_1 = 3$, so the case $n=1$ recovers the large-N form of Lemma S2 (see Table I for values of C_n up to $n = 20$). To prove Lemma S3, we first need the following:

Lemma S4. *Let $\alpha_1, \ldots, \alpha_\ell$ be a sequence of pairs of qubits whose union totals $v \leq N$ qubits and with $\ell \geq 2$ fixed as $N \to \infty$. Define the traceless transpositions $\widetilde{F}_\alpha \coloneqq F_\alpha - \langle F_\alpha \rangle \mathbb{I}$. Then*

$$\left\langle \widetilde{F}_{\alpha_1} \cdots \widetilde{F}_{\alpha_\ell} \right\rangle = \frac{k}{2N} \operatorname{tr}\left(\prod_{a=1}^{\ell} L_\alpha\right) + O(N^{-2}), \tag{S14}$$

where $L_\alpha = (P_\alpha - \mathbb{I})$, with P_α the $v \times v$ permutation matrix associated with the transposition α, acting on the space of v labels.

n	C_n
0	1
1	3
2	28
3	408
4	7698
5	173682
6	4498622
7	130698192
8	4199406588
9	147876395596
10	5671974937140
11	235911748619404
12	10602128617075710
13	513225453419669250
14	26682263414687027790
15	1485579557699327016216
16	88328721495283696013796
17	5592824183754640556807628
18	376096726732217578613778896
19	26789128136617248915600755328
20	2016058168256938037502316523336

TABLE I. Values of C_n as defined by Eq. (S12) up to $n = 20$.

Proof. Consider an arbitrary permutation $\pi \in S_N$ with support size $s = |\mathrm{supp}(\pi)| \leq \ell$, and let F_π be the associated unitary acting on $\mathcal{P}$. The normalized character associated with the permutation π is

$$\phi_\pi := \langle F_\pi \rangle = 1 - \frac{ks}{2N} + O(N^{-2}).$$

Indeed, this follows from elementary representation theory. Since k is even, the Young diagram associated with the representation has two rows, $\left(N - \frac{k}{2}, \frac{k}{2}\right)$. Denote $[N] = \{1, \dots, N\}$. Let $m_n := \left|\left\{S \subseteq [N] \mid |S| = n, \quad \pi(S) \subseteq S\right\}\right|$ count the number of subsets of $[N]$ of size n that are fixed by π. By the Murnaghan–Nakayama rule

$$\phi_\pi = \frac{1}{d_{\mathcal{P}}} \left(m_{k/2} - m_{k/2-1}\right).$$

A subset of size n which is fixed by π either avoids $\mathrm{supp}(\pi)$, or contains an entire nontrivial cycle of π. There are $\binom{N-s}{n}$ options for the former, and since every nontrivial cycle has length at least 2, the latter contribution is $O(N^{n-2})$. Hence

$$m_{k/2} = \binom{N-s}{k/2} + O(N^{k/2-2}), \qquad m_{k/2-1} = \binom{N-s}{k/2-1} + O(N^{k/2-3}).$$

Since

$$d_{\mathcal{P}} = \binom{N}{k/2} - \binom{N}{k/2-1},$$

expanding in powers of $1/N$ gives

$$\phi_\pi = 1 - \frac{k|\mathrm{supp}(\pi)|}{2N} + O(N^{-2}). \tag{S15}$$

In particular, $\phi_2 = 1 - \frac{k}{N} + O(N^{-2})$ for a transposition. Now expand the product of traceless transpositions:

$$\left\langle \widetilde{F}_{\alpha_1} \cdots \widetilde{F}_{\alpha_\ell} \right\rangle = \sum_{A \subseteq [\ell]} (-\phi_2)^{\ell - |A|} \phi\left(\overrightarrow{\prod_{a \in A}} \pi_{\alpha_a}\right),$$

where the arrow means that the product is taken in the original order. Using Eq. (S15),

$$\phi\left(\prod_{a\in A}^{\rightarrow}\pi_{\alpha_a}\right)=1-\frac{k}{2N}\left|\operatorname{supp}\left(\prod_{a\in A}^{\rightarrow}\pi_{\alpha_a}\right)\right|+O(N^{-2}).$$

Also,

$$(-\phi_2)^{\ell-|A|}=(-1)^{\ell-|A|}\left(1-\frac{k(\ell-|A|)}{N}\right)+O(N^{-2}).$$

Upon multiplying, using $\sum_{A\subseteq[\ell]}(-1)^{\ell-|A|}=0$, and $\sum_{A\subseteq[\ell]}(-1)^{\ell-|A|}(\ell-|A|)=0$, we get

$$\left\langle\widetilde{F}_{\alpha_1}\cdots\widetilde{F}_{\alpha_\ell}\right\rangle=-\frac{k}{2N}\sum_{A\subseteq[\ell]}(-1)^{\ell-|A|}\left|\operatorname{supp}\left(\prod_{a\in A}^{\rightarrow}\pi_{\alpha_a}\right)\right|+O(N^{-2}).$$

Since $|\operatorname{supp}(\pi)|=\operatorname{tr}(I-P_\pi)$ and $P_{\prod_a\pi_{\alpha_a}}=\prod_a P_{\alpha_a}$ we get

$$\left\langle\widetilde{F}_{\alpha_1}\cdots\widetilde{F}_{\alpha_\ell}\right\rangle=\frac{k}{2N}\operatorname{tr}\left(\sum_{A\subseteq[\ell]}(-1)^{\ell-|A|}\prod_{a\in A}^{\rightarrow}P_{\alpha_a}\right)+O(N^{-2})=\frac{k}{2N}\operatorname{tr}\left(\prod_{a=1}^{\ell}L_\alpha\right)+O(N^{-2}).\qquad\square$$

Now we prove Lemma S3.

Proof of Lemma S3: The case $n=0$ is the normalization $\mathbb{E}[\langle\hat{K}_1^2\rangle]=1=C_0$. We henceforth assume $n\geq 1$. We expand the commutators using

$$[\hat{K}_0,\hat{K}_1]_n=\sum_{a=0}^{n}(-1)^a\binom{n}{a}\hat{K}_0^{n-a}\hat{K}_1\hat{K}_0^a.$$

By Hermiticity of $\hat{K}_0,\hat{K}_1$ and cyclicity of the trace,

$$\begin{aligned}\left\langle[\hat{K}_0,\hat{K}_1]_n^\dagger[\hat{K}_0,\hat{K}_1]_n\right\rangle&=\sum_{a,b=0}^{n}(-1)^{a+b}\binom{n}{a}\binom{n}{b}\left\langle\hat{K}_0^{a+b}\hat{K}_1\hat{K}_0^{2n-a-b}\hat{K}_1\right\rangle\\&=\sum_{p=0}^{2n}(-1)^p\binom{2n}{p}\left\langle\hat{K}_0^{2n-p}\hat{K}_1\hat{K}_0^p\hat{K}_1\right\rangle.\end{aligned}$$

We now perform the average over the Gaussian disorder. Note that, in terms of the traceless transpositions $\widetilde{F}_\alpha\coloneqq F_\alpha-\langle F_\alpha\rangle\mathbb{I}$, we can write $\hat{K}_\mu=2\sum_\alpha\tilde{c}_\alpha^{(\mu)}\widetilde{F}_\alpha$, where α runs over all unordered pairs of qubits and $\tilde{c}_\alpha^{(\mu)}$ are Gaussian random numbers with zero mean and variance σ^2. Then, we obtain

$$\begin{aligned}\mathbb{E}\left[\left\langle[\hat{K}_0,\hat{K}_1]_n^\dagger[\hat{K}_0,\hat{K}_1]_n\right\rangle\right]&=\sum_{p=0}^{2n}(-1)^p\binom{2n}{p}\mathbb{E}\left[\left\langle\hat{K}_0^{2n-p}\hat{K}_1\hat{K}_0^p\hat{K}_1\right\rangle\right]\\&=2^{2n+2}\sum_{p=0}^{2n}(-1)^p\binom{2n}{p}\sum_{\alpha_1,\ldots,\alpha_{2n}}\sum_{\beta,\beta'}\mathbb{E}\left[\tilde{c}_\beta^{(1)}\tilde{c}_{\beta'}^{(1)}\prod_{j=1}^{2n}\tilde{c}_{\alpha_j}^{(0)}\right]\left\langle\widetilde{F}_{\alpha_1}\cdots\widetilde{F}_{\alpha_{2n-p}}\widetilde{F}_\beta\widetilde{F}_{\alpha_{2n-p+1}}\cdots\widetilde{F}_{\alpha_{2n}}\widetilde{F}_{\beta'}\right\rangle.\end{aligned}\tag{S16}$$

By Wick's theorem, the expectation reduces to contractions over pairings (here, *pairings* means pairings of the variables α_j or β, which themselves denote pairs of qubits), with covariances $\mathbb{E}[\tilde{c}_\alpha^{(\mu)}\tilde{c}_{\alpha'}^{(\mu')}]=\sigma^2\delta_{\mu\mu'}\delta_{\alpha\alpha'}$,

$$\mathbb{E}\left[\tilde{c}_\beta^{(1)}\tilde{c}_{\beta'}^{(1)}\prod_{j=1}^{2n}\tilde{c}_{\alpha_j}^{(0)}\right]=\sigma^{2n+2}\delta_{\beta\beta'}\sum_{\Pi\in\mathrm{Pair}(2n)}\prod_{\{i,j\}\in\Pi}\delta_{\alpha_i\alpha_j},$$

where $\mathrm{Pair}(2n)$ denotes the set of pairings of the labels $\{1,\ldots,2n\}$ (e.g., $\mathrm{Pair}(4)=\big\{\{\{1,2\}\,\{3,4\}\},\{\{1,3\},\{2,4\}\},\{\{1,4\},\{2,3\}\}\big\}$). Thus, Eq. (S16) reduces to

$$\mathbb{E}\left[\left\langle[\hat{K}_0,\hat{K}_1]_n^\dagger[\hat{K}_0,\hat{K}_1]_n\right\rangle\right]=(4\sigma^2)^{n+1}\sum_{p=0}^{2n}(-1)^p\binom{2n}{p}\sum_{\Pi\in\mathrm{Pair}(2n)}\sum_{\boldsymbol{\alpha},\beta}\left\langle\widetilde{F}_{\Pi,p}(\boldsymbol{\alpha};\beta)\right\rangle,\tag{S17}$$

where

$$\widetilde{F}_{\Pi,p}(\boldsymbol{\alpha};\beta) = \widetilde{F}_{\alpha_{\Pi(1)}} \cdots \widetilde{F}_{\alpha_{\Pi(2n-p)}} \widetilde{F}_{\beta} \widetilde{F}_{\alpha_{\Pi(2n-p+1)}} \cdots \widetilde{F}_{\alpha_{\Pi(2n)}} \widetilde{F}_{\beta}, \tag{S18}$$

and $\Pi(j)$ is the pair containing the label $j \in \{1, \ldots, 2n\}$, and now each α_π is labeled by a pair $\pi \in \Pi$, forming the n-tuple $\boldsymbol{\alpha} = (\alpha_\pi)_{\pi\in\Pi}$. The sum $\sum_{\boldsymbol{\alpha}}$ contains a sum over each α_π, each running over the N_p possible pairs of qubits.

For fixed $\Pi, \boldsymbol{\alpha}, \beta$, we say that a label α_π is *connected* to β if there exist labels $\alpha_{\pi_1}, \ldots, \alpha_{\pi_s}$, with $\pi_s = \pi \in \Pi$, such that $\beta \cap \alpha_{\pi_1} \neq \varnothing$, and $\alpha_{\pi_i} \cap \alpha_{\pi_{i+1}} \neq \varnothing \quad (1 \leq i < s)$. That is, β and α_{π_1} share a qubit, and also α_{π_i} and $\alpha_{\pi_{i+1}}$ for each $1 \leq i < s$. Let

$$\mathrm{dis}(\boldsymbol{\alpha},\beta) = \{\pi \in \Pi \,|\, \alpha_\pi \text{ is not connected to } \beta\}. \tag{S19}$$

We split the sum into the connected component of β and the rest, which contains some disconnected α_π:

$$Q_p \coloneqq \sum_{\Pi\in\mathrm{Pair}(2n)} \sum_{\substack{\boldsymbol{\alpha},\beta \\ \mathrm{dis}(\boldsymbol{\alpha},\beta)=\varnothing}} \left\langle \widetilde{F}_{\Pi,p}(\boldsymbol{\alpha};\beta) \right\rangle, \qquad D_p \coloneqq \sum_{\Pi\in\mathrm{Pair}(2n)} \sum_{\substack{\boldsymbol{\alpha},\beta \\ \mathrm{dis}(\boldsymbol{\alpha},\beta)\neq\varnothing}} \left\langle \widetilde{F}_{\Pi,p}(\boldsymbol{\alpha};\beta) \right\rangle \tag{S20}$$

so

$$\mathbb{E}\left[\left\langle [\hat{K}_0, \hat{K}_1]_n^\dagger [\hat{K}_0, \hat{K}_1]_n \right\rangle\right] = (4\sigma^2)^{n+1} \sum_{p=0}^{2n} (-1)^p \binom{2n}{p} (Q_p + D_p)\,.$$

Claim 1 (Only the connected component contributes)**.** *We have*

$$\sum_{p=0}^{2n} (-1)^p \binom{2n}{p} D_p = 0. \tag{S21}$$

Proof. Define the functional $\Sigma[\,\cdot\,]$ acting on a function $p \mapsto f(p)$ by

$$\Sigma[f] \coloneqq \sum_{p=0}^{2n} (-1)^p \binom{2n}{p} f(p).$$

Note that the functions $f_{a,b}(p) = \binom{p}{a}\binom{2n-p}{b}$ with $a, b \geq 0$ and $a + b < 2n$ are annihilated by this functional:

$$\Sigma[f_{a,b}] = \sum_{p=0}^{2n} (-1)^p \binom{2n}{p} \binom{p}{a} \binom{2n-p}{b} = (-1)^a \frac{(2n)!}{a!\,b!\,(2n-a-b)!} \sum_{q=0}^{2n-a-b} (-1)^q \binom{2n-a-b}{q} = 0. \tag{S22}$$

We now show that D_p is a linear combination of the functions $f_{a,b}(p)$. Fix $\boldsymbol{\alpha}, \beta$ and let s be the size of $\Pi \setminus \mathrm{dis}(\boldsymbol{\alpha},\beta)$. If $\mathrm{dis}(\boldsymbol{\alpha},\beta) \neq \varnothing$, then $s < n$. Moreover, if $\pi \in \mathrm{dis}(\boldsymbol{\alpha},\beta)$ and $\pi' \notin \mathrm{dis}(\boldsymbol{\alpha},\beta)$, then

$$\alpha_\pi \cap \alpha_{\pi'} = \varnothing, \qquad \alpha_\pi \cap \beta = \varnothing,$$

because otherwise α_π would also be connected to β. Hence

$$[\widetilde{F}_{\alpha_\pi}, \widetilde{F}_{\alpha_{\pi'}}] = 0, \qquad [\widetilde{F}_{\alpha_\pi}, \widetilde{F}_{\beta}] = 0 \qquad (\pi \in \mathrm{dis}(\boldsymbol{\alpha},\beta),\ \pi' \notin \mathrm{dis}(\boldsymbol{\alpha},\beta)). \tag{S23}$$

Write $i_1 < \cdots < i_{2s}$ for the labels $j \in \{1, \ldots, 2n\}$ such that $\Pi(j) \notin \mathrm{dis}(\boldsymbol{\alpha},\beta)$, and write $j_1 < \cdots < j_{2n-2s}$ for the remaining labels, so $\Pi(j_q) \in \mathrm{dis}(\boldsymbol{\alpha},\beta)$. Suppose that exactly a of $i_1, \ldots, i_{2s}$ are in $\{2n-p+1, \ldots, 2n\}$, i.e., $i_{2s-a} \leq 2n-p < i_{2s-a+1}$.

By Eq. (S23) we may perform the following commutation:

$$\widetilde{F}_{\Pi,p}(\boldsymbol{\alpha};\beta) = \left(\prod_{r=1}^{2s-a} \widetilde{F}_{\alpha_{\Pi(i_r)}}\right) \underbrace{\left(\prod_{q:\, j_q \leq 2n-p} \widetilde{F}_{\alpha_{\Pi(j_q)}}\right)}_{(\star)} \widetilde{F}_{\beta} \left(\prod_{r=2s-a+1}^{2s} \widetilde{F}_{\alpha_{\Pi(i_r)}}\right) \underbrace{\left(\prod_{q:\, j_q > 2n-p} \widetilde{F}_{\alpha_{\Pi(j_q)}}\right)}_{(\star\star)} \widetilde{F}_{\beta}$$

$$= \underbrace{\left(\prod_{r=1}^{2s-a} \widetilde{F}_{\alpha_{\Pi(i_r)}}\right) \widetilde{F}_\beta \left(\prod_{r=2s-a+1}^{2s} \widetilde{F}_{\alpha_{\Pi(i_r)}}\right) \widetilde{F}_\beta}_{} \underbrace{\left(\prod_{q=1}^{2n-2s} \widetilde{F}_{\alpha_{\Pi(j_q)}}\right)}_{(\star)\times(\star\star)},$$

and hence

$$\left\langle \widetilde{F}_{\Pi,p}(\boldsymbol{\alpha};\beta)\right\rangle = \left\langle \Big(\prod_{r=1}^{2s-a} \widetilde{F}_{\alpha_{\Pi(i_r)}}\Big)\widetilde{F}_\beta\Big(\prod_{r=2s-a+1}^{2s} \widetilde{F}_{\alpha_{\Pi(i_r)}}\Big)\widetilde{F}_\beta\Big(\prod_{q=1}^{2n-2s} \widetilde{F}_{\alpha_{\Pi(j_q)}}\Big)\right\rangle =: W_{s,a},$$

where the dependence of the right-hand side on p is now entirely through a. Thus, we can collect

$$D_p = \sum_{\Pi\in \mathrm{Pair}(2n)} \sum_{\substack{\boldsymbol{\alpha},\beta \\ \mathrm{dis}(\boldsymbol{\alpha},\beta)\neq\varnothing}} \left\langle \widetilde{F}_{\Pi,p}(\boldsymbol{\alpha};\beta)\right\rangle = \sum_{s=0}^{n-1}\sum_{a=0}^{2s} W_{s,a} m_{s,a,p},$$

where $m_{s,a,p}$ counts the possible choices for a and the upper limit $s \le n-1$ follows from $\mathrm{dis}(\boldsymbol{\alpha},\beta)\neq\varnothing$. Let us count the possible choices for a. Recall that $s = |\Pi \setminus \mathrm{dis}(\boldsymbol{\alpha},\beta)|$, and suppose that exactly a of the $2s$ positions in the word $\widetilde{F}_{\Pi,p}(\boldsymbol{\alpha},\beta)$ whose labels are not in $\mathrm{dis}(\boldsymbol{\alpha},\beta)$ occur to the right of the first $\widetilde{F}_\beta$, i.e., among the last p positions. Then the other $2s-a$ such positions occur to the left of $\widetilde{F}_\beta$. The number of choices of these positions is then exactly $m_{s,a,p} = \binom{p}{a}\binom{2n-p}{2s-a}$.

Applying the functional Σ we can then conclude

$$\sum_{p=0}^{2n}(-1)^p\binom{2n}{p}D_p = \Sigma\left[p\mapsto \sum_{s=0}^{n-1}\sum_{a=0}^{2s} W_{s,a}m_{s,a,p}\right] = \sum_{s=0}^{n-1}\sum_{a=0}^{2s} W_{s,a}\Sigma\left[p\mapsto\binom{p}{a}\binom{2n-p}{2s-a}\right] = 0,$$

where we used $a+(2s-a) = 2s < 2n$ to apply Eq. (S22) with $b = 2s-a$. □

Because of Claim 1, we obtain

$$\mathbb{E}\left[\left\langle [\hat{K}_0,\hat{K}_1]_n^\dagger[\hat{K}_0,\hat{K}_1]_n\right\rangle\right] = (4\sigma^2)^{n+1}\sum_{p=0}^{2n}(-1)^p\binom{2n}{p}Q_p.$$

The proof is complete once we prove the following.

Claim 2. *For fixed $p, n,$ and k, with $P_{n,p}$ and g_r defined by Eqs.* (S10) *and* (S11),

$$(4\sigma^2)^{n+1}Q_p = \frac{1}{2k^n}\left(P_{n,p} + \begin{cases} g_{p/2}g_{n-p/2}, & p \text{ even,}\\ 0, & p\text{ odd}\end{cases}\right) + O(N^{-1}). \tag{S24}$$

Proof. We begin by applying Lemma S4 to Q_p:

$$Q_p = \sum_{\Pi\in\mathrm{Pair}(2n)}\sum_{\substack{\boldsymbol{\alpha},\beta\\ \mathrm{dis}(\boldsymbol{\alpha},\beta)=\varnothing}}\left[\frac{k}{2N}\mathrm{tr}\big(L_{\alpha_{\Pi(1)}}\cdots L_{\alpha_{\Pi(2n-p)}}L_\beta L_{\alpha_{\Pi(2n-p+1)}}\cdots L_{\alpha_{\Pi(2n)}}L_\beta\big) + O(N^{-2})\right].$$

Here the trace is taken over $\mathbb{R}^v$, where v counts the total number of qubits appearing in $\boldsymbol{\alpha},\beta$, each labeling a canonical basis vector e_i, and $L_{\{i,j\}} = (e_i-e_j)(e_i-e_j)^T = -(P_{\{i,j\}}-\mathbb{I})$ (the sign cancels since the number of terms is even).

We now identify the terms that contribute at leading order in N. These terms are associated with *maximal trees*, in the following sense. Let $G(\boldsymbol{\alpha},\beta)$ be the graph whose vertices are the qubits appearing in the pairs β and α_Π, and whose edges are those pairs. Let E be the number of distinct edges and v the number of distinct qubits in this graph. Because we are summing only over configurations with $\mathrm{dis}(\boldsymbol{\alpha},\beta)=\varnothing$, the graph $G(\boldsymbol{\alpha},\beta)$ is connected. Hence $v\le E+1$. Moreover $E\le n+1$: there are at most n distinct α_π edges, plus the distinguished edge β. Therefore $v\le n+2$. For a fixed graph using v distinct qubits, the number of embeddings into $\{1,\ldots,N\}$ is $O(N^v)$. Thus, the leading order corresponds to graphs with the maximal $v=n+2$, and hence $E=n+1$: a tree with $n+1$ edges. Since $(4\sigma^2)^{n+1} = \frac{1}{N^{n+1}k^{n+1}}(1+O(N^{-1}))$, we obtain

$$(4\sigma^2)^{n+1}Q_p = \frac{1}{2N^{n+2}k^n}\sum_{\Pi\in\mathrm{Pair}(2n)}\sum_{\substack{\boldsymbol{\alpha},\beta\\ G(\boldsymbol{\alpha},\beta)\text{ is a tree}\\ |E(G)|=n+1}}\mathrm{tr}\big(L_{\alpha_{\Pi(1)}}\cdots L_{\alpha_{\Pi(2n-p)}}L_\beta L_{\alpha_{\Pi(2n-p+1)}}\cdots L_{\alpha_{\Pi(2n)}}L_\beta\big) + O(N^{-1}),$$

where we summed the error term over the $O(N^{n+2})$ leading tree configurations.

We now transform the sums over pairings Π and over pairs of qubits $\boldsymbol{\alpha},\beta$ into sums over trees and *words*. This reduces the problem to counting such objects. Let us label qubits such that $\beta=\{0,1\}$, which we will take to be the *root* of the tree. Denote by $\mathcal{T}_n$ the set of trees on the vertex set $\{0,1,\dots,n+1\}$ which contain the distinguished edge β. For $T\in\mathcal{T}_n$, write $E(T)\setminus\{\beta\}=\{e_1,\dots,e_n\}$, and let $\mathcal{W}(T)$ be the set of words $w=w_1\cdots w_{2n}$ in the alphabet $E(T)\setminus\{\beta\}$ such that each non-root edge appears exactly twice. The data of a pairing $\Pi\in\mathrm{Pair}(2n)$, together with an assignment $\pi\mapsto\alpha_\pi$ of distinct non-root edges to the n pairs $\pi\in\Pi$, is equivalent to such a word: the letter in position j is the edge assigned to the pair $\Pi(j)$. Conversely, any word in which every edge appears exactly twice determines the pairing by pairing the two positions occupied by the same edge.

The dependence on N now enters only through the choice of the $n+2$ qubits supporting the maximal tree. We may first choose this support, which gives $\binom{N}{n+2}$ choices. Once the support is chosen, we simply have to select which pair of qubits forms the distinguished edge β, giving $\frac{1}{2}(n+2)(n+1)$ more options. Therefore

$$\begin{aligned}\sum_{\Pi\in\mathrm{Pair}(2n)}\ \sum_{\substack{\boldsymbol{\alpha},\beta\\ G(\boldsymbol{\alpha},\beta)\text{ is a tree}\\ |E(G)|=n+1}} &\mathrm{tr}\big(L_{\alpha_{\Pi(1)}}\cdots L_{\alpha_{\Pi(2n-p)}}L_\beta L_{\alpha_{\Pi(2n-p+1)}}\cdots L_{\alpha_{\Pi(2n)}}L_\beta\big)\\ &=\binom{N}{n+2}\frac{(n+1)(n+2)}{2}\sum_{T\in\mathcal{T}_n}\sum_{w\in\mathcal{W}(T)}\mathrm{tr}\big(L_{w_1}\cdots L_{w_{2n-p}}L_\beta L_{w_{2n-p+1}}\cdots L_{w_{2n}}L_\beta\big)\,.\end{aligned}$$

Since $\binom{N}{n+2}=N^{n+2}+O(N^{n+1})$, we obtain

$$(4\sigma^2)^{n+1}Q_p=\frac{A_{n,p}}{2k^n}+O(N^{-1}),$$

where we defined

$$A_{n,p}\coloneqq\frac{1}{2n!}\sum_{T\in\mathcal{T}_n}\sum_{w\in\mathcal{W}(T)}\mathrm{tr}\big(L_{w_1}\cdots L_{w_{2n-p}}L_\beta L_{w_{2n-p+1}}\cdots L_{w_{2n}}L_\beta\big)\,,\tag{S25}$$

which is independent of N. Thus, we have removed all the N dependence, and it simply remains to compute the coefficients $A_{n,p}$.

To compute the coefficients $A_{n,p}$, we analyze the combinatorics in the space of trees. Write, for a word $u=u_1\cdots u_m$ in edges of $T\setminus\{\beta\}$,

$$L_u\coloneqq L_{u_1}\cdots L_{u_m},\qquad L_\varnothing=\mathbb{I}.$$

Since $L_\beta=(e_0-e_1)(e_0-e_1)^T$, if $u=w_1\cdots w_{2n-p}$ and $v=w_{2n-p+1}\cdots w_{2n}$, then

$$\begin{aligned}A_{n,p}&=\frac{1}{2n!}\sum_{\substack{T\in\mathcal{T}_n\\ w\in\mathcal{W}(T)}}\mathrm{tr}\big(L_u(e_0-e_1)(e_0-e_1)^TL_v(e_0-e_1)(e_0-e_1)^T\big)\\ &=\frac{1}{2n!}\sum_{\substack{T\in\mathcal{T}_n\\ w\in\mathcal{W}(T)}}\big((e_0-e_1)^TL_u(e_0-e_1)\big)\big((e_0-e_1)^TL_v(e_0-e_1)\big)\\ &=\frac{1}{2n!}\sum_{\substack{T\in\mathcal{T}_n\\ w\in\mathcal{W}(T)}}\big(e_0^TL_ue_0+e_1^TL_ue_1\big)\big(e_0^TL_ve_0+e_1^TL_ve_1\big)\\ &=\underbrace{\frac{1}{2n!}\sum_{\substack{T\in\mathcal{T}_n\\ w\in\mathcal{W}(T)}}\big[(e_0^TL_ue_0)(e_0^TL_ve_0)+(e_1^TL_ue_1)(e_1^TL_ve_1)\big]}_{=:\,P_{n,p}}+\underbrace{\frac{1}{2n!}\sum_{\substack{T\in\mathcal{T}_n\\ w\in\mathcal{W}(T)}}\big[(e_0^TL_ue_0)(e_1^TL_ve_1)+(e_1^TL_ue_1)(e_0^TL_ve_0)\big]}_{(\star)}\,.\end{aligned}$$

Let us focus on $(\star)$. The factors $e_a^TL_ue_a$ are zero unless the word u is supported on the side of the tree attached to the vertex a of β. Thus $e_0^TL_ue_0$ vanishes unless u lies entirely on the 0-side of β, while $e_1^TL_ve_1$ vanishes unless v lies entirely on the 1-side. Hence the cross terms in $(\star)$ can be nonzero only when u and v lie on opposite sides of β, which forces p to be even. For even $p=2r$, we can split into two separate contributions where u uses exactly the $n-r$ edges on the 0 side of β, and v uses exactly the r edges on the 1 side, weighted by the combinatorial factor $\binom{n}{r}$. To write this in equations, let us denote by $\mathcal{T}_m^{(a)}$ the set of rooted trees with $m+1$ vertices, root $a \in \{0,1\}$, and with vertex set disjoint from the other endpoint of β. For $T \in \mathcal{T}_m^{(a)}$, $\mathcal{W}(T)$ denotes the set of words in the m edges of T, with each edge appearing exactly twice, and define

$$g_m := \frac{1}{m!} \sum_{T \in \mathcal{T}_m^{(a)}} \sum_{w \in \mathcal{W}(T)} e_a^T L_w e_a, \qquad a \in \{0,1\}. \tag{S26}$$

Then

$$(\star) = \frac{1}{2n!} 2\binom{n}{r} \Bigg[\sum_{T_0 \in \mathcal{T}_{n-r}^{(0)}} \sum_{u \in \mathcal{W}(T_0)} e_0^T L_u e_0 \Bigg] \Bigg[\sum_{T_1 \in \mathcal{T}_r^{(1)}} \sum_{v \in \mathcal{W}(T_1)} e_1^T L_v e_1 \Bigg] = \frac{1}{2n!} 2\binom{n}{r} \big((n-r)! g_{n-r}\big)\big(r! g_r\big) = g_r g_{n-r}.$$

Therefore, we have shown

$$A_{n,p} = P_{n,p} + \begin{cases} g_{p/2} g_{n-p/2}, & p \text{ even}, \\ 0, & p \text{ odd}. \end{cases}$$

It remains to show that $P_{n,p}$ indeed satisfies Eq. (S11) and that $G(y) = \sum_{n \geq 0} g_n y^n$ satisfies Eq. (S10).

First observe that

$$P_{n,p} = \frac{1}{n!} \sum_{\substack{T \in \mathcal{T}_n^{(0)} \\ w \in \mathcal{W}(T)}} (e_0^T L_u e_0)(e_0^T L_v e_0) = \frac{1}{n!} \sum_{\substack{T \in \mathcal{T}_n^{(1)} \\ w \in \mathcal{W}(T)}} (e_1^T L_u e_1)(e_1^T L_v e_1)$$

for $u = w_1 \cdots w_{2n-p}$ and $v = w_{2n-p+1} \cdots w_{2n}$, for any p. Note first that if $n = 0$ or $p = 0$, then trivially $g_n = P_{n,p}$. Thus assume $n \neq 0$ and $p \neq 0$. We calculate by inserting a resolution of the identity $\sum_x e_x e_x^T = \mathbb{I}$:

$$\begin{aligned}
g_n &= \frac{1}{n!} \sum_{T \in \mathcal{T}_n^{(0)}} \sum_{w \in \mathcal{W}(T)} e_0^T L_u L_v e_0 \\
&= \frac{1}{n!} \sum_{T \in \mathcal{T}_n^{(0)}} \sum_{w \in \mathcal{W}(T)} \sum_{x=0}^{n+1} \left(e_0^T L_u e_x\right) \left(e_x^T L_v e_0\right) \\
&= P_{n,p} + \frac{1}{n!} \sum_{T \in \mathcal{T}_n^{(0)}} \sum_{w \in \mathcal{W}(T)} \sum_{x=1}^{n+1} \left(e_0^T L_u e_x\right) \left(e_x^T L_v e_0\right) \\
&= P_{n,p} + \frac{1}{n!} \sum_{\substack{a+b=n-1 \\ q+r=p-1}} \binom{n}{a,b,1} \Bigg[\sum_{T \in \mathcal{T}_a^{(0)}} \sum_{\substack{w=uv \in \mathcal{W}(T) \\ |v|=q}} \left(e_0^T L_u e_0\right) \left(e_0^T L_v e_0\right) \Bigg] \\
&\qquad \times \Bigg[\sum_{T \in \mathcal{T}_b^{(1)}} \sum_{\substack{w=uv \in \mathcal{W}(T) \\ |v|=r}} \sum_{x=1}^{b+1} \left(e_1^T L_u e_x\right) \left(e_x^T L_v e_1\right) \Bigg] \\
&= P_{n,p} + \frac{1}{n!} \sum_{\substack{a+b=n-1 \\ q+r=p-1}} \binom{n}{a,b,1} \Bigg[\sum_{T \in \mathcal{T}_a^{(0)}} \sum_{\substack{w=uv \in \mathcal{W}(T) \\ |v|=q}} \left(e_0^T L_u e_0\right) \left(e_0^T L_v e_0\right) \Bigg] \Bigg[\sum_{T \in \mathcal{T}_b^{(1)}} \sum_{w \in \mathcal{W}(T)} e_1^T L_w e_1 \Bigg] \\
&= P_{n,p} + \frac{1}{n!} \sum_{\substack{a+b=n-1 \\ q+r=p-1}} \frac{n!}{a!\, b!} \left(a! P_{a,q}\right) \left(b! g_b\right) \\
&= P_{n,p} + \sum_{\substack{a+b=n-1 \\ q+r=p-1}} P_{a,q} g_b.
\end{aligned}$$

The fourth equality is the only nontrivial step. It follows from the following decomposition. For the summand $(e_0^T L_u e_x)(e_x^T L_v e_0)$ to be nonzero, the first edge on the path from 0 to x must be crossed once by u and once by v.

Removing this edge separates T into a component containing 0, with a edges, and a component containing x, with b edges, so $a+b=n-1$. If q and r are the numbers of letters of v lying in these two components, then $q+r=p-1$, since the removed edge also appears in v. The first component gives $a!P_{a,q}$. For the second component, we relabel the endpoint of the removed edge as 1, so the component becomes an element of $\mathcal{T}_b^{(1)}$. Under this relabeling, the sum over x becomes the resolution of the identity on this component with $b+1$ vertices, $\sum_{x=1}^{b+1} e_x e_x^T = I$, and gives $b!g_b$. Finally, the multinomial coefficient $\binom{n}{a,b,1}$ counts the choice of the two components and the separating edge.

Therefore, defining

$$H(y,z) = \sum_{n\geq 0} g_n y^n \sum_{p=0}^{2n} z^p \qquad \text{and} \qquad P(y,z) = \sum_{n\geq 0}\sum_{p=0}^{2n} P_{n,p} z^p y^n,$$

we obtain the relation

$$\begin{aligned} H(y,z) &= \sum_{n\geq 0}\sum_{p=0}^{2n} P_{n,p} z^p y^n + \sum_{n\geq 1}\sum_{p=1}^{2n} \sum_{\substack{a+b=n-1\\ q+r=p-1}} P_{a,q} g_b z^p y^n = P(y,z) + \sum_{a,b\geq 0}\sum_{q=0}^{2a}\sum_{r=0}^{2b} P_{a,q} g_b z^{q+r+1} y^{a+b+1} \\ &= P(y,z) + zy\left(\sum_{a\geq 0}\sum_{q=0}^{2a} P_{a,q} z^q y^a\right)\left(\sum_{b\geq 0}\sum_{r=0}^{2b} g_b z^r y^b\right) = P(y,z) + zyP(y,z)H(y,z)\,, \end{aligned}$$

which implies Eq. (S11). Further, $H(y,1) = P(y,1) + yP(y,1)H(y,1)$ and

$$H(y,1) = \sum_{n\geq 0}(2n+1) g_n y^n = \sum_{n\geq 0} g_n y^n + 2y\sum_{n\geq 1} n g_n y^{n-1} = G(y) + 2yG'(y).$$

So

$$P(y,1) = \frac{H(y,1)}{1+yH(y,1)} = \frac{G(y)+2yG'(y)}{1+yG(y)+2y^2G'(y)}.$$

From the above we get Eq. (S10):

$$\begin{aligned} \frac{1}{1+yG(y)+2y^2G'(y)} &= \frac{1}{1+y\big(G(y)+2yG'(y)\big)} = \frac{1}{1+yH(y,1)} = 1 - y\frac{H(y,1)}{1+yH(y,1)} = 1 - yP(y,1) \\ &= 1 - \big(G(y) - 1 - yG(y)^2\big) = 2 - G(y) + yG(y)^2. \end{aligned}$$

□

D. Moments of random chiral couplings

We can generalize the ensemble of 2-local RHCs to 3-local operators by replacing transpositions with 3-cycles. We define a random chiral coupling (RCC) by

$$\hat{K} = \sum_{i<j<\ell} c_{ij\ell}\, i\left(F_{(ij\ell)} - F_{(i\ell j)}\right) = \frac{1}{2}\sum_{i<j<\ell} c_{ij\ell}\, \boldsymbol{\sigma}_i \cdot (\boldsymbol{\sigma}_j \times \boldsymbol{\sigma}_\ell)\,, \tag{S27}$$

where $\boldsymbol{\sigma}_i = (\hat{X}_i, \hat{Y}_i, \hat{Z}_i)$ and $F_{(ij\ell)} = F_{ij}F_{j\ell}$. The second equality follows from $F_{ij} = (\mathbb{I} + \boldsymbol{\sigma}_i\cdot\boldsymbol{\sigma}_j)/2$. We take the coefficients to be independent centered Gaussians with variance σ_3^2 and choose σ_3 so that $\mathbb{E}[\langle \hat{K}^2\rangle] = 1$. Since $\left\langle \big(F_{(ij\ell)} - F_{(i\ell j)}\big)^2 \right\rangle = 2(\phi_3 - 1)$, by Eq. (S15) the normalization is

$$\sigma_3^{-2} = 2\binom{N}{3}(1-\phi_3) = \frac{kN^2}{2} + O(N). \tag{S28}$$

The commutator moments of RCCs obey a simpler formula than the corresponding moments of RHCs.

Lemma S5. *Let $\hat{K}_0$ and $\hat{K}_1$ be independent RCCs defined as in Eq.* (S27)*. For each fixed n and fixed k,*

$$\mathbb{E}\left[\left\langle [\hat{K}_0, \hat{K}_1]_n^\dagger [\hat{K}_0, \hat{K}_1]_n \right\rangle\right] = \frac{C_n^{(3)}}{k^n} + O(N^{-1}), \qquad \textit{where} \qquad C_n^{(3)} = \frac{2^n}{(n+1)(n+2)}\binom{2n}{n}\binom{2n+2}{n+1}. \tag{S29}$$

Proof. We follow the proof of Lemma S3 step by step. Let $\alpha = \{i, j, \ell\}$ denote a triple of sites, and write

$$\widetilde{F}_\alpha := i\left(F_{(ij\ell)} - F_{(i\ell j)}\right), \qquad \hat{K}_\mu = \sum_\alpha c_\alpha^{(\mu)} \widetilde{F}_\alpha.$$

The commutator expansion is exactly the same one used to obtain Eq. (S16). Applying Wick's theorem to the Gaussian coefficients gives the same expression as Eq. (S17),

$$\mathbb{E}\left[\left\langle [\hat{K}_0, \hat{K}_1]_n^\dagger [\hat{K}_0, \hat{K}_1]_n \right\rangle\right] = \sigma_3^{2n+2} \sum_{p=0}^{2n} (-1)^p \binom{2n}{p} \sum_{\Pi \in \mathrm{Pair}(2n)} \sum_{\boldsymbol{\alpha}, \beta} \left\langle \widetilde{F}_{\Pi,p}(\boldsymbol{\alpha}; \beta) \right\rangle. \tag{S30}$$

Here $\widetilde{F}_{\Pi,p}$ is defined by the same word as in Eq. (S18), with β and the α_π's now triples.

The next step parallels Lemma S4. For a fixed word of triples, let L_α be the finite permutation matrix $i(P_{(ij\ell)} - P_{(i\ell j)})$, acting on the labels that appear in the word. Since each $\widetilde{F}_\alpha$ is a difference of two permutations with coefficients summing to zero, the proof of Lemma S4 applies without change: only the support size of the resulting permutation enters the $O(N^{-1})$ term. Therefore

$$\left\langle \widetilde{F}_{\alpha_1} \cdots \widetilde{F}_{\alpha_m} \right\rangle = \frac{k}{2N} \operatorname{tr}\left(L_{\alpha_1} \cdots L_{\alpha_m}\right) + O(N^{-2}). \tag{S31}$$

We use the definition of connectedness from Eq. (S19), with α_π and β now triples. Equivalently, connectedness is computed in the 3-uniform hypergraph where two triples are adjacent if they share at least one site. The disconnected part of Eq. (S30) vanishes by the same argument as Claim 1. Indeed, disjoint triples commute, and after commuting disconnected components to the end, the remaining dependence on p is again killed by the finite-difference identity Eq. (S22).

It remains to evaluate the terms in which the triples form a connected configuration. After applying Wick's theorem there are n triples from $\hat{K}_0$, together with the distinguished triple β from $\hat{K}_1$. A connected 3-uniform hypergraph with m hyperedges has at most $1 + 2m$ vertices, so here the number of vertices is at most $2n + 3$. Combining Eq. (S31) with Eq. (S28) gives

$$\sigma_3^{2n+2} \frac{k}{2N} = \frac{2^n}{k^n N^{2n+3}} + O(N^{-2n-4}).$$

Thus a connected configuration with v vertices contributes at order $N^{v-(2n+3)}$. Only the maximal case $v = 2n + 3$ survives as $N \to \infty$. These maximal connected configurations are *loose hypertrees* made of triples: connected collections in which each added triple shares exactly one site with the previous collection and contributes two new sites.

We can now define the coefficient $A_{n,p}^{(3)}$, analogously to $A_{n,p}$ in Eq. (S25). Fix $\beta = \{0, 1, 2\}$, which plays the role of the root, and let $\mathcal{T}_n^{(3)}$ be the set of such loose hypertrees T with $V(T) = \{0, 1, \ldots, 2n+2\}$ and $\beta \in E(T)$. For $T \in \mathcal{T}_n^{(3)}$, let $\mathcal{W}(T)$ be the set of words in the n hyperedges of T other than β, with each such hyperedge appearing exactly twice. Each term that survives at leading order uses $2n + 3$ distinct sites. Choosing these sites and then choosing which three of them form β gives

$$\binom{N}{2n+3} \binom{2n+3}{3} = \frac{N^{2n+3}}{6(2n)!} + O(N^{2n+2}).$$

Combining this with the factor $2^n/(k^n N^{2n+3})$ above, one arrives at

$$A_{n,p}^{(3)} := \frac{2^n}{6(2n)!} \sum_{T \in \mathcal{T}_n^{(3)}} \sum_{w \in \mathcal{W}(T)} \operatorname{tr}\big(L_{w_1} \cdots L_{w_{2n-p}} L_\beta L_{w_{2n-p+1}} \cdots L_{w_{2n}} L_\beta\big), \tag{S32}$$

so that

$$\mathbb{E}\left[\left\langle [\hat{K}_0, \hat{K}_1]_n^\dagger [\hat{K}_0, \hat{K}_1]_n \right\rangle\right] = \frac{1}{k^n} \sum_{p=0}^{2n} (-1)^p \binom{2n}{p} A_{n,p}^{(3)} + O(N^{-1}).$$

We finally evaluate $A_{n,p}^{(3)}$. Write $u = w_1 \cdots w_{2n-p}$ and $v = w_{2n-p+1} \cdots w_{2n}$, and set $L_u = L_{u_1} \cdots L_{u_{|u|}}$, with the analogous definition for L_v. The matrix L_β has zero diagonal on the three vertices of β and satisfies $(L_\beta)_{ab}(L_\beta)_{ba} = 1$ for $a \neq b$. Therefore the only terms that survive in the trace have the form

$$\operatorname{tr}(L_u L_\beta L_v L_\beta) = \sum_{a \neq b} (e_a^T L_u e_a)(e_b^T L_v e_b),$$

with $a, b \in \{0,1,2\}$. Since L_α has no identity part, a diagonal element $e_a^T L_u e_a$ based at a can be nonzero only when the word u uses hyperedges entirely in the component attached to a after removing β. Thus u must use one component attached to β, v must use a second one, and the third such component must be empty. In particular, p must be even. For $p = 2r$, the two nonempty components have $n - r$ and r hyperedges, respectively.

We define $g_m^{(3)}$ analogously to g_n in Eq. (S26), but with the sum running over loose hypertrees made of triples, rooted at one vertex, with m hyperedges. To compute $g_m^{(3)}$, consider a word that starts at the root and returns to it. If the word is nonempty, let α be the hyperedge used to leave the root for the first time. Since L_α has no identity part, the next return to the root must use α again. Between these two uses, the word lies entirely in one of the two branches beyond α, and after the return the remaining letters form an independent word rooted at the original vertex. Therefore, for $m \geq 1$, $g_m^{(3)} = 2\sum_{a+b=m-1} g_a^{(3)} g_b^{(3)}$, where the factor 2 chooses the branch beyond α. Thus the generating function $G^{(3)}(y) = \sum_{m\geq 0} g_m^{(3)} y^m$ satisfies

$$G^{(3)}(y) = 1 + 2yG^{(3)}(y)^2,$$

and hence $g_m^{(3)} = 2^m \frac{1}{m+1}\binom{2m}{m}$. After summing over the choices of the two nonempty components attached to β and over the partitions of labels away from β, the prefactor in Eq. (S32) accounts for the remaining combinatorial factors. Thus

$$A_{n,p}^{(3)} = \begin{cases} g_r^{(3)} g_{n-r}^{(3)}, & p = 2r \\ 0, & p \text{ odd} \end{cases}.$$

Combining this with the alternating sum over p gives

$$C_n^{(3)} = \sum_{r=0}^{n} \binom{2n}{2r} g_r^{(3)} g_{n-r}^{(3)} = 2^n (2n)! \sum_{r=0}^{n} \frac{1}{r!(r+1)!(n-r)!(n-r+1)!} = \frac{2^n}{(n+1)(n+2)} \binom{2n}{n} \binom{2n+2}{n+1}. \qquad \square$$

IV. MICROSCOPIC DERIVATION OF THE LINDBLAD EQUATION

We now give a heuristic derivation of the effective Lindblad equation

$$\frac{\partial \rho}{\partial t} = \mathcal{L}_t[\rho] = -i[\hat{H}_{KT}(t), \rho] - \gamma \sum_{\mu=x,y,z} \tfrac{1}{2}[\hat{S}_\mu, [\hat{S}_\mu, \rho]]. \tag{S33}$$

To see why this equation should arise, recall the global Hamiltonian:

$$\hat{H}(t) = \hat{H}_{\mathrm{KT}}(t) + \varepsilon H_{\mathrm{dis}} \qquad\qquad \hat{H}_{\mathrm{dis}} = \hat{K}_x \hat{S}_x + \hat{K}_y \hat{S}_y + \hat{K}_z \hat{S}_z. \tag{S34}$$

The matrices $\hat{K}_x, \hat{K}_y, \hat{K}_z$ are independent samples from a bath ensemble. In the main text we focus on random Heisenberg couplings; here we also treat the Gaussian orthogonal ensemble (GOE). Recall that $H_{\mathrm{KT}}(t)$ and the collective spins $\hat{S}_\mu$ only act on $\mathcal{S}$, while each $\hat{K}_\mu$ only acts on $\mathcal{P}$. To derive the Lindblad equation, we first rewrite the total Hamiltonian in the form $H_{\mathcal{S}} + H_{\mathcal{P}} + H_{\mathcal{SP}}$. Although no bare bath Hamiltonian is present at first sight, an effective bath Hamiltonian emerges after expanding around a localized spin-coherent state.

A. Effective bath Hamiltonian

When the system state is localized near the north pole (positive z direction) for large N, the state is an approximate eigenstate of $\hat{S}_z$ (with eigenvalue S), so the disorder Hamiltonian $\hat{H}_{\mathrm{dis}}$ naturally breaks up into two parts, an effective bath term $S\hat{K}_z$ and an interaction $\hat{K}_x\hat{S}_x + \hat{K}_y\hat{S}_y$, which is analogous (as $N \to \infty$) to the standard diffusion interaction $\hat{x}B_x + \hat{p}B_p$ for a free particle in flat phase space.

For a system initialized in a coherent state $|\Omega\rangle$ centered at $\Omega = (\Omega_x, \Omega_y, \Omega_z)$ on the sphere, we can split the action of a spin operator on this state as

$$\hat{S}_\mu |\Omega\rangle = S\Omega_\mu |\Omega\rangle + (\hat{S}_\mu - S\Omega_\mu)|\Omega\rangle\,,$$

where the norm of the second term is $O(\sqrt{S})$, and is therefore small relative to the first one, which scales as S. This suggests decomposing the disorder into $\varepsilon H_{\mathrm{dis}} = \mathbb{I}_{\mathcal{S}} \otimes H_{\mathcal{P}}^{(\Omega)} + H_{\mathcal{SP}}^{(\Omega)}$ where

$$H_{\mathcal{P}}^{(\Omega)} = \varepsilon S \sum_{\mu=x,y,z} \Omega_\mu \hat{K}_\mu$$

acts only on the permutation sector for any Ω, and where

$$H_{\mathcal{SP}}^{(\Omega)} = \varepsilon \sum_{\mu=x,y,z} (\hat{S}_\mu - S\Omega_\mu) \otimes \hat{K}_\mu.$$

Thus, when acting on a state $|\psi\rangle = |\Omega\rangle_{\mathcal{S}} \otimes |\phi\rangle_{\mathcal{P}}$, the disorder splits as $\varepsilon H_{\mathrm{dis}} |\psi\rangle = \mathbb{I}_{\mathcal{S}} \otimes H_{\mathcal{P}}^{(\Omega)} |\psi\rangle + H_{\mathcal{SP}}^{(\Omega)} |\psi\rangle$.

We make a semiclassical approximation for the collective-spin dynamics: an initially coherent state remains localized near a coherent state $|\Omega(t)\rangle$, whose center follows a classical trajectory on the sphere. This is exactly true in the case of no system dynamics or only rotations of the sphere (we will study these cases in detail below), but we also expect it to be approximately true in the limit of large S. For any specified classical trajectory $\Omega(t)$, we naturally extend the above interaction and bath operators to be time-dependent:

$$H_{\mathcal{P}}^{(\Omega)}(t) := H_{\mathcal{P}}^{(\Omega(t))} = \varepsilon S \sum_\mu \Omega_\mu(t) \hat{K}_\mu, \qquad H_{\mathcal{SP}}^{(\Omega)}(t) := H_{\mathcal{SP}}^{(\Omega(t))} = \varepsilon \sum_\mu (\hat{S}_\mu - S\Omega_\mu(t)) \otimes \hat{K}_\mu\,. \tag{S35}$$

We move into the interaction picture with respect to $H_{\mathcal{S}}(t) + H_{\mathcal{P}}^{(\Omega)}(t)$, and define

$$U^{(\Omega)}(t) = \mathcal{T} \exp\left[-i \int_0^t \mathrm{d}t' \, \left(H_{\mathcal{S}}(t') \otimes \mathbb{I}_{\mathcal{P}} + \mathbb{I}_{\mathcal{S}} \otimes H_{\mathcal{P}}^{(\Omega)}(t')\right)\right] = U_{\mathcal{S}}(t) \otimes U_{\mathcal{P}}^{(\Omega)}(t).$$

The interaction term in the interaction picture is, then,

$$\widetilde{H}_{\mathcal{SP}}^{(\Omega)}(t) = U^{(\Omega)\dagger}(t) H_{\mathcal{SP}}^{(\Omega)}(t) U^{(\Omega)}(t) = \varepsilon \sum_\mu \Delta\widetilde{S}_\mu(t) \otimes \widetilde{K}_\mu(t),$$

where

$$\Delta\widetilde{S}_\mu(t) = U_{\mathcal{S}}^\dagger(t)(\hat{S}_\mu - S\Omega_\mu(t))U_{\mathcal{S}}(t), \qquad \widetilde{K}_\mu(t) = U_{\mathcal{P}}^{(\Omega)\dagger}(t)\hat{K}_\mu U_{\mathcal{P}}^{(\Omega)}(t).$$

B. Dyson series

Having moved to the interaction picture, the full unitary dynamics are simply given by the Schrödinger equation $i\partial_t \widetilde{\rho}_{\mathcal{SP}}(t) = [\widetilde{H}_{\mathcal{SP}}^{(\Omega)}(t), \widetilde{\rho}_{\mathcal{SP}}(t)]$, starting at $\widetilde{\rho}_{\mathcal{SP}}(0) = \rho_{\mathcal{SP}}(0)$. We integrate these dynamics in a Dyson series up to a certain *observation time* T for which we ask about the empirical rate γ, which, as we will see, may in principle depend on T.

$$\widetilde{\rho}_{\mathcal{SP}}(T) = \widetilde{\rho}_{\mathcal{SP}}(0) - i \int_0^T \mathrm{d}t_1 \, [\widetilde{H}_{\mathcal{SP}}^{(\Omega)}(t_1), \widetilde{\rho}_{\mathcal{SP}}(0)] - \int_0^T \mathrm{d}t_1 \int_0^{t_1} \mathrm{d}t_2 \, [\widetilde{H}_{\mathcal{SP}}^{(\Omega)}(t_1), [\widetilde{H}_{\mathcal{SP}}^{(\Omega)}(t_2), \widetilde{\rho}_{\mathcal{SP}}(0)]] + \cdots\,. \tag{S36}$$

We compare this to the leading change from the dissipative part of the Lindblad equation (S33) in the weak-decoherence regime, $\gamma T \ll 1$:

$$\widetilde{\rho}_{\mathcal{S}}(T) - \rho_{\mathcal{S}}(0) = -\frac{\gamma}{2} \sum_\mu \int_0^T \mathrm{d}s \, [\widetilde{S}_\mu(s), [\widetilde{S}_\mu(s), \rho_{\mathcal{S}}(0)]] + O((\gamma T)^2), \tag{S37}$$

where

$$\widetilde{S}_\mu(s) = U_{\mathcal{S}}^\dagger(s) \hat{S}_\mu U_{\mathcal{S}}(s)\,, \qquad \widetilde{\rho}_{\mathcal{S}}(t) = U_{\mathcal{S}}^\dagger(t) \rho_{\mathcal{S}}(t) U_{\mathcal{S}}(t). \tag{S38}$$

The rate γ can be extracted by matching the second-order microscopic change to the coefficient multiplying the double commutator in this weak-decoherence expansion. The higher-order terms in the Dyson series generate the $O((\gamma T)^2)$

terms in Eq. (S37), so for the purposes of extracting γ, we may truncate them. We then further approximate the bath as initially being in an infinite-temperature state

$$\widetilde{\rho}_{\mathcal{SP}}(0) = \rho_{\mathcal{S}}(0) \otimes \frac{\mathbb{I}_{\mathcal{P}}}{d_{\mathcal{P}}}, \tag{S39}$$

but do not invoke the Born approximation in the usual sense.

By Eq. (S39), the first-order term vanishes after tracing over $\mathcal{P}$, since $\langle \hat{K}_\mu \rangle = 0$. Thus, tracing out the bath yields

$$\begin{aligned}
\widetilde{\rho}_{\mathcal{S}}(T) - \rho_{\mathcal{S}}(0) &\approx -\operatorname{tr}_{\mathcal{P}} \int_0^T \mathrm{d}t_1 \int_0^{t_1} \mathrm{d}t_2 \left[\widetilde{H}^{(\Omega)}_{\mathcal{SP}}(t_1), \left[\widetilde{H}^{(\Omega)}_{\mathcal{SP}}(t_2), \rho_{\mathcal{S}}(0) \otimes \frac{\mathbb{I}_{\mathcal{P}}}{d_{\mathcal{P}}}\right]\right] \\
&= -\varepsilon^2 \sum_{\mu,\nu} \int_0^T \mathrm{d}t_1 \int_0^{t_1} \mathrm{d}t_2 \operatorname{tr}_{\mathcal{P}} \left(\left[\Delta\widetilde{S}_\mu(t_1) \otimes \widetilde{K}_\mu(t_1), \left[\Delta\widetilde{S}_\nu(t_2) \otimes \widetilde{K}_\nu(t_2), \rho_{\mathcal{S}}(0) \otimes \frac{\mathbb{I}_{\mathcal{P}}}{d_{\mathcal{P}}}\right]\right]\right) \qquad \text{(S40)} \\
&= -\varepsilon^2 \sum_{\mu,\nu} \int_0^T dt_1 \int_0^{t_1} dt_2 \, \langle \widetilde{K}_\mu(t_1) \widetilde{K}_\nu(t_2) \rangle \left[\Delta\widetilde{S}_\mu(t_1), \left[\Delta\widetilde{S}_\nu(t_2), \rho_{\mathcal{S}}(0)\right]\right] \qquad \text{(S41)} \\
&= -\varepsilon^2 \sum_{\mu,\nu} \int_0^T \mathrm{d}t_1 \int_0^{t_1} \mathrm{d}t_2 \, B_{\mu\nu}(t_1,t_2) \left[\widetilde{S}_\mu(t_1), \left[\widetilde{S}_\nu(t_2), \rho_{\mathcal{S}}(0)\right]\right], \qquad \text{(S42)}
\end{aligned}$$

where we introduced the bath correlation function

$$B_{\mu\nu}(t_1,t_2) = \left\langle \widetilde{K}_\mu(t_1) \widetilde{K}_\nu(t_2) \right\rangle = \left\langle \hat{K}_\mu U_{\mathcal{P}}(t_1,t_2) \, \hat{K}_\nu \, U^\dagger_{\mathcal{P}}(t_1,t_2) \right\rangle,$$

with $U_{\mathcal{P}}(t_1,t_2) = \mathcal{T} e^{-i\varepsilon S \int_{t_2}^{t_1} ds \, \hat{K}_{\Omega(s)}}$ and $\hat{K}_\Omega = \sum_\sigma \Omega_\sigma \hat{K}_\sigma$.

We first study the case where there are no system dynamics, $H_{\mathcal{S}} = 0$ (i.e., $\kappa = 0 = p$ in the kicked-top Hamiltonian).

C. Diffusion rate without system dynamics

In the case of no system dynamics, the trajectory $\Omega(t) = \Omega$ is constant, so we can write

$$B_{\mu\nu}(\tau_1,\tau_2) = \langle \hat{K}_\mu e^{-i(\tau_1-\tau_2)\hat{K}_\Omega} \hat{K}_\nu e^{i(\tau_1-\tau_2)\hat{K}_\Omega} \rangle, \tag{S43}$$

where we introduced the scaled time $\tau \coloneqq \varepsilon S t$. Further, in this case $U_{\mathcal{S}}(t) = \mathbb{I}$, so $\widetilde{S}_\mu(t) = \hat{S}_\mu$ is also constant and

$$\widetilde{\rho}_{\mathcal{S}}(T) - \rho_{\mathcal{S}}(0) = -\frac{T}{2} \sum_{\mu\nu} \gamma_{\mu\nu}(T) \left[\hat{S}_\mu, \left[\hat{S}_\nu, \rho_{\mathcal{S}}(0)\right]\right], \tag{S44}$$

where we introduced the directional rates

$$\gamma_{\mu\nu}(T) = \frac{2}{S^2 T} \int_0^{\varepsilon S T} \mathrm{d}\tau_1 \int_0^{\tau_1} \mathrm{d}\tau_2 \, B_{\mu\nu}(\tau_1,\tau_2) = \frac{2\varepsilon}{S} \int_0^{\varepsilon S T} \mathrm{d}\tau \left(1 - \frac{\tau}{\varepsilon S T}\right) B_{\mu\nu}(\tau). \tag{S45}$$

In the last equality we substituted $\tau = \tau_1 - \tau_2$ and performed one of the integrals.

We now average over the disorder in $\hat{K}_\mu$ to obtain an average prediction over the ensemble, remaining agnostic for the moment as to whether the $\hat{K}_\mu$ are RHCs or GOE operators. We compute

$$\mathbb{E}[\gamma_{\mu\nu}(T)] = \frac{2\varepsilon}{S} \int_0^{\varepsilon S T} \mathrm{d}\tau \left(1 - \frac{\tau}{\varepsilon S T}\right) \mathbb{E}[B_{\mu\nu}(\tau)]. \tag{S46}$$

Without loss of generality, take $\Omega = x$. The correlators with $\mu \neq \nu$ vanish, because they always contain a sole average $\mathbb{E}_{\hat{K}_\mu}[\hat{K}_\mu] = 0$. For instance,

$$\mathbb{E}[B_{xy}(\tau)] = \mathop{\mathbb{E}}_{\hat{K}_x}[\langle \hat{K}_x e^{-i\tau\hat{K}_x} \cancel{\mathop{\mathbb{E}}_{\hat{K}_y}[\hat{K}_y]} e^{i\tau\hat{K}_x}]\rangle = 0. \tag{S47}$$

Further, for the direction parallel to Ω, namely $\mu = \nu = x$, the commutator vanishes $\left[\hat{S}_x, \left[\hat{S}_x, \rho_{\mathcal{S}}(0)\right]\right] = 0$, so the only relevant correlators are those in the transverse directions to Ω, $\mathbb{E}[B_{yy}]$ and $\mathbb{E}[B_{zz}]$. These two have to be equal,

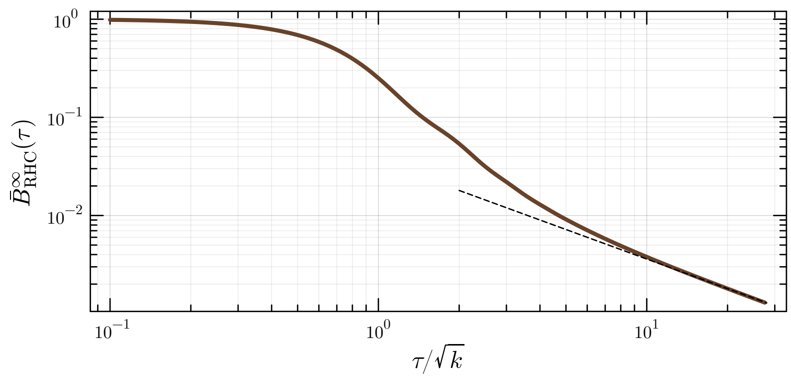

FIG. S2. Ensemble-averaged bath correlator for random Heisenberg couplings $\bar{B}^{\infty}_{\mathrm{RHC}}(\tau)$, constructed by computing C_n up to $n = 2500$ and truncating the rest of the Taylor series. The dashed line is a power-law decay $\sim \sqrt{k}/\tau$, i.e. $\sim \tilde{\tau}^{-1}$ with $\tilde{\tau} := \tau/\sqrt{k}$.

since the ensemble of matrices $\hat{K}_\mu$ is isotropic, meaning that for any rotation matrix $R_{\mu\nu}$ the matrix $\hat{K}'_\mu = \sum_\nu R_{\mu\nu}\hat{K}_\nu$ is distributed identically to $\hat{K}_\mu$ (this follows directly from expanding the matrices as sums of transpositions with Gaussian coefficients for the random Heisenberg couplings, and is also true if $\hat{K}_\mu$ is sampled from random-matrix ensembles, such as GOE). An additional average over rotations that leave $\Omega = x$ invariant would not change the result, so $\mathbb{E}[B_{yy}(\tau)] = \mathbb{E}[B_{zz}(\tau)]$. The single relevant quantity is

$$\bar{\gamma}(T) = \mathbb{E}[\gamma_{zz}(T)] = \mathbb{E}[\gamma_{yy}(T)] = \frac{\varepsilon}{S}\bar{J}(\varepsilon S T), \tag{S48}$$

where

$$\bar{J}(\tau) = \int_{-\tau}^{\tau} \mathrm{d}\tau' \left(1 - \frac{|\tau'|}{\tau}\right)\bar{B}(\tau'), \qquad \bar{B}(\tau) = \mathbb{E}[\langle \hat{K}_0 e^{-i\tau\hat{K}_1}\hat{K}_0 e^{i\tau\hat{K}_1}\rangle], \tag{S49}$$

with independent samples $\hat{K}_0, \hat{K}_1$. Next, we compute the integral $\bar{J}(\tau)$ when $\hat{K}_0$ and $\hat{K}_1$ are RHCs and also when they are sampled from the GOE, in the limit $N \to \infty$.

1. *Correlator for random Heisenberg couplings*

Expanding in nested commutators and using Lemma S3 gives:

$$\bar{B}^{\infty}_{\mathrm{RHC}}(\tau) = \lim_{N\to\infty}\mathbb{E}[\langle \hat{K}_0 e^{-i\tau\hat{K}_1}\hat{K}_0 e^{i\tau\hat{K}_1}\rangle] = \sum_{n=0}^{\infty}\frac{(-1)^n\tau^{2n}}{(2n)!}\lim_{N\to\infty}\mathbb{E}[\langle[\hat{K}_0,\hat{K}_1]_n[\hat{K}_0,\hat{K}_1]_n^\dagger\rangle] = \sum_{n=0}^{\infty}\frac{(-1)^n\tau^{2n}}{(2n)!}\frac{C_n}{k^n}, \tag{S50}$$

where C_n are defined in terms of a recursive expression (S12). Performing the integral yields

$$\bar{J}^{\infty}_{\mathrm{RHC}}(\tau) := \int_{-\tau}^{\tau}\mathrm{d}\tau'\left(1 - \frac{|\tau'|}{\tau}\right)\bar{B}^{\infty}_{\mathrm{RHC}}(\tau') = \sum_{n=0}^{\infty}\frac{(-1)^n C_n}{(2n)!k^n(1+3n+2n^2)}\tau^{1+2n}. \tag{S51}$$

We show a plot of $\bar{B}^{\infty}_{\mathrm{RHC}}(\tau)$ up to the value $\tilde{\tau} := \tau/\sqrt{k} \sim 30$ in Fig. S2. Up to the accessible times $\tilde{\tau} \sim 30$, $\bar{B}^{\infty}_{\mathrm{RHC}}$ appears to have a power-law tail $\sim \tilde{\tau}^{-1}$. However, a preliminary asymptotic analysis for much later times (not shown) suggests instead $\sim (\tilde{\tau}\sqrt{\log\tilde{\tau}})^{-1}$. In any case, such a tail implies a logarithmic-type divergence for $\bar{J}^{\infty}_{\mathrm{RHC}}(\tau)$. As we will see below, this slow divergence will not prevent Markovianity of the bath once the system Hamiltonian is turned on.

2. *Correlator for GOE matrices*

In the case of GOE matrices, we can compute the correlator using free probability [S18]. Averages of products involving different GOE matrices simplify much like products of independent random variables, provided one keeps the operator ordering. Concretely, it allows us to decompose:

$$\bar{B}^{\infty}_{\mathrm{GOE}}(\tau) := \lim_{N\to\infty} \mathbb{E}[\langle \hat{K}_0 e^{-i\tau\hat{K}_1}\hat{K}_0 e^{i\tau\hat{K}_1}\rangle] = \lim_{N\to\infty} \mathbb{E}[\langle \hat{K}_0^2\rangle]\,\mathbb{E}[\langle e^{-i\tau\hat{K}_1}\rangle]\,\mathbb{E}[\langle e^{i\tau\hat{K}_1}\rangle] = \left(\frac{J_1(2\tau)}{\tau}\right)^2, \tag{S52}$$

where $J_j(\tau)$ is the Bessel function of the first kind of order j, and we used $\lim_{N\to\infty}\mathbb{E}[\langle e^{i\tau\hat{K}}\rangle] = J_1(2\tau)/\tau$. Integrating yields

$$\bar{J}^{\infty}_{\mathrm{GOE}}(\tau) := \int_{-\tau}^{\tau} \mathrm{d}\tau' \left(1 - \frac{|\tau'|}{\tau}\right) \bar{B}^{\infty}_{\mathrm{GOE}}(\tau') = \frac{1}{3\tau}[(3+16\tau^2)J_0(2\tau)^2 - 8\tau J_0(2\tau)J_1(2\tau) + (1+16\tau^2)J_1(2\tau)^2 - 3]. \tag{S53}$$

3. *Correlator for random chiral couplings*

The 2-local RHC ensemble can be generalized to the 3-local random chiral couplings (RCCs) introduced in Sec. III D. We do not use RCCs in our numerical analysis, but their correlator is a useful comparison point: interestingly, it takes a much simpler form than the RHC correlator, closer to what we found for GOE matrices.

Expanding in nested commutators as in the RHC case and using Lemma S5 gives

$$\bar{B}^{\infty}_{\mathrm{RCC}}(\tau) := \lim_{N\to\infty} \mathbb{E}[\langle \hat{K}_0 e^{-i\tau\hat{K}_1}\hat{K}_0 e^{i\tau\hat{K}_1}\rangle] = \sum_{n=0}^{\infty} \frac{(-1)^n\tau^{2n}}{(2n)!}\frac{C_n^{(3)}}{k^n}, \tag{S54}$$

where $C_n^{(3)}$ is given by Eq. (S29). In this case the series can be summed explicitly. To see this, use the Taylor series

$$\frac{J_1(2x)}{x} = \sum_{m=0}^{\infty} \frac{(-1)^m x^{2m}}{m!(m+1)!}.$$

Comparing coefficients with Eq. (S29), one sees that the square of this Taylor series reproduces Eq. (S54) after setting $x = \sqrt{2/k}\,\tau$. Thus

$$\bar{B}^{\infty}_{\mathrm{RCC}}(\tau) = \left[\frac{J_1\left(2\sqrt{2/k}\,\tau\right)}{\sqrt{2/k}\,\tau}\right]^2 = \bar{B}^{\infty}_{\mathrm{GOE}}\left(\sqrt{\frac{2}{k}}\,\tau\right), \tag{S55}$$

where in the last equality we used Eq. (S52). Therefore the integrated correlator in this case is the same as for GOE, but with a rescaling:

$$\bar{J}^{\infty}_{\mathrm{RCC}}(\tau) = \sqrt{\frac{k}{2}}\,\bar{J}^{\infty}_{\mathrm{GOE}}\left(\sqrt{\frac{2}{k}}\,\tau\right). \tag{S56}$$

Thus, unlike the RHC correlator in Fig. S2, the RCC correlator has the same integrable tail as the GOE correlator. This suggests that the logarithmic-type divergence found for RHCs is special to the 2-local couplings.

D. Diffusion rate with system dynamics

Fig. S3 shows an empirical rate $\gamma(T)$ obtained by fitting a time-dependent instantaneous rate to the trajectory of the reduced density matrix and minimizing the trace distance to multiple disorder realizations. The prediction $J^{\infty}(TS\varepsilon)\frac{\varepsilon}{S}$ agrees well with $\gamma(T)$ for both GOE and RHCs in the case of no system dynamics. However, in the presence of a system Hamiltonian (either the full kicked top or only kicks), the empirical rate $\gamma(T)$ flattens and plateaus near $J^{\infty}(T_*S\varepsilon)\frac{\varepsilon}{S}$, for some T_*. To understand this effect, consider a single kick at time $T_* = 1$ with $p = \pi/2$, without the nonlinear term ($\kappa = 0$) in the kicked-top Hamiltonian. We will explain that, after the kick, $\gamma(T)$ becomes independent of the observation time T. It takes exactly the same form as the case with no dynamics, but with T replaced by T_*:

$$\gamma = \gamma(T_*) = \frac{\varepsilon}{S}J(\varepsilon S T_*). \tag{S57}$$

This can be proven rigorously upon averaging for GOE random matrices $\hat{K}_\mu$, using free probability. We only prove the statement considering the immediate effect of a single kick, but a similar statement can be made for later times.

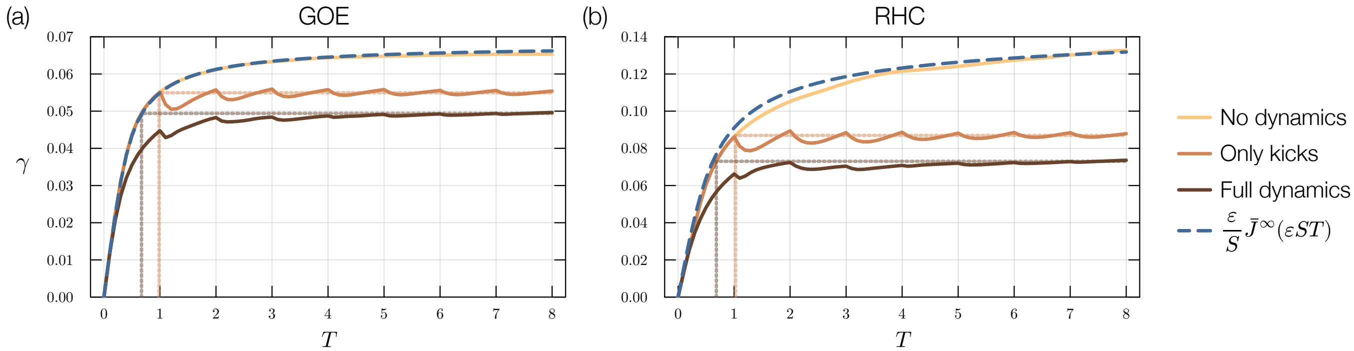

FIG. S3. Time-dependent rates extracted from exact disorder-sampled dynamics. For each bath ensemble we sample M independent realizations of $(\hat{K}_x, \hat{K}_y, \hat{K}_z)$, evolve the corresponding global states $|\psi^{(i)}(t)\rangle$, and form $\rho_{\mathcal{S}}^{(i)}(t) = \mathrm{tr}_{\mathcal{P}}\, \psi^{(i)}(t)$. We then evolve a single reduced density matrix $\rho_\gamma(t)$ with the same system dynamics and a piecewise-constant instantaneous Lindblad rate $\gamma_{\mathrm{inst}}(t)$. At each time step, $\gamma_{\mathrm{inst}}(t)$ is chosen to minimize the trace distance to all samples $M^{-1}\sum_{i=1}^{M} \frac{1}{2}\|\rho_{\mathcal{S}}^{(i)}(t) - \rho_\gamma(t)\|_1$. The plotted quantity is the cumulative rate $\gamma(T) = T^{-1}\int_0^T dt\gamma_{\mathrm{inst}}(t)$. Panel (a) shows GOE bath operators ($N = 150, M = 10$), with a resulting average trace distance ~ 0.02, while panel (b) shows random Heisenberg couplings (RHC) with average trace distance ~ 0.07 ($N = 200, M = 20$). In each panel we compare no system dynamics ($\kappa = 0, p = 0$), kicks only ($\kappa = 0, p = \pi/2$), and full kicked-top dynamics ($\kappa = 4.2, p = \pi/2$). The dashed blue curve J is the prediction obtained from the bath correlator in the absence of system dynamics. The dotted vertical lines indicate the effective cutoff times selected by the only-kicks and full-dynamics curves ($k = 4$, $\theta_0 = 0.5$, $\varphi_0 = 1.1$).

Proposition S1. *Let $\hat{K}_x, \hat{K}_y, \hat{K}_z$ be independent GOE matrices in $\mathcal{P}$ with $\mathbb{E}[\langle \hat{K}_\mu^2\rangle] = 1$. For $\kappa = 0$, $p = \pi/2$, and $k \geq 4$, consider the initial state $\rho(0) = |\Omega(0)\rangle\langle\Omega(0)|$ with $\Omega(0) = x$, and a single kick applied at time $T_* = 1$. At the observation time $T = 2T_*$, i.e. right before the next kick would occur, the empirical ensemble-averaged rate satisfies $\mathbb{E}[\gamma(T)] = \mathbb{E}[\gamma(T_*)]$:*

$$\mathbb{E}[\text{Eq. (S42)}] = -\frac{\mathbb{E}[\gamma(T_*)]}{2} \sum_{\mu=x,y,z} \int_0^{2T_*} \mathrm{d}s \left[\widetilde{S}_\mu(s), \left[\widetilde{S}_\mu(s), \rho_{\mathcal{S}}(0)\right]\right] + O\left(\frac{1}{S^2}\right), \tag{S58}$$

Proof. We split the double integral in Eq. (S42) into cases depending on whether t_1, t_2 are larger or smaller than T_*:

$$\text{(S42)} = \int_0^T \mathrm{d}t_1 \int_0^{t_1} \mathrm{d}t_2\,(\cdots) = \underbrace{\int_0^{T_*} \mathrm{d}t_1 \int_0^{t_1} \mathrm{d}t_2\,(\cdots)}_{I_1:\quad t_1,t_2 \leq T_*} + \underbrace{\int_{T_*}^{2T_*} \mathrm{d}t_1 \int_{T_*}^{t_1} \mathrm{d}t_2\,(\cdots)}_{I_2:\quad t_1,t_2 \geq T_*} + \underbrace{\int_{T_*}^{2T_*} \mathrm{d}t_1 \int_0^{T_*} \mathrm{d}t_2\,(\cdots)}_{I_3:\quad t_2 \leq T_* \leq t_1}. \tag{S59}$$

The first two integrals I_1 and I_2 encompass the cases when t_1 and t_2 are not separated by the kick and take the same form as the equation with no system dynamics. The last integral I_3, in which t_1 and t_2 are separated by a kick, gives a vanishing contribution proportional to $1/S^2$. To compute these integrals, recall that the only terms that contribute to the dephasing correspond to the directions perpendicular to $\Omega(t)$. These are:

$$\Omega(t) = x \quad \Longrightarrow \quad \Omega_{\perp,1} = y, \quad \Omega_{\perp,2} = z, \quad (t < T_*) \tag{S60}$$

$$\Omega(t) = y \quad \Longrightarrow \quad \Omega_{\perp,1} = x, \quad \Omega_{\perp,2} = z, \quad (t > T_*). \tag{S61}$$

Let us compute the three integrals:

I_1 : This integral is exactly the same as the one we already performed in the case without dynamics, where the transverse directions to $\Omega(t \leq T_*) = x$ are y and z, and the bath evolution is simply $U_{\mathcal{P}}(\tau_1, \tau_2) = e^{-i(\tau_1 - \tau_2)\hat{K}_x}$, giving

$$I_1 = -T_* \frac{\bar{\gamma}_*}{2} \left[\hat{S}_y, \left[\hat{S}_y, \rho_{\mathcal{S}}(0)\right]\right] - T_* \frac{\bar{\gamma}_*}{2} \left[\hat{S}_z, \left[\hat{S}_z, \rho_{\mathcal{S}}(0)\right]\right], \tag{S62}$$

with $\bar{\gamma}_* = \mathbb{E}[\gamma(T_*)]$.

I_2 : Here, the center of the coherent state has been rotated to $\Omega(t) = y$, so the transverse directions are x and z. Thus, in the interaction picture,

$$I_2 = -T_* \frac{\bar{\gamma}_*}{2} \left[\widetilde{S}_x(s), \left[\widetilde{S}_x(s), \rho_{\mathcal{S}}(0)\right]\right] - T_* \frac{\bar{\gamma}_*}{2} \left[\widetilde{S}_z(s), \left[\widetilde{S}_z(s), \rho_{\mathcal{S}}(0)\right]\right] \tag{S63}$$

$$= -T_* \frac{\bar{\gamma}_*}{2}\left[\hat{S}_y, \left[\hat{S}_y, \rho_{\mathcal{S}}(0)\right]\right] - T_* \frac{\bar{\gamma}_*}{2}\left[\hat{S}_z, \left[\hat{S}_z, \rho_{\mathcal{S}}(0)\right]\right], \qquad T_* < s < 2T_*, \tag{S64}$$

yielding the same result as I_1.

I_3 : The bath evolution from t_2 to t_1 is $U_{\mathcal{P}}(t_1, t_2) = e^{-i\tau_1 \hat{K}_y} e^{-i\tau_2 \hat{K}_x}$, where we have introduced shifted scaled times $\tau_1 = \varepsilon S(t_1 - T_*)$ and $\tau_2 = \varepsilon S(T_* - t_2)$. Expanding I_3 and changing variables gives four terms, corresponding to the pairs of possible transverse directions before and after the kick:

$$I_3 = -\frac{1}{S^2}\int_0^{\varepsilon ST_*} \mathrm{d}\tau_1 \int_0^{\varepsilon ST_*} \mathrm{d}\tau_2 \Big(\bar{B}_{xz}(\tau_1,\tau_2)[\widetilde{S}_x(t_1), [\widetilde{S}_z(t_2), \rho_{\mathcal{S}}(0)]] + \bar{B}_{zz}(\tau_1,\tau_2)[\widetilde{S}_z(t_1), [\widetilde{S}_z(t_2), \rho_{\mathcal{S}}(0)]] \tag{S65}$$

$$+ \bar{B}_{xy}(\tau_1,\tau_2)[\widetilde{S}_x(t_1), [\widetilde{S}_y(t_2), \rho_{\mathcal{S}}(0)]] + \bar{B}_{zy}(\tau_1,\tau_2)[\widetilde{S}_z(t_1), [\widetilde{S}_y(t_2), \rho_{\mathcal{S}}(0)]]\Big). \tag{S66}$$

The xz and zy correlators vanish because they contain a single $\hat{K}_z$, which averages to zero (since $\hat{K}_z$ does not appear in the evolution operator). The remaining terms can be computed using free probability, up to $O(d_{\mathcal{P}}^{-1}) = O(1/S^2)$ corrections:

$$\bar{B}_{zz}(\tau_1,\tau_2) = \mathbb{E}\left[\langle \hat{K}_z e^{-i\tau_1\hat{K}_y} e^{-i\tau_2\hat{K}_x} \hat{K}_z e^{i\tau_2\hat{K}_x} e^{i\tau_1\hat{K}_y}\rangle\right]$$

$$= \mathbb{E}\Big[\langle e^{-i\tau_1\hat{K}_y}\rangle\Big]\,\mathbb{E}\Big[\langle e^{-i\tau_2\hat{K}_x}\rangle\Big]\,\mathbb{E}\Big[\langle e^{i\tau_2\hat{K}_x}\rangle\Big]\,\mathbb{E}\Big[\langle e^{i\tau_1\hat{K}_y}\rangle\Big] = \bar{B}_{\mathrm{GOE}}(\tau_1)\bar{B}_{\mathrm{GOE}}(\tau_2). \tag{S67}$$

The resulting integral is bounded independently of S,

$$\int_0^{\varepsilon ST_*}\mathrm{d}\tau_1 \int_0^{\varepsilon ST_*}\mathrm{d}\tau_2 \bar{B}_{zz}(\tau_1,\tau_2) = \left(\int_0^{\varepsilon ST_*}\mathrm{d}\tau \bar{B}_{\mathrm{GOE}}(\tau)\right)^2 = \left(\int_0^{\varepsilon ST_*}\mathrm{d}\tau\left(\frac{J_1(2\tau)}{\tau}\right)^2\right)^2 \le \left(\int_0^{\infty}\mathrm{d}\tau\left(\frac{J_1(2\tau)}{\tau}\right)^2\right)^2 = \left(\frac{8}{3\pi}\right)^2. \tag{S68}$$

The same analysis applies to B_{xy}:

$$\bar{B}_{xy}(\tau_1,\tau_2) = \mathbb{E}\Big[\Big\langle \hat{K}_x e^{-i\tau_1\hat{K}_y} e^{-i\tau_2\hat{K}_x} \hat{K}_y e^{i\tau_2\hat{K}_x} e^{i\tau_1\hat{K}_y}\Big\rangle\Big] = 2\,\mathbb{E}[\langle e^{-i\tau_1\hat{K}_y}\rangle]\,\mathbb{E}[\langle e^{i\tau_2\hat{K}_x}\rangle]\,\mathbb{E}[\langle \hat{K}_x e^{-i\tau_2\hat{K}_x}\rangle]\,\mathbb{E}[\langle \hat{K}_y e^{i\tau_1\hat{K}_y}\rangle]$$

$$= 2\,B_{1/2}(\tau_1)B_{1/2}(\tau_2)\left(i\frac{\mathrm{d}}{\mathrm{d}\tau_2}B_{1/2}(\tau_2)\right)\left(-i\frac{\mathrm{d}}{\mathrm{d}\tau_1}B_{1/2}(\tau_1)\right), \tag{S69}$$

where we used $\mathbb{E}[\langle Xe^{-i\tau X}\rangle] = i\,\frac{\mathrm{d}}{\mathrm{d}\tau}\,\mathbb{E}[\langle e^{-i\tau X}\rangle]$ and $B_{1/2}(\tau) \coloneqq \mathbb{E}[\langle e^{i\tau\hat{K}}\rangle] = J_1(2\tau)/\tau$. Integrating by parts gives the same $O(1)$ bound, using $B_{1/2}(\tau)^2 = \bar{B}_{\mathrm{GOE}}(\tau)$. With the overall prefactor $1/S^2$, this gives $I_3 = O(1/S^2)$, completing the proof of Eq. (S58). □

As confirmed by the numerics in Fig. S3, in the kick-only dynamics, $\gamma(T)$ becomes time independent exactly at the first kick time, $T_* = 1$. When the nonlinear term is also included, $\gamma(T)$ instead deviates smoothly from the integrated correlator and plateaus near $\frac{\varepsilon}{S}J(\varepsilon ST_*)$, with a slightly smaller fitted value $T_* \approx 0.6$ for the parameters used here. The parameter T_* is simply a characteristic timescale of the system dynamics. We remark that its precise value is not necessary to predict the effective rate γ in the thermodynamic limit, as the relative error between $\bar{J}^\infty(\varepsilon T_* S)$ and $\bar{J}^\infty(\varepsilon T_*' S)$ for constant T_* and T_*' vanishes in the limit $N \to \infty$ for both the correlators of RHCs and GOE. In both Fig. 2 of the main text (RHCs) and Fig. S4 (GOE) we find excellent agreement between the predicted rate of Eq. (S57) and the empirical value from numerics, across a wide range of system sizes and disorder strengths ε.

E. Intuition

To understand how stronger system dynamics can reduce the effective bath-induced decoherence, we can get intuition from a simplified model closely related to the Coleman-Hepp model [S19]. Consider a system spin moving through a one-dimensional bath of spins with spatial density χ, where the two states of the system spin generate opposite local magnetic fields on each bath spin. If the system moves with speed ν and the field profile has integrated strength $G = \int g(u)\,du$, then each bath spin is only rotated by an angle G/ν, so the overlap of the two conditional bath states is $\cos(G/\nu)$. Since the system encounters $\chi\nu$ bath spins per unit time, the system's coherence decays at rate

$$\Gamma(\nu) = -\chi\nu\log|\cos(G/\nu)| \simeq \frac{\chi G^2}{2\nu} \tag{S70}$$

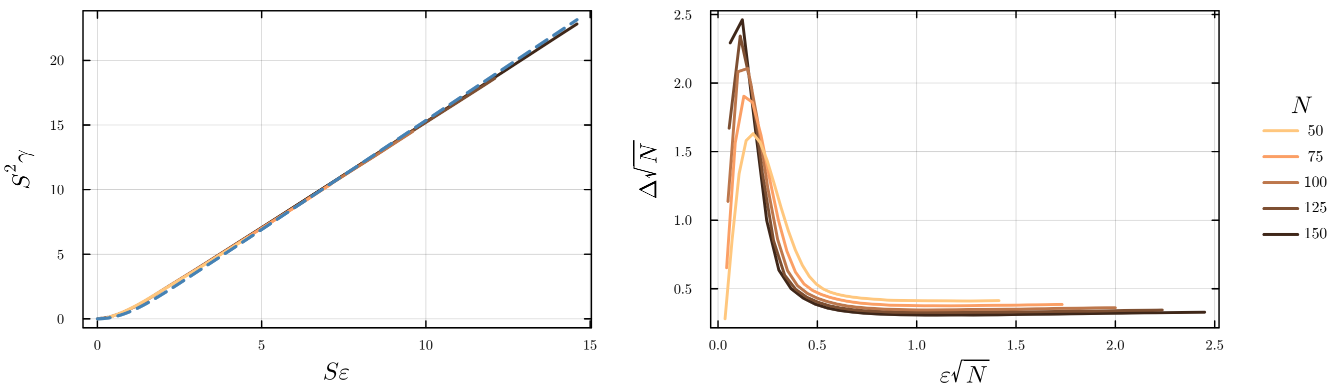

FIG. S4. Effective Lindblad dynamics for couplings sampled from GOE. (a) Optimized rate γ obtained by minimizing average trace distance Δ to exact quantum dynamics, with the permutation-sector couplings $\hat{K}_\mu$ sampled from the GOE. The dashed line is $\frac{\varepsilon}{S}\bar{J}^{\infty}_{\mathrm{GOE}}(\varepsilon ST)$, [see Eq. (S53)]. The vertical axis is scaled by S^2 and the horizontal axis by S, which collapses all curves. (b) Trace distance of the optimization. Axes are scaled by $\sqrt{N}$. All plots are averaged over 20 random-matrix realizations ($k = 4$, $\kappa = 4.2$, $p = \pi/2$, $\theta_0 = 0.5$, $\varphi_0 = 1.1$).

for $G/\nu \ll 1$. Thus faster system motion increases the number of bath spins sampled per unit time but decreases the distinguishability imprinted on each one more strongly, making the net decoherence rate smaller.

In the present model, the analogous role is played by the system Hamiltonian itself: rapid motion of the collective spin changes the interaction-picture system operators and cuts off the effective memory integral, preventing the Markov-limit rate from diverging even when the static bath correlator has a slowly decaying tail. This effect is reminiscent of dynamical decoupling [S20], Zeno-bang-bang effects [S21], and open-system motional narrowing [S22].

V. DETAILED PROOF OF THEOREM 1

Here we provide a more detailed proof of Theorem 1 in the main text. We recall the basic notation. We denote by $\hat{\Omega} = |\Omega\rangle\langle\Omega|$ a spin coherent-state projector and use the measure $\mathrm{d}\Omega = \frac{2S+1}{4\pi}\sin\theta\,\mathrm{d}\theta\,\mathrm{d}\varphi$. We write $S_\mu(\Omega) = S\Omega_\mu$ and use the Poisson bracket $\{f, g\} = \boldsymbol{S}\cdot\left(\frac{\partial f}{\partial \boldsymbol{S}} \times \frac{\partial g}{\partial \boldsymbol{S}}\right)$, which satisfies $\{S_\mu, S_\nu\} = \sum_\lambda \epsilon_{\mu\nu\lambda} S_\lambda$.

The following Lemma serves as a dictionary to transform commutators in the operator picture to Poisson brackets in the phase space picture.

Lemma S6 (Dictionary from commutators to Poisson brackets)**.** *Let* $\rho = \int \mathrm{d}\Omega\, P(\Omega)\hat{\Omega}$. *Then*

$$-i[\hat{S}_\mu, \rho] = \int \mathrm{d}\Omega\,\{S_\mu, P\}\hat{\Omega}, \tag{S71}$$

$$-[\hat{S}_\mu, [\hat{S}_\nu, \rho]] = \int \mathrm{d}\Omega\,\{S_\mu, \{S_\nu, P\}\}\hat{\Omega}, \tag{S72}$$

$$-i[\hat{S}_\mu^2, \rho] = \int \mathrm{d}\Omega\,\left[\{S_\mu^2, P\} + \frac{1}{S}\sum_{\nu,\lambda}\epsilon_{\mu\nu\lambda}\{S_\mu, \{S_\nu, S_\lambda P\}\}\right]\hat{\Omega}. \tag{S73}$$

Proof. The commutator $-i[\hat{S}_\mu, \cdot\,]$ generates rotations of coherent-state projectors about the μ axis, while the Poisson bracket $\{S_\mu, \cdot\,\}$ generates the corresponding classical rotation on the sphere. Then, integration by parts gives the equality

$$-i\int \mathrm{d}\Omega\, F(\Omega)[\hat{S}_\mu, \hat{\Omega}] = \int \mathrm{d}\Omega\,\{S_\mu, F\}\hat{\Omega}, \tag{S74}$$

for any smooth function $F(\Omega)$. Equation (S71) follows by picking $F = P$. Now, for Eq. (S72) note that

$$-[\hat{S}_\mu, [\hat{S}_\nu, \rho]] = -i\left[\hat{S}_\mu, -i[\hat{S}_\nu, \rho]\right] = -i\left[\hat{S}_\mu, \int \mathrm{d}\Omega\,\{S_\nu, P\}\hat{\Omega}\right] = -i\int \mathrm{d}\Omega\,\{S_\nu, P\}[\hat{S}_\mu, \hat{\Omega}] = \int \mathrm{d}\Omega\,\{S_\mu, \{S_\nu, P\}\}\hat{\Omega}, \tag{S75}$$

where in the last equality we used $F = \{S_\nu, P\}$ in Eq. (S74). We finally derive the identity for the quadratic term. For this, we show

$$\hat{S}_\mu \hat{\Omega} + \hat{\Omega}\hat{S}_\mu = 2S_\mu \hat{\Omega} - \frac{i}{S}\sum_{\nu,\lambda} \epsilon_{\mu\nu\lambda} S_\lambda [\hat{S}_\nu, \hat{\Omega}]. \tag{S76}$$

Indeed, by rotational invariance, it is enough to check Eq. (S76) at the north pole $\hat{z} = |S,S\rangle\langle S,S|$. Using $\hat{S}_+\hat{z} = 0$ and $\hat{z}\hat{S}_- = 0$, one obtains

$$\hat{S}_x\hat{z} + \hat{z}\hat{S}_x = -i[\hat{S}_y, \hat{z}], \qquad \hat{S}_y\hat{z} + \hat{z}\hat{S}_y = i[\hat{S}_x, \hat{z}], \qquad \hat{S}_z\hat{z} + \hat{z}\hat{S}_z = 2S\hat{z}. \tag{S77}$$

It follows that

$$[\hat{S}_\mu^2, \hat{\Omega}] = [\hat{S}_\mu, \hat{S}_\mu\hat{\Omega} + \hat{\Omega}\hat{S}_\mu] = 2S_\mu[\hat{S}_\mu, \hat{\Omega}] - \frac{i}{S}\sum_{\nu,\lambda} \epsilon_{\mu\nu\lambda} S_\lambda [\hat{S}_\mu, [\hat{S}_\nu, \hat{\Omega}]]. \tag{S78}$$

Using Eq. (S74) with $F = 2S_\mu P$ gives

$$-i\int \mathrm{d}\Omega\, 2S_\mu P[\hat{S}_\mu, \hat{\Omega}] = \int \mathrm{d}\Omega\, \{S_\mu, 2S_\mu P\}\hat{\Omega} = \int \mathrm{d}\Omega\, \{S_\mu^2, P\}\hat{\Omega}. \tag{S79}$$

For the remaining terms, note that in general

$$\int \mathrm{d}\Omega\, F[\hat{S}_\mu, [\hat{S}_\nu, \hat{\Omega}]] = -\int \mathrm{d}\Omega\, \{S_\mu, \{S_\nu, F\}\}\hat{\Omega}, \tag{S80}$$

so taking $F = S_\lambda P$ gives

$$-\frac{1}{S}\int \mathrm{d}\Omega\, P\sum_{\nu,\lambda} \epsilon_{\mu\nu\lambda} S_\lambda [\hat{S}_\mu, [\hat{S}_\nu, \hat{\Omega}]] = \frac{1}{S}\int \mathrm{d}\Omega \sum_{\nu,\lambda} \epsilon_{\mu\nu\lambda}\{S_\mu, \{S_\nu, S_\lambda P\}\}\hat{\Omega}. \tag{S81}$$

Combining Eqs. (S79) and (S81) gives Eq. (S73). □

To prove Theorem 1, we apply Lemma S6 to the terms in the Lindblad equation (S33), for $\rho = \int \mathrm{d}\Omega\, P(\Omega)\hat{\Omega}$, giving

$$\int \mathrm{d}\Omega\, \frac{\partial P}{\partial t}\hat{\Omega} = \int \mathrm{d}\Omega \left[\frac{\kappa}{2S+1}\Big(\{S_x^2, P\} + \frac{1}{S}\sum_{\nu,\lambda} \epsilon_{x\nu\lambda}\{S_x, \{S_\nu, S_\lambda P\}\}\Big) + p\sum_{n=1}^{\infty} \delta(t-n)\{S_z, P\} + \frac{\gamma}{2}\sum_{\mu}\{S_\mu, \{S_\mu, P\}\}\right]\hat{\Omega}. \tag{S82}$$

This equation is satisfied whenever the coefficients in the integrands are equal, yielding an equation for P. Note that

$$\begin{aligned}
\sum_{\mu,\nu} \epsilon_{\sigma\mu\nu}\{S_\sigma, \{S_\mu, S_\nu P\}\} &= \{S_\sigma^2, P\} + \sum_{\mu,\nu} \epsilon_{\sigma\mu\nu}\{S_\sigma, S_\nu\}\{S_\mu, P\} + \sum_{\mu,\nu} \epsilon_{\sigma\mu\nu} S_\nu \{S_\sigma, \{S_\mu, P\}\} \\
&= \frac{3}{2}\{S_\sigma^2, P\} + \sum_{\mu,\nu} \epsilon_{\sigma\mu\nu} S_\nu \{S_\sigma, \{S_\mu, P\}\} \\
&= \frac{3}{2}\{S_\sigma^2, P\} + \frac{1}{2}\sum_{\mu,\nu} \epsilon_{\sigma\mu\nu} S_\nu \left(\{S_\sigma, \{S_\mu, P\}\} + \{S_\mu, \{S_\sigma, P\}\} + \{\{S_\sigma, S_\mu\}, P\}\right) \\
&= \frac{5}{4}\{S_\sigma^2, P\} + \frac{1}{2}\sum_{\mu,\nu} \epsilon_{\sigma\mu\nu} S_\nu \left(\{S_\sigma, \{S_\mu, P\}\} + \{S_\mu, \{S_\sigma, P\}\}\right) \\
&= \frac{5}{4}\{S_\sigma^2, P\} + \frac{1}{2}\sum_{\mu,\nu,\lambda} \left(\delta_{\sigma\mu}\epsilon_{\sigma\nu\lambda} + \delta_{\sigma\nu}\epsilon_{\sigma\mu\lambda}\right) S_\lambda \{S_\mu, \{S_\nu, P\}\},
\end{aligned}$$

where the first equality is the product rule and $\{S_\mu, S_\nu\} = \sum_\lambda \epsilon_{\mu\nu\lambda} S_\lambda$, the second uses the contraction of two Levi-Civita symbols, together with $\{S_x^2 + S_y^2 + S_z^2, P\} = 0$, and the third equality is a symmetrization using the Jacobi identity. Then, the equation for P becomes

$$\frac{\partial P}{\partial t} = \frac{\kappa}{2S+1}\left(1 + \frac{5}{4S}\right)\{S_x^2, P\} + p\sum_{n=1}^{\infty} \delta(t-n)\{S_z, P\} +$$

$$+\frac{\kappa}{2S(2S+1)}\sum_{\mu,\nu,\lambda}\left(\delta_{x\mu}\epsilon_{x\nu\lambda}+\delta_{x\nu}\epsilon_{x\mu\lambda}\right)S_\lambda\{S_\mu,\{S_\nu,P\}\}+\frac{\gamma}{2}\sum_\mu\{S_\mu,\{S_\mu,P\}\}$$
$$=\{\widetilde{H}_{\mathrm{KT}}(t),P\}+\frac{1}{2}\sum_{\mu,\nu}\Lambda_{\mu\nu}\{S_\mu,\{S_\nu,P\}\},$$

where $\widetilde{H}_{\mathrm{KT}(t)}=(\frac{\kappa}{2S}+\frac{3c}{4})S_x^2+p\sum_{n=1}^\infty\delta(t-n)S_z$, with $c=\kappa/(S(2S+1))$ and

$$\Lambda_{\mu\nu}=\gamma\delta_{\mu\nu}+c\sum_\lambda\left(\delta_{x\mu}\epsilon_{x\nu\lambda}+\delta_{x\nu}\epsilon_{x\mu\lambda}\right)S_\lambda=\begin{pmatrix}\gamma & cS_z & -cS_y\\ cS_z & \gamma & 0\\ -cS_y & 0 & \gamma\end{pmatrix}_{\mu\nu},$$

whose eigenvalues are $\gamma,\gamma\pm c\sqrt{S_z^2+S_y^2}$, which are positive if $\gamma\geq|c|S$, as stated in Theorem 1.

VI. CLASSICALITY FOR $\gamma\gg O(S^{-4/3})$ WITH NOT-TOO-SQUEEZED STATES

In this section, we extend Theorem 1 of the main text to general Hamiltonians and weaker noise by allowing mixtures of squeezed spin states. Following the ideas of Refs. [S6, S23], which study flat phase space, we prove an approximation by mixtures of *not-too-squeezed* (NTS) states.

Let $|\Omega\rangle$ be the spin coherent state centered at $\Omega\in\mathbb{S}^2$. Choose a unit vector $u\perp\Omega$, set $v=\Omega\times u$, and write $\hat{S}_a=\sum_\mu a_\mu\hat{S}_\mu$ for the spin along an axis a. We use the *two-axis-countertwisted squeezed states* [S24]

$$|\Omega;\sigma\rangle=\exp\left[\frac{i\log\zeta}{4S}(\hat{S}_u\hat{S}_v+\hat{S}_v\hat{S}_u)\right]|\Omega\rangle,\qquad\sigma=\frac{1}{2S}\left(\zeta^{-1}uu^\mathsf{T}+\zeta vv^\mathsf{T}\right).\tag{S83}$$

Here Ω is the center about which squeezing is applied, and $\zeta\geq1$ controls its strength, with $\zeta=1$ giving a coherent state. At leading order, u is the squeezed axis and v the broadened axis: σ approximates the tangent covariance of the normalized spin $\hat{\boldsymbol{S}}/S$, with curvature corrections $O(S^{-2})$ at fixed ζ. For $\zeta_{\max}\geq1$, we consider the set $\mathrm{NTS}_{\zeta_{\max}}$ of labels (Ω,σ) such that $1\leq\zeta\leq\zeta_{\max}$.

Consider a collective-spin Hamiltonian of the form

$$\widehat{H}(t)=\sum_{a,b,c\geq0}\frac{\kappa_{a,b,c}(t)}{S^{a+b+c-1}}\,\mathrm{Sym}\big(\hat{S}_x^a\hat{S}_y^b\hat{S}_z^c\big),\tag{S84}$$

where the coefficients $\kappa_{a,b,c}(t)$ are real and Sym averages over all orderings of the spin factors.[4] Consider the Lindblad generator with isotropic noise with rate $\gamma>0$,

$$\mathcal{L}_t[\rho]=-i[\widehat{H}(t),\rho]-\frac{\gamma}{2}\sum_{\mu=x,y,z}[\hat{S}_\mu,[\hat{S}_\mu,\rho]].\tag{S85}$$

Theorem S1 (Approximation by mixtures of NTS states)**.** *Consider an initial coherent state $\rho(0)=|\Omega_0\rangle\langle\Omega_0|$, suppose $\gamma\geq KS^{-4/3}$, and set $\zeta_{\max}=\max\{1,K/(S\gamma)\}$. Then for all times $t\geq0$ there is a normalized, nonnegative probability distribution $p_t(\Omega,\sigma)$, supported on $\mathrm{NTS}_{\zeta_{\max}}$, such that*

$$\widetilde{\rho}(t)=\int_{\mathrm{NTS}_{\zeta_{\max}}}\mathrm{d}\Omega\,\mathrm{d}\sigma\,p_t(\Omega,\sigma)|\Omega;\sigma\rangle\langle\Omega;\sigma|,\qquad\qquad\|\rho(t)-\widetilde{\rho}(t)\|_1\leq r\,t,\tag{S86}$$

with an error rate $r\coloneqq100(K+K_3)\max\{S^{-1/2},\,K^{3/2}S^{-2}\gamma^{-3/2}\}$, which is small when $\gamma\gg O(S^{-4/3})$.

Here the constants K and K_3 are assumed to be finite, and given by

$$K=\frac{S}{2}\sup_{t,\Omega}\big[\lambda_{\max}(A(t,\Omega))-\lambda_{\min}(A(t,\Omega))\big],\qquad K_3=\sup_t\sum_{n=3}^\infty n(n-1)(n-2)\sum_{a+b+c=n}|\kappa_{a,b,c}(t)|,\tag{S87}$$

---

[4] For example, $\mathrm{Sym}(\hat{S}_x^2\hat{S}_y)=(\hat{S}_x^2\hat{S}_y+\hat{S}_x\hat{S}_y\hat{S}_x+\hat{S}_y\hat{S}_x^2)/3$.

$$A_{\mu\nu}(t,\Omega) = \frac{1}{S}\left[\frac{\partial^2 h(\Omega,t)}{\partial\Omega_\mu\partial\Omega_\nu} - \frac{\delta_{\mu\nu}}{3}\sum_\lambda \frac{\partial^2 h(\Omega,t)}{\partial\Omega_\lambda^2}\right] \qquad h(\Omega,t) = \sum_{a,b,c\geq 0}\kappa_{a,b,c}(t)\Omega_x^a\Omega_y^b\Omega_z^c.$$

Here the components Ω_μ are treated as independent when differentiating h. The quantities $\lambda_{\max}$ and $\lambda_{\min}$ are the largest and smallest eigenvalues of the real symmetric 3×3 matrix $A(t,\Omega)$. The integral over $\mathrm{NTS}_{\zeta_{\max}}$ is defined in terms of the measure $\mathrm{d}\sigma = \mathrm{d}\zeta\,\mathrm{d}\varphi/\pi$, where $\varphi\in[0,\pi)$ is the angle of u in the plane tangent to the sphere at Ω. For the kicked top of the main text, $K = S|\kappa|/(2S+1)$ and $K_3 = 0$.

As will be apparent below, the evolution of $p_t(\Omega,\sigma)$ constructed in the proof has a direct classical interpretation: the motion of the centers Ω and deformation of the covariances σ of the squeezed states follow the dynamics of the classical Hamiltonian $h(\Omega,t)$, with an added diffusion term, resulting in the emergence of classical Fokker–Planck dynamics. A precise statement capturing this can be phrased as is done in Refs. [S23, S25] for flat phase space (we do not present it here).

Proof of Theorem S1. Our proof follows the same construction as Ref. [S6]. We perform a local quadratic approximation, which we use to construct a distribution over the space of labels (Ω,σ) so that the corresponding mixture approximately follows the quantum evolution.

At each center Ω, we use the quadratic Taylor approximation

$$\widehat{H}_\Omega^{(2)} = Sh(\Omega,t) + \sum_\mu \frac{\partial h(\Omega,t)}{\partial\Omega_\mu}(\hat{S}_\mu - S\Omega_\mu) + \frac{1}{4S}\sum_{\mu,\nu}\frac{\partial^2 h(\Omega,t)}{\partial\Omega_\mu\partial\Omega_\nu}\big[(\hat{S}_\mu - S\Omega_\mu)(\hat{S}_\nu - S\Omega_\nu) + (\hat{S}_\nu - S\Omega_\nu)(\hat{S}_\mu - S\Omega_\mu)\big]. \tag{S88}$$

Up to a scalar, this has the quadratic form $\widehat{H}_\Omega^{(2)} = \sum_\mu b_\mu\hat{S}_\mu + \frac{1}{4}\sum_{\mu,\nu}A_{\mu\nu}(\hat{S}_\mu\hat{S}_\nu + \hat{S}_\nu\hat{S}_\mu)$, with A from Eq. (S87) and $b_\mu(t,\Omega) = \frac{\partial h(\Omega,t)}{\partial\Omega_\mu} - \sum_\nu\Omega_\nu\frac{\partial^2 h(\Omega,t)}{\partial\Omega_\mu\partial\Omega_\nu}$. The leading-order Hamiltonian motion changes the variables Ω and σ as:

$$\mathrm{d}\Omega = (\omega\times\Omega)\,\mathrm{d}t, \qquad \mathrm{d}\sigma = \big[\omega\times\sigma + (\omega\times\sigma)^\mathsf{T} + B\sigma + \sigma B\big]\,\mathrm{d}t. \qquad \text{(Only Hamiltonian)} \tag{S89}$$

Here $\omega\times\sigma$ means taking the cross product with each column of σ, and the angular velocity ω and the symmetric stretching matrix B are

$$\omega_\mu = b_\mu + S\sum_\nu A_{\mu\nu}\Omega_\nu + \frac{S}{2}A_{\Omega\Omega}\Omega_\mu, \qquad B = SA_{uv}(uu^\mathsf{T} - vv^\mathsf{T}) + \frac{S}{2}(A_{vv} - A_{uu})(uv^\mathsf{T} + vu^\mathsf{T}), \tag{S90}$$

where $A_{ab} = \sum_{\mu,\nu}a_\mu A_{\mu\nu}(t,\Omega)b_\nu$. All coefficients are evaluated at the current center Ω. Along the squeezed axis, the variance changes at rate $\mathrm{d}\sigma_{uu}/\mathrm{d}t = 2B_{uu}\sigma_{uu} = A_{uv}/\zeta$. Since $S|A_{uv}|\leq K$, this rate can be as negative as $-K/(S\zeta)$ in the worst case. At $\zeta = \zeta_{\max}$, such a contraction could take the squeezed state outside the NTS set.

We leverage the noise to counteract such a contraction. It spreads the centers of the squeezed states through random rotations, adding tangent covariance at rate $\gamma\Omega_\perp$, with $\Omega_\perp = I - \Omega\Omega^\mathsf{T}$. Thus $\gamma\geq K/(S\zeta_{\max})$ provides enough broadening to counteract the squeezing. We divide the non-rotational covariance change as follows:

$$B\sigma + \sigma B + \gamma\Omega_\perp = \Sigma_{\mathrm{shape}} + \Sigma_{\mathrm{diff}}, \qquad \Sigma_{\mathrm{diff}} = \gamma\Omega_\perp + \frac{K}{S\zeta_{\max}}\frac{4S^2\sigma^2 - \Omega_\perp}{1-\zeta_{\max}^{-2}}. \tag{S91}$$

The matrix Σ_{diff} is the full tangent covariance rate from center diffusion; Σ_{shape}, determined by the first equality, is the rate of change of each state's squeezing matrix at fixed Ω. This is analogous to Eqs. (D.9)–(D.11) of Ref. [S6].

To describe the resulting motion, we introduce some notation: $\partial/\partial\theta_\mu$ will mean differentiation under a rotation of Ω and σ about the Cartesian μ axis, that is, for any function F on $\mathrm{NTS}_{\zeta_{\max}}$,

$$\frac{\partial F}{\partial\theta_\mu} = \frac{\mathrm{d}}{\mathrm{d}\theta}F(R_\mu(\theta)\Omega, R_\mu(\theta)\sigma R_\mu(\theta)^\mathsf{T})\bigg|_{\theta=0}. \tag{S92}$$

The expression $\sum_{\mu,\nu}(\Sigma_{\mathrm{shape}})_{\mu\nu}\partial F/\partial\sigma_{\mu\nu}$ similarly means the derivative at fixed Ω when the squeezing matrix changes at rate Σ_{shape}, along the family in Eq. (S83). We define the classical evolution on the set $\mathrm{NTS}_{\zeta_{\max}}$ by specifying the following generator, acting on a function $F(\Omega,\sigma)$.

$$\mathcal{L}_t^{(\mathrm{cl})}[F] \coloneqq \sum_\mu \omega_\mu\frac{\partial F}{\partial\theta_\mu} + \sum_{\mu,\nu}(\Sigma_{\mathrm{shape}})_{\mu\nu}\frac{\partial F}{\partial\sigma_{\mu\nu}} + \frac{1}{2}\sum_{\mu,\nu}\left[\gamma\Omega_\mu\Omega_\nu + (\Sigma_{\mathrm{diff}})_{vv}u_\mu u_\nu + (\Sigma_{\mathrm{diff}})_{uu}v_\mu v_\nu\right]\frac{\partial^2 F}{\partial\theta_\mu\,\partial\theta_\nu}.$$

The three terms in this equation rotate the squeezed state, change its squeezing parameter, and add random rotations, respectively. The three terms in the square brackets describe random rotations about Ω, u, and v, with rates γ, $(\Sigma_{\text{diff}})_{vv}$, and $(\Sigma_{\text{diff}})_{uu}$, respectively. Rotation about Ω turns the squeezing axes without moving the center. The diffusion rates along u and v are exchanged because rotation about u displaces the center along v, and conversely. The evolution of a distribution is then simply $\frac{\mathrm{d}}{\mathrm{d}t}\int p_t F = \int p_t \mathcal{L}_t^{(\mathrm{cl})}[F]$. For a squeezed state $\rho_{\Omega,\sigma} = |\Omega;\sigma\rangle\langle\Omega;\sigma|$, the action $\mathcal{L}_t^{(\mathrm{cl})}[\rho_{\Omega,\sigma}]$ differentiates its dependence on Ω, σ, entry by entry in a fixed spin basis: it is not a quantum superoperator acting on the density matrix. Our main technical result is that the evolution given by $\mathcal{L}_t^{(\mathrm{cl})}$ remains close to the actual Lindblad evolution by $\mathcal{L}_t$.

Lemma S7. *If $\gamma \geq K/(S\zeta_{\max})$ and $1 < \zeta_{\max} \leq S^{1/3}$,*

$$\left\|\mathcal{L}_t[\rho_{\Omega,\sigma}] - \mathcal{L}_t^{(\mathrm{cl})}[\rho_{\Omega,\sigma}]\right\|_1 \leq \frac{100(K+K_3)\zeta_{\max}^{3/2}}{\sqrt{S}}. \tag{S93}$$

We prove Lemma S7 below, but first use it to finish the proof of Theorem S1. With $\zeta_{\max} = \max\{1, K/(S\gamma)\}$, the hypotheses of Lemma S7 hold: $\gamma \geq K/(S\zeta_{\max})$ by construction, and $\zeta_{\max} \leq S^{1/3}$ is equivalent to $\gamma \geq KS^{-4/3}$. Evolve the initial delta distribution at $(\Omega_0, (\Omega_0)_\perp/(2S))$ with the label dynamics above. The corresponding mixture obeys $\dot{\widetilde{\rho}} = \int \mathrm{d}\Omega\,\mathrm{d}\sigma\, p_t(\Omega,\sigma)\mathcal{L}_t^{(\mathrm{cl})}[\rho_{\Omega,\sigma}]$. Let $\mathcal{N}_{t,s}$ be the quantum propagator from time s to t. To accumulate the local errors, differentiate the proposed mixture after propagating it from s to the final time: $\frac{\mathrm{d}}{\mathrm{d}s}\big(\mathcal{N}_{t,s}[\widetilde{\rho}(s)]\big) = \mathcal{N}_{t,s}\big[\dot{\widetilde{\rho}}(s) - \mathcal{L}_s[\widetilde{\rho}(s)]\big]$. Integrating from $s=0$ to $s=t$, and using $\widetilde{\rho}(0) = \rho(0)$, gives Duhamel's formula,

$$\rho(t) - \widetilde{\rho}(t) = \int_0^t \mathcal{N}_{t,s}\big[\mathcal{L}_s[\widetilde{\rho}(s)] - \dot{\widetilde{\rho}}(s)\big]\,\mathrm{d}s. \tag{S94}$$

Thus the final error is the accumulated local mismatch, propagated by the quantum evolution. Trace-norm contractivity and the positivity and normalization of p_s give

$$\|\rho(t) - \widetilde{\rho}(t)\|_1 \leq \int_0^t \mathrm{d}s \int \mathrm{d}\Omega\,\mathrm{d}\sigma\, p_s(\Omega,\sigma)\left\|\mathcal{L}_s[\rho_{\Omega,\sigma}] - \mathcal{L}_s^{(\mathrm{cl})}[\rho_{\Omega,\sigma}]\right\|_1 \leq \frac{100(K+K_3)\zeta_{\max}^{3/2}}{\sqrt{S}}\, t = r\,t, \tag{S95}$$

which proves Eq. (S86). □

To prove Lemma S7, we require the following two intermediate lemmas.

Lemma S8 (Bounds on spin operators acting on squeezed states)**.** *Define the operator $\hat{a}_\zeta := (\hat{S}_u + i\zeta^{-1}\hat{S}_v)/\sqrt{S}$. For the squeezed states in Eq.* (S83) *and k an integer, the following bounds hold:*

$$\left\|(S - \hat{S}_\Omega)^{k/2}|\Omega;\sigma\rangle\right\| \leq \sqrt{(2k-1)!!}\,(\zeta^{k/2} - 1), \qquad k \geq 1, \tag{S96}$$

$$\left\|(S + 1 - \hat{S}_\Omega)^{k/2}\hat{a}_\zeta|\Omega;\sigma\rangle\right\| \leq \sqrt{\frac{(2k+5)!!}{8}\,\frac{(\zeta^2-1)\zeta^{(k-1)/2}}{S}}, \qquad k \geq 0, \tag{S97}$$

$$\left\|(\hat{S}_\Theta - S\Theta\cdot\Omega)^k|\Omega;\sigma\rangle\right\| \leq 2^k\sqrt{(2k-1)!!}\,(S\zeta)^{k/2}, \qquad k \geq 1, \quad \Theta \in \mathbb{S}^2. \tag{S98}$$

Proof. In the basis $(S - \hat{S}_\Omega)|m\rangle = m|m\rangle$,

$$\begin{aligned} \frac{i(\hat{S}_u\hat{S}_v + \hat{S}_v\hat{S}_u)}{4S} &= \frac{(\hat{S}_u + i\hat{S}_v)^2 - (\hat{S}_u - i\hat{S}_v)^2}{8S}, \\ \left|\langle m+2|\frac{i(\hat{S}_u\hat{S}_v + \hat{S}_v\hat{S}_u)}{4S}|m\rangle\right| &= \frac{\sqrt{(m+1)(m+2)(2S-m)(2S-m-1)}}{8S} \leq \frac{\sqrt{(m+1)(m+2)}}{4} \leq \frac{m+2}{4}. \end{aligned} \tag{S99}$$

From Eq. (S99), for $k \geq 1$ and any vector $|\psi\rangle$,

$$\begin{aligned} &\left|\langle\psi|\Big[\prod_{j=1}^k (S + 2j - 1 - \hat{S}_\Omega), \frac{i(\hat{S}_u\hat{S}_v + \hat{S}_v\hat{S}_u)}{4S}\Big]|\psi\rangle\right| \\ &\leq \frac{1}{2}\sum_{m=0}^{2S-2}(m+2)|\langle m|\psi\rangle\langle\psi|m+2\rangle|\Big[\prod_{j=1}^k (m+2j+1) - \prod_{j=1}^k (m+2j-1)\Big] \\ &\leq \frac{k}{2}\sum_{m=0}^{2S}|\langle m|\psi\rangle|^2\prod_{j=1}^k (m+2j-1)\Big(\frac{m+2}{m+1} + \frac{m}{m+2k-1}\Big) \leq k\langle\psi|\prod_{j=1}^k (S+2j-1-\hat{S}_\Omega)|\psi\rangle. \end{aligned} \tag{S100}$$

The second inequality in Eq. (S100) uses $2|ab| \leq |a|^2 + |b|^2$. Integrating Eq. (S100) gives, for $1 \leq \zeta' \leq \zeta$,

$$\Big\|\Big[\prod_{j=1}^{k}(S+2j-1-\hat{S}_\Omega)\Big]^{1/2} e^{\frac{i\log(\zeta/\zeta')}{4S}(\hat{S}_u\hat{S}_v+\hat{S}_v\hat{S}_u)}|\psi\rangle\Big\| \leq \Big(\frac{\zeta'}{\zeta}\Big)^{k/2}\Big\|\Big[\prod_{j=1}^{k}(S+2j-1-\hat{S}_\Omega)\Big]^{1/2}|\psi\rangle\Big\|,$$
$$\Big\|\Big[\prod_{j=1}^{k}(S+2j-1-\hat{S}_\Omega)\Big]^{1/2}|\Omega;\sigma\rangle\Big\| \leq \sqrt{(2k-1)!!}\,\zeta^{k/2}. \tag{S101}$$

For $k=0$, the first inequality in Eq. (S101) is an equality, with an empty product.

For $k \geq 2$, Eq. (S96) follows by integration from the coherent state, writing σ' for the covariance matrix with squeezing ζ':

$$\begin{aligned}\Big\|(S-\hat{S}_\Omega)^{k/2}|\Omega;\sigma\rangle\Big\| &\leq \int_1^\zeta \frac{\mathrm{d}\zeta'}{4S\zeta'}\Big\|\big[(S-\hat{S}_\Omega)^{k/2}, \hat{S}_u\hat{S}_v+\hat{S}_v\hat{S}_u\big]|\Omega;\sigma'\rangle\Big\| \\ &\leq \frac{k}{2}\int_1^\zeta \frac{\mathrm{d}\zeta'}{\zeta'}\Big\|\Big[\prod_{j=1}^{k}(S+2j-1-\hat{S}_\Omega)\Big]^{1/2}|\Omega;\sigma'\rangle\Big\| \\ &\leq \frac{k}{2}\sqrt{(2k-1)!!}\int_1^\zeta \zeta'^{k/2-1}\,\mathrm{d}\zeta' = \sqrt{(2k-1)!!}\,(\zeta^{k/2}-1).\end{aligned} \tag{S102}$$

The second inequality in Eq. (S102) uses Eq. (S99) and $(m+2)^{k/2} - m^{k/2} \leq k(m+2)^{k/2-1}$; the last uses Eq. (S101). For $k=1$, Cauchy–Schwarz gives

$$\zeta\partial_\zeta\langle\Omega;\sigma|(S-\hat{S}_\Omega)|\Omega;\sigma\rangle = -\frac{\mathrm{Re}\langle\Omega;\sigma|(\hat{S}_u+i\hat{S}_v)^2|\Omega;\sigma\rangle}{2S} \leq \Big[\langle\Omega;\sigma|(S-\hat{S}_\Omega)|\Omega;\sigma\rangle\big(1+\langle\Omega;\sigma|(S-\hat{S}_\Omega)|\Omega;\sigma\rangle\big)\Big]^{1/2},$$
$$\Big\|(S-\hat{S}_\Omega)^{1/2}|\Omega;\sigma\rangle\Big\| \leq \frac{\sqrt{\zeta}-\zeta^{-1/2}}{2} \leq \sqrt{\zeta}-1, \tag{S103}$$

where the last line of Eq. (S103) integrates its first line from $\zeta = 1$. This proves Eq. (S96).

To prove Eq. (S97), direct differentiation gives

$$2\zeta\partial_\zeta\big(\hat{a}_\zeta|\Omega;\sigma\rangle\big) = \Big[\frac{i(\hat{S}_u\hat{S}_v+\hat{S}_v\hat{S}_u)}{2S}-1\Big]\hat{a}_\zeta|\Omega;\sigma\rangle + \frac{\hat{a}_\zeta^\dagger(S-\hat{S}_\Omega)+(S-\hat{S}_\Omega)\hat{a}_\zeta^\dagger}{2S}|\Omega;\sigma\rangle. \tag{S104}$$

To bound the last term in Eq. (S104), we first compute the nonzero matrix elements of $\hat{S}_\Theta$ in the basis $(S-\hat{S}_\Omega)|m\rangle = m|m\rangle$,

$$\big|\langle m|(\hat{S}_\Theta - S\Theta\cdot\Omega)|m\rangle\big| = |\Theta\cdot\Omega|\,m, \qquad \big|\langle m+1|\hat{S}_\Theta|m\rangle\big| = \frac{\sqrt{1-(\Theta\cdot\Omega)^2}}{2}\sqrt{(m+1)(2S-m)}, \tag{S105}$$

which are also used below. We then use

$$\hat{a}_{\zeta'}^\dagger = \frac{1-\zeta'^{-1}}{2}\,\frac{\hat{S}_u+i\hat{S}_v}{\sqrt{S}} + \frac{1+\zeta'^{-1}}{2}\,\frac{\hat{S}_u-i\hat{S}_v}{\sqrt{S}}, \tag{S106}$$

$$2m(2m-1)^2\prod_{j=1}^{k}(m+2j-2) \leq 2(m+1)(2m+1)^2\prod_{j=1}^{k}(m+2j) \leq 8\prod_{j=1}^{k+3}(m+2j-1). \tag{S107}$$

Eqs. (S105), (S106), and (S107), together with convexity of the squared norm, give

$$\begin{aligned}&\Big\|\Big[\prod_{j=1}^{k}(S+2j-1-\hat{S}_\Omega)\Big]^{1/2}\big[\hat{a}_{\zeta'}^\dagger(S-\hat{S}_\Omega)+(S-\hat{S}_\Omega)\hat{a}_{\zeta'}^\dagger\big]|\Omega;\sigma'\rangle\Big\|^2 \\ &\qquad \leq 8\langle\Omega;\sigma'|\prod_{j=1}^{k+3}(S+2j-1-\hat{S}_\Omega)|\Omega;\sigma'\rangle \leq 8(2k+5)!!\,\zeta'^{k+3}.\end{aligned} \tag{S108}$$

The last inequality in Eq. (S108) uses Eq. (S101). Finally, $\hat{a}_1|\Omega\rangle = 0$ and Eqs. (S101), (S104), and (S108) give

$$\begin{aligned}\Big\|(S+1-\hat{S}_\Omega)^{k/2}\hat{a}_\zeta|\Omega;\sigma\rangle\Big\| &\leq \Big\|\Big[\prod_{j=1}^{k}(S+2j-1-\hat{S}_\Omega)\Big]^{1/2}\hat{a}_\zeta|\Omega;\sigma\rangle\Big\| \\ &\leq \frac{1}{S}\sqrt{\frac{(2k+5)!!}{2}}\,\zeta^{(k-1)/2}\int_1^\zeta \zeta'\,\mathrm{d}\zeta' = \sqrt{\frac{(2k+5)!!}{8}}\,\frac{(\zeta^2-1)\zeta^{(k-1)/2}}{S},\end{aligned}$$

which proves Eq. (S97).

Equations (S98) and (S105) give, for every integer $k \geq 0$ and any vector $|\psi\rangle$,

$$\begin{aligned} &\Big\| \Big[\prod_{\ell=1}^{k}(S+\ell-\hat{S}_\Omega)\Big]^{1/2}(\hat{S}_\Theta - S\Theta\cdot\Omega)|\psi\rangle\Big\| \\ &\quad\leq \sqrt{2S}\big(|\Theta\cdot\Omega| + \sqrt{1-(\Theta\cdot\Omega)^2}\big)\Big\|\Big[\prod_{\ell=1}^{k+1}(S+\ell-\hat{S}_\Omega)\Big]^{1/2}|\psi\rangle\Big\| \\ &\quad\leq 2\sqrt{S}\Big\|\Big[\prod_{\ell=1}^{k+1}(S+\ell-\hat{S}_\Omega)\Big]^{1/2}|\psi\rangle\Big\|. \end{aligned} \tag{S109}$$

The first inequality in Eq. (S109) applies Eq. (S105) to the two off-diagonals and the diagonal separately, using $m^2 \leq 2S(m+1)$; the second is Cauchy–Schwarz. Iterating Eq. (S109) k times and applying Eq. (S101) gives

$$\begin{aligned} \Big\|(\hat{S}_\Theta - S\Theta\cdot\Omega)^k|\Omega;\sigma\rangle\Big\| &\leq 2^k S^{k/2}\Big\|\Big[\prod_{\ell=1}^{k}(S+\ell-\hat{S}_\Omega)\Big]^{1/2}|\Omega;\sigma\rangle\Big\| \\ &\leq 2^k S^{k/2}\Big\|\Big[\prod_{\ell=1}^{k}(S+2\ell-1-\hat{S}_\Omega)\Big]^{1/2}|\Omega;\sigma\rangle\Big\| \leq 2^k\sqrt{(2k-1)!!}\,(S\zeta)^{k/2}, \end{aligned}$$

which proves Eq. (S98). ☐

Lemma S9 (Taylor remainder)**.** *For the Hamiltonian in Eq.* (S84) *and its quadratic approximation in Eq.* (S88)*,*

$$\Big\|-i[\widehat{H}-\widehat{H}^{(2)}_\Omega, \rho_{\Omega,\sigma}]\Big\|_1 \leq \frac{100K_3\zeta^{3/2}}{\sqrt{S}}. \tag{S110}$$

Proof. By Theorem 5.1 of Ref. [S26], any monomial of degree $n = a+b+c$ admits a finite real decomposition of the following form:

$$x^a y^b z^c = \sum_j w_j(\Theta^{(j)}_x x + \Theta^{(j)}_y y + \Theta^{(j)}_z z)^n, \qquad \Theta^{(j)} \in \mathbb{S}^2, \qquad \sum_j |w_j| \leq 1. \tag{S111}$$

For $n \geq 3$, let $f_n(s,y)$ denote the second-order Taylor remainder of s^n about y, for which Taylor's theorem gives

$$\begin{aligned} f_n(s,y) &:= s^n - y^n - ny^{n-1}(s-y) - \tfrac{1}{2}n(n-1)y^{n-2}(s-y)^2, \\ |f_n(s,y)| &\leq \frac{n(n-1)(n-2)}{6}|s-y|^3, \qquad s,y\in[-1,1]. \end{aligned} \tag{S112}$$

Symmetric ordering preserves Eq. (S111) as an operator identity, giving $\mathrm{Sym}(\hat{S}^a_x\hat{S}^b_y\hat{S}^c_z) = \sum_j w_j\hat{S}^n_{\Theta^{(j)}}$. Eqs. (S84) and (S88) give

$$\widehat{H}-\widehat{H}^{(2)}_\Omega = S\sum_{n=3}^{\infty}\sum_{a+b+c=n}\kappa_{a,b,c}(t)\sum_j w_j\, f_n\Big(\frac{\hat{S}_{\Theta^{(j)}}}{S},\,\Theta^{(j)}\cdot\Omega\Big), \tag{S113}$$

where $\Theta^{(j)}$ and w_j depend on (a,b,c). Therefore

$$\begin{aligned} \Big\|-i[\widehat{H}-\widehat{H}^{(2)}_\Omega,\rho_{\Omega,\sigma}]\Big\|_1 &\leq 2\Big\|(\widehat{H}-\widehat{H}^{(2)}_\Omega)|\Omega;\sigma\rangle\Big\| \\ &\leq 2S\sum_{n=3}^{\infty}\sum_{a+b+c=n}|\kappa_{a,b,c}(t)|\sum_j|w_j|\,\Big\|f_n\Big(\frac{\hat{S}_{\Theta^{(j)}}}{S},\,\Theta^{(j)}\cdot\Omega\Big)|\Omega;\sigma\rangle\Big\| \\ &\leq \frac{2S}{6S^3}\sum_{n=3}^{\infty}n(n-1)(n-2)\sum_{a+b+c=n}|\kappa_{a,b,c}(t)|\sum_j|w_j|\,\Big\|(\hat{S}_{\Theta^{(j)}} - S\Theta^{(j)}\cdot\Omega)^3|\Omega;\sigma\rangle\Big\| \\ &\leq \frac{1}{3S^2}\sum_{n=3}^{\infty}n(n-1)(n-2)\sum_{a+b+c=n}|\kappa_{a,b,c}(t)|\sup_{\Theta\in\mathbb{S}^2}\Big\|(\hat{S}_\Theta - S\Theta\cdot\Omega)^3|\Omega;\sigma\rangle\Big\| \\ &\leq \frac{8\sqrt{15}}{3}\frac{K_3\zeta^{3/2}}{\sqrt{S}} \leq \frac{100K_3\zeta^{3/2}}{\sqrt{S}}. \end{aligned} \tag{S114}$$

The last inequality applies Lemma S8, Eq. (S98), with $k=3$, together with the definition of K_3 in Eq. (S87). ☐

Proof of Lemma S7. Let $\mathcal{L}^{(2)}_{t,\Omega}$ be $\mathcal{L}_t$ with $\widehat{H}$ replaced by $\widehat{H}^{(2)}_\Omega$. Eq. (S110) bounds the error in this replacement. We now compare $\mathcal{L}^{(2)}_{t,\Omega}$ with $\mathcal{L}^{(\mathrm{cl})}_t$, keeping the Taylor center fixed in the following calculation. We start by subtracting the two generators. A rigid rotation gives $\partial\rho_{\Omega,\sigma}/\partial\theta_\mu = -i[\hat{S}_\mu, \rho_{\Omega,\sigma}]$, so the noise about Ω cancels exactly. The difference is

$$\begin{aligned}\mathcal{L}^{(2)}_{t,\Omega}[\rho_{\Omega,\sigma}] - \mathcal{L}^{(\mathrm{cl})}_t[\rho_{\Omega,\sigma}] = &-i\left[\widehat{H}^{(2)}_\Omega - \sum_\mu \omega_\mu \hat{S}_\mu, \rho_{\Omega,\sigma}\right] - \sum_{\mu,\nu} (\Sigma_{\mathrm{shape}})_{\mu\nu} \frac{\partial \rho_{\Omega,\sigma}}{\partial \sigma_{\mu\nu}} \\ &+ \frac{1}{2}\sum_{\mu,\nu} \left[(\mathrm{Tr}(\Sigma_{\mathrm{diff}}) - \gamma)(\Omega_\perp)_{\mu\nu} - (\Sigma_{\mathrm{diff}})_{\mu\nu}\right] [\hat{S}_\mu, [\hat{S}_\nu, \rho_{\Omega,\sigma}]]. \end{aligned} \tag{S115}$$

The quadratic Hamiltonian separates into rotation, tangent squeezing, and terms containing longitudinal fluctuations:

$$\widehat{H}^{(2)}_\Omega = \sum_\mu \omega_\mu \hat{S}_\mu + \frac{A_{uu} - A_{vv}}{4}(\hat{S}_u^2 - \hat{S}_v^2) + \frac{A_{uv}}{2}(\hat{S}_u\hat{S}_v + \hat{S}_v\hat{S}_u) + \widehat{H}_{\mathrm{rem}} \quad \text{(up to a scalar)}, \tag{S116}$$

$$\widehat{H}_{\mathrm{rem}} = -\frac{1}{2}\sum_{a=u,v} A_{a\Omega}\left[(S - \hat{S}_\Omega)\hat{S}_a + \hat{S}_a(S - \hat{S}_\Omega)\right] + \frac{3}{4}A_{\Omega\Omega}(S - \hat{S}_\Omega)^2. \tag{S117}$$

To evaluate the second term in Eq. (S115), recall that φ is the angle of the squeezed axis u in a fixed tangent frame at Ω. The two rates $\dot\zeta$ and $\dot\varphi$ describe only the shape change: $\Sigma_{\mathrm{shape}} = (\partial_\zeta\sigma)\dot\zeta + (\partial_\varphi\sigma)\dot\varphi$, with Ω fixed. They let us replace the matrix derivative in Eq. (S115) by $\dot\zeta\,\partial_\zeta\rho_{\Omega,\sigma} + \dot\varphi\,\partial_\varphi\rho_{\Omega,\sigma}$. In the frame (u, v), Eqs. (S83) and (S91) give

$$(\Sigma_{\mathrm{diff}})_{uu} = \gamma - \frac{K}{S\zeta_{\max}}\frac{1 - \zeta^{-2}}{1 - \zeta_{\max}^{-2}}, \qquad (\Sigma_{\mathrm{diff}})_{vv} = \gamma + \frac{K}{S\zeta_{\max}}\frac{\zeta^2 - 1}{1 - \zeta_{\max}^{-2}}. \tag{S118}$$

Differentiating σ in Eq. (S83) and using Eq. (S91) gives the shape rates

$$\frac{\dot\zeta}{2\zeta} = -SA_{uv} - \frac{K}{\zeta_{\max}}\frac{\zeta - \zeta^{-1}}{1 - \zeta_{\max}^{-2}}, \qquad \dot\varphi = -\frac{S}{2}(A_{vv} - A_{uu})\frac{\zeta^2 + 1}{\zeta^2 - 1}. \tag{S119}$$

For $1 \le \zeta \le \zeta_{\max}$, $(\Sigma_{\mathrm{diff}})_{uu} \ge \gamma - K/(S\zeta_{\max}) \ge 0$ and $(\Sigma_{\mathrm{diff}})_{vv} \ge \gamma$. At $\zeta = \zeta_{\max}$, $\dot\zeta/(2\zeta) = -SA_{uv} - K \le 0$, so shape evolution cannot increase the squeezing beyond $\zeta_{\max}$.

Substituting Eqs. (S116), (S118), and (S119) into Eq. (S115), using $\partial_\zeta\rho_{\Omega,\sigma} = i[\hat{S}_u\hat{S}_v + \hat{S}_v\hat{S}_u, \rho_{\Omega,\sigma}]/(4S\zeta)$ from Eq. (S83), gives

$$\begin{aligned}\mathcal{L}^{(2)}_{t,\Omega}[\rho_{\Omega,\sigma}] - \mathcal{L}^{(\mathrm{cl})}_t[\rho_{\Omega,\sigma}] = &\underbrace{-i[\widehat{H}_{\mathrm{rem}}, \rho_{\Omega,\sigma}]}_{(\star)} + \underbrace{\frac{iS(A_{vv} - A_{uu})}{2}\left[\frac{\hat{S}_u^2 - \hat{S}_v^2}{2S} - \frac{\zeta^2+1}{\zeta^2-1}\hat{S}_\Omega, \rho_{\Omega,\sigma}\right]}_{(\star\star)} \\ &+ \underbrace{\frac{K(\zeta^2 - 1)}{2\zeta_{\max}(1 - \zeta_{\max}^{-2})}\left(\frac{[\hat{S}_u, [\hat{S}_u, \rho_{\Omega,\sigma}]]}{S} - \frac{[\hat{S}_v, [\hat{S}_v, \rho_{\Omega,\sigma}]]}{S\zeta^2} + 4\frac{\partial\rho_{\Omega,\sigma}}{\partial\zeta}\right)}_{(\star\star\star)} \end{aligned} \tag{S120}$$

We now use Eqs. (S96) and (S97) to bound the three terms in Eq. (S120).

$$\begin{aligned}\|(\star)\|_1 &\le 2\left\|\widehat{H}_{\mathrm{rem}}|\Omega;\sigma\rangle\right\| \\ &\le \sum_{a=u,v}|A_{a\Omega}|\left\|[(S - \hat{S}_\Omega)\hat{S}_a + \hat{S}_a(S - \hat{S}_\Omega)]|\Omega;\sigma\rangle\right\| + \frac{3}{2}|A_{\Omega\Omega}|\left\|(S - \hat{S}_\Omega)^2|\Omega;\sigma\rangle\right\| \\ &\le \frac{4\sqrt{2}K}{3\sqrt{S}}\left[\langle\Omega;\sigma|\big(8(S - \hat{S}_\Omega)^3 + 4(S - \hat{S}_\Omega)^2 + 6(S - \hat{S}_\Omega) + 1\big)|\Omega;\sigma\rangle\right]^{1/2} + \frac{2K}{S}\left\|(S - \hat{S}_\Omega)^2|\Omega;\sigma\rangle\right\| \\ &\le \frac{4\sqrt{278}}{3}\frac{K\zeta^{3/2}}{\sqrt{S}} + 2\sqrt{105}\frac{K\zeta^2}{S} \le \frac{24K\zeta^{3/2}}{\sqrt{S}} + \frac{21K\zeta^2}{S}. \end{aligned} \tag{S121}$$

The first two inequalities in Eq. (S121) use the rank-one trace norm and Eq. (S117). The next uses Eq. (S105) with $\Theta = u, v$, $\sum_{a=u,v} |A_{a\Omega}| \le \sqrt{2}\|A\|_\infty$, and $S\|A\|_\infty \le 4K/3$, following from Eq. (S87). The final bounds use Eq. (S96) with $k = 1, 2, 3, 4$.

$$\begin{aligned}
\|(\star\star)\|_1 &= \frac{S|A_{vv} - A_{uu}|}{2(1-\zeta^{-2})} \left\| \left[\hat{a}_\zeta^\dagger \hat{a}_\zeta + \frac{(1+\zeta^{-2})(S-\hat{S}_\Omega)^2 - 2\zeta^{-1}(S-\hat{S}_\Omega)}{2S}, \rho_{\Omega,\sigma} \right] \right\|_1 \\
&\le \frac{2K}{1-\zeta^{-2}} \left(\left\| \hat{a}_\zeta^\dagger \hat{a}_\zeta |\Omega;\sigma\rangle \right\| + \frac{1+\zeta^{-2}}{2S} \left\| (S-\hat{S}_\Omega)^2 |\Omega;\sigma\rangle \right\| + \frac{\zeta^{-1}}{S} \left\| (S-\hat{S}_\Omega)|\Omega;\sigma\rangle \right\| \right) \\
&\le \frac{2K}{1-\zeta^{-2}} \left(\sqrt{2} \left\| (S+1-\hat{S}_\Omega)^{1/2} \hat{a}_\zeta |\Omega;\sigma\rangle \right\| + \frac{1+\zeta^{-2}}{2S} \left\| (S-\hat{S}_\Omega)^2 |\Omega;\sigma\rangle \right\| + \frac{\zeta^{-1}}{S} \left\| (S-\hat{S}_\Omega)|\Omega;\sigma\rangle \right\| \right) \\
&\le \frac{2K}{S} \left[\frac{\sqrt{105}}{2}(2\zeta^2+1) + \frac{\sqrt{3}\,\zeta}{\zeta+1} \right] \le (3\sqrt{105}+\sqrt{3}) \frac{K\zeta^2}{S} \le \frac{33K\zeta^2}{S}.
\end{aligned} \tag{S122}$$

The equality in Eq. (S122) uses $\hat{S}_u^2 + \hat{S}_v^2 + \hat{S}_\Omega^2 = S(S+1)$; scalar terms disappear inside the commutator. The first inequality uses $S|A_{vv} - A_{uu}| \le 2K$, from Eq. (S87). The second uses Eqs. (S106) and (S105), which give $\left\| \hat{a}_\zeta^\dagger |\psi\rangle \right\| \le \sqrt{2} \left\| (S+1-\hat{S}_\Omega)^{1/2} |\psi\rangle \right\|$. The final bounds use Eq. (S96) with $k = 2, 4$ and Eq. (S97) with $k = 1$.

$$\begin{aligned}
\|(\star\star\star)\|_1 &= \frac{K(\zeta^2-1)}{2\zeta_{\max}(1-\zeta_{\max}^{-2})} \left\| \hat{a}_\zeta^2 \rho_{\Omega,\sigma} + \rho_{\Omega,\sigma} (\hat{a}_\zeta^\dagger)^2 - \hat{a}_\zeta \rho_{\Omega,\sigma} \hat{a}_\zeta - \hat{a}_\zeta^\dagger \rho_{\Omega,\sigma} \hat{a}_\zeta^\dagger \right\|_1 \\
&\le K\zeta \left(\left\| \hat{a}_\zeta^2 |\Omega;\sigma\rangle \right\| + \| \hat{a}_\zeta |\Omega;\sigma\rangle \| \left\| \hat{a}_\zeta^\dagger |\Omega;\sigma\rangle \right\| \right) \\
&\le \sqrt{2} K\zeta \left(\left\| (S+1-\hat{S}_\Omega)^{1/2} \hat{a}_\zeta |\Omega;\sigma\rangle \right\| + \| \hat{a}_\zeta |\Omega;\sigma\rangle \| \left[1 + \left\| (S-\hat{S}_\Omega)^{1/2} |\Omega;\sigma\rangle \right\|^2 \right]^{1/2} \right) \\
&\le \frac{\sqrt{105}+\sqrt{15}}{2} \frac{K\zeta(\zeta^2-1)}{S} \le \frac{8K\zeta^3}{S}.
\end{aligned} \tag{S123}$$

The equality in Eq. (S123) expands $\hat{a}_\zeta$ using Eq. (S106) and its adjoint, and uses $\partial_\zeta \rho_{\Omega,\sigma} = i[\hat{S}_u \hat{S}_v + \hat{S}_v \hat{S}_u, \rho_{\Omega,\sigma}]/(4S\zeta)$ from Eq. (S83). The first inequality in Eq. (S123) uses the rank-one trace norm and $(\zeta - \zeta^{-1})/(\zeta_{\max} - \zeta_{\max}^{-1}) \le 1$. The second uses Eq. (S106) and its adjoint, together with Eq. (S105), for $\hat{a}_\zeta$ and $\hat{a}_\zeta^\dagger$. The final bounds use Eq. (S96) with $k = 1$, Eq. (S97) with $k = 0, 1$, and $1 + (\sqrt{\zeta} - 1)^2 \le \zeta$.

Combining Eqs. (S121), (S122), (S123), and (S110) gives

$$\begin{aligned}
\left\| \mathcal{L}_t[\rho_{\Omega,\sigma}] - \mathcal{L}_t^{(\mathrm{cl})}[\rho_{\Omega,\sigma}] \right\|_1 &\le \left\| -i[\widehat{H} - \widehat{H}_\Omega^{(2)}, \rho_{\Omega,\sigma}] \right\|_1 + \left\| \mathcal{L}_{t,\Omega}^{(2)}[\rho_{\Omega,\sigma}] - \mathcal{L}_t^{(\mathrm{cl})}[\rho_{\Omega,\sigma}] \right\|_1 \\
&\le K \left(\frac{24\zeta^{3/2}}{\sqrt{S}} + \frac{54\zeta^2 + 8\zeta^3}{S} \right) + \frac{100K_3\zeta^{3/2}}{\sqrt{S}} \le \frac{100(K+K_3)\zeta_{\max}^{3/2}}{\sqrt{S}}.
\end{aligned} \tag{S124}$$

The last inequality in Eq. (S124) uses $\zeta \le \zeta_{\max}$ and $\zeta_{\max}^3 \le S$, proving Eq. (S93). The calculation is written for $\zeta > 1$; the bound extends to coherent labels by smoothness in σ. □

VII. FIDELITY OF RECORDS IN THE LINDBLAD REGIME

In this section, we estimate the overlap between two branches specified by sequences of spin-coherent-state projections. Using the effective Lindblad description, we obtain a simple estimate in which the branch overlap is exponentially suppressed by the time-integrated separation between the two histories. We then test this prediction numerically.

A. Factorization in time from effective Lindblad

The branch overlap can be expressed using the effective Lindblad description as

$$|\langle \phi_{\mathbf{\Theta}} | \phi_{\mathbf{\Omega}} \rangle|^2 = \frac{1}{|c_{\mathbf{\Omega}}|^2 |c_{\mathbf{\Theta}}|^2} \left| \mathrm{tr} \Big(\hat{\Omega}_M U_M \cdots \hat{\Omega}_2 U_2 \hat{\Omega}_1 U_1 \, |\psi(0)\rangle\langle\psi(0)| \, U_1^\dagger \hat{\Theta}_1 U_2^\dagger \hat{\Theta}_2 \cdots U_M^\dagger \hat{\Theta}_M \Big) \right|^2 \tag{S125}$$

$$\approx \frac{1}{|c_{\mathbf{\Omega}}|^2 |c_{\mathbf{\Theta}}|^2} \left| \mathrm{tr}\Big(\hat{\Omega}_M \mathcal{N}_M \Big[\cdots \hat{\Omega}_2 \mathcal{N}_2 \Big[\hat{\Omega}_1 \mathcal{N}_1 \big[\, |\Omega_0\rangle\langle\Theta_0| \, \big] \hat{\Theta}_1 \Big] \hat{\Theta}_2 \cdots \Big] \hat{\Theta}_M \Big) \right|^2 \tag{S126}$$

$$= \frac{1}{|c_{\mathbf{\Omega}}|^2 |c_{\mathbf{\Theta}}|^2} |\langle\Theta_M|\Omega_M\rangle|^2 \prod_{m=1}^{M} \left| \langle\Omega_m| \, \mathcal{N}_m \big[\, |\Omega_{m-1}\rangle\langle\Theta_{m-1}| \, \big] \, |\Theta_m\rangle \right|^2, \tag{S127}$$

where $\mathcal{N}_m = \mathcal{T} \exp \int_{t_{m-1}}^{t_m} \mathrm{d}t \mathcal{L}_t$. In this approximation, the effective Lindblad evolution applies not only to the initial state, but also after each intermediate projection into the coherent states $\hat{\Omega}_m$ and $\hat{\Theta}_m$. Under the same Lindbladian approximation, the normalization coefficients can be expanded as

$$|c_{\mathbf{\Omega}}|^2 \approx \prod_{m=1}^{M} \langle\Omega_m| \, \mathcal{N}_m \big[\hat{\Omega}_{m-1}\big] \, |\Omega_m\rangle \,, \qquad |c_{\mathbf{\Theta}}|^2 \approx \prod_{m=1}^{M} \langle\Theta_m| \, \mathcal{N}_m \big[\hat{\Theta}_{m-1}\big] \, |\Theta_m\rangle \,. \tag{S128}$$

Thus, the fidelity of records factorizes in time:

$$|\langle R_{\mathbf{\Theta}}|R_{\mathbf{\Omega}}\rangle|^2 = \frac{|\langle\phi_{\mathbf{\Theta}}|\phi_{\mathbf{\Omega}}\rangle|^2}{|\langle\Theta_M|\Omega_M\rangle|^2} \approx \prod_{m=1}^{M} \frac{\left|\langle\Omega_m| \, \mathcal{N}_m \big[\, |\Omega_{m-1}\rangle\langle\Theta_{m-1}| \, \big] \, |\Theta_m\rangle\right|^2}{\langle\Theta_m| \, \mathcal{N}_m \big[\hat{\Theta}_{m-1}\big] \, |\Theta_m\rangle \, \langle\Omega_m| \, \mathcal{N}_m \big[\hat{\Omega}_{m-1}\big] \, |\Omega_m\rangle}. \tag{S129}$$

B. Off-diagonal decay under Lindblad dynamics

To estimate each factor in Eq. (S129), we first present an elementary result for coherent states in flat phase space undergoing pure isotropic diffusion.

Proposition S2. *Let $\alpha, \beta, \alpha', \beta' \in \mathbb{C}$ be the centers of coherent states of a harmonic oscillator, i.e., eigenstates of the annihilation operator $\hat{a} = (\hat{x} + i\hat{p})/\sqrt{2\hbar}$, $\hat{a}\,|\alpha\rangle = \alpha\,|\alpha\rangle$. Consider evolution under pure isotropic diffusion $\mathcal{N} = \exp(t\mathcal{L})$, with $\mathcal{L}[\rho] = -\frac{\gamma}{2\hbar^2}\left([\hat{p},[\hat{p},\rho]] + [\hat{x},[\hat{x},\rho]]\right)$. Then*

$$\frac{|\langle\alpha'| \, \mathcal{N}[|\alpha\rangle\langle\beta|] \, |\beta'\rangle|^2}{\langle\alpha'| \, \mathcal{N}[|\alpha\rangle\langle\alpha|] \, |\alpha'\rangle \, \langle\beta'| \, \mathcal{N}[|\beta\rangle\langle\beta|] \, |\beta'\rangle} = \exp\!\left[-\frac{\gamma t/\hbar}{1+\gamma t/\hbar}\Big(|\alpha-\beta|^2 + |\alpha'-\beta'|^2\Big)\right]. \tag{S130}$$

Proof. The channel $\mathcal{N}$ is simply a Gaussian average over displacements,

$$\mathcal{N}[\rho] = \int_{\mathbb{C}} \frac{\mathrm{d}\xi}{\pi\nu} \exp\!\left[-\frac{|\xi|^2}{\nu}\right] D(\xi)\rho D(\xi)^\dagger, \qquad \text{where} \qquad D(\xi) = \exp\!\big(\xi\hat{a}^\dagger - \xi^*\hat{a}\big) \tag{S131}$$

is the displacement operator and $\nu = \gamma t/\hbar$. To see this, evaluate the action on the displacement-operator basis $D(\eta)$,

$$\mathcal{L}[D(\eta)] = -\frac{\gamma}{2\hbar^2}\left([\hat{x},[\hat{x},D(\eta)]] + [\hat{p},[\hat{p},D(\eta)]]\right) = -\frac{\gamma}{2\hbar^2}\left(2\hbar(\mathrm{Re}\,\eta)^2 + 2\hbar(\mathrm{Im}\,\eta)^2\right) D(\eta) = -\frac{\gamma}{\hbar}|\eta|^2 D(\eta).$$

Thus $D(\eta)$ is an eigenoperator of $\mathcal{L}$ with eigenvalue $-\nu|\eta|^2/t$. Therefore

$$e^{t\mathcal{L}}[D(\eta)] = e^{-\nu|\eta|^2} D(\eta) = \int_{\mathbb{C}} \frac{\mathrm{d}^2\xi}{\pi\nu} \exp\!\left[-\frac{|\xi|^2}{\nu}\right] \exp(\eta^*\xi - \eta\xi^*) D(\eta) = \int_{\mathbb{C}} \frac{\mathrm{d}^2\xi}{\pi\nu} \exp\!\left[-\frac{|\xi|^2}{\nu}\right] D(\xi)D(\eta)D(\xi)^\dagger.$$

Inserting the off-diagonal operator $|\alpha\rangle\langle\beta|$ into Eq. (S131) yields

$$\begin{aligned}
\langle\alpha'| \, \mathcal{N}[|\alpha\rangle\langle\beta|] \, |\beta'\rangle &= \int_{\mathbb{C}} \frac{\mathrm{d}\xi}{\pi\nu} e^{-|\xi|^2/\nu} \, \langle\alpha'| \, D(\xi) \, |\alpha\rangle \, \langle\beta| \, D(\xi)^\dagger \, |\beta'\rangle \\
&= \int_{\mathbb{C}} \frac{\mathrm{d}^2\xi}{\pi\nu} \exp\!\left[-\frac{|\xi|^2}{\nu} - |\xi|^2 - \frac{|\alpha'|^2 + |\alpha|^2 + |\beta|^2 + |\beta'|^2}{2} + \alpha'^*\alpha + \beta^*\beta' + \xi(\alpha'^* - \beta^*) + \xi^*(\beta' - \alpha)\right] \\
&= \frac{1}{1+\nu} \exp\!\left[-\frac{|\alpha'|^2 + |\alpha|^2 + |\beta|^2 + |\beta'|^2}{2} + \alpha'^*\alpha + \beta^*\beta' + \frac{\nu}{1+\nu}(\alpha'^* - \beta^*)(\beta' - \alpha)\right],
\end{aligned}$$

where we used the coherent-state identity

$$\langle z|\, D(\xi)\, |w\rangle = \exp\left[-\frac{|z|^2+|w|^2+|\xi|^2}{2} + z^*w + \xi z^* - \xi^* w\right],$$

and performed the Gaussian integral. Thus

$$|\langle\alpha'|\,\mathcal{N}[|\alpha\rangle\!\langle\beta|]\,|\beta'\rangle|^2 = \frac{1}{(1+\nu)^2}\exp\left[-\frac{|\alpha'-\alpha|^2+|\beta'-\beta|^2}{1+\nu} - \frac{\nu}{1+\nu}\left(|\alpha-\beta|^2+|\alpha'-\beta'|^2\right)\right]. \tag{S132}$$

The diagonal terms follow by setting $\beta=\alpha$ and $\beta'=\alpha'$:

$$\langle\alpha'|\,\mathcal{N}[|\alpha\rangle\!\langle\alpha|]\,|\alpha'\rangle = \frac{1}{1+\nu}\exp\left[-\frac{|\alpha'-\alpha|^2}{1+\nu}\right] \qquad \langle\beta'|\,\mathcal{N}[|\beta\rangle\!\langle\beta|]\,|\beta'\rangle = \frac{1}{1+\nu}\exp\left[-\frac{|\beta'-\beta|^2}{1+\nu}\right],$$

which combine to give the stated expression. □

An analogous result holds for spin coherent states under pure isotropic diffusion $\mathcal{N} = \exp\Big(t\sum_\mu \frac{\gamma}{2}[\hat{S}_\mu,[\hat{S}_\mu,\,\cdot\,]]\Big)$ in the spherical phase space. The isotropic diffusion on the sphere can be approximated by an average over Gaussian rotations, for short times $\sqrt{\gamma t} \ll 1$, and the overlap between coherent states is approximately Gaussian for large S, yielding the same result. The resulting formula follows by making the replacements

$$\hbar \to \frac{1}{S} \qquad \text{and} \qquad |\alpha-\beta|^2 \to \frac{S}{2}d^{(2)}(\Omega,\Theta)$$

in Proposition S2, where $d^{(2)}(\Omega,\Theta) = 2(1-\cos d(\Omega,\Theta)) \approx d(\Omega,\Theta)^2$. We obtain

$$\frac{|\langle\Omega'|\,\mathcal{N}[|\Omega\rangle\!\langle\Theta|]\,|\Theta'\rangle|^2}{\langle\Omega'|\,\mathcal{N}[|\Omega\rangle\!\langle\Omega|]\,|\Omega'\rangle\,\langle\Theta'|\,\mathcal{N}[|\Theta\rangle\!\langle\Theta|]\,|\Theta'\rangle} \approx \exp\left[-\frac{\gamma S^2 t}{1+\gamma S t}\frac{1}{2}\left(d^{(2)}(\Omega,\Theta)+d^{(2)}(\Omega',\Theta')\right)\right]. \tag{S133}$$

C. Full fidelity of records

Assuming equal temporal spacings $\Delta t = t_m - t_{m-1}$, Eq. (S133) reduces Eq. (S129) to a simple expression for the fidelity of records in the case where there is no Hamiltonian term in the Lindbladian:

$$|\langle R_{\mathbf{\Theta}}|R_{\mathbf{\Omega}}\rangle|^2 \approx \exp\Big(-\Gamma D^{(2)}_{\mathbf{\Omega},\mathbf{\Theta}}\Big), \tag{S134}$$

where

$$\Gamma \coloneqq \frac{\gamma S^2\Delta t}{1+\gamma S\Delta t} \qquad \text{and} \qquad D^{(2)}_{\mathbf{\Omega},\mathbf{\Theta}} \coloneqq \frac{1}{2}\sum_{m=1}^{M}\left[d^{(2)}(\Omega_{m-1},\Theta_{m-1}) + d^{(2)}(\Omega_m,\Theta_m)\right]. \tag{S135}$$

Although the derivation above assumed that there was no Hamiltonian term in the effective Lindbladian, and hence no term acting solely on $\mathcal{S}$ in the global Hamiltonian, Eq. (S134) still describes the fidelity of branches in the presence of such a term. We show this numerically by considering the unitary evolution under the disordered kicked-top Hamiltonian, starting in the pure state $|\psi(0)\rangle = |\theta_0,\varphi_0\rangle^{\otimes(N-k)} \otimes [\frac{1}{\sqrt{2}}(|01\rangle - |10\rangle)]^{\otimes k/2}$. After evolving for one period, $\Delta t = 1$, we compute the Husimi distribution $Q_1(\Omega) = \langle\Omega|\,\mathrm{tr}_{\mathcal{P}}(|\psi(\Delta t)\rangle\!\langle\psi(\Delta t)|)\,|\Omega\rangle$, and sample $\Omega_1 \sim Q_1$. Note that the Husimi function is normalized with respect to the measure $\mathrm{d}\Omega = \frac{2S+1}{4\pi}\sin\theta\,\mathrm{d}\theta\,\mathrm{d}\varphi$, i.e., $\int \mathrm{d}\Omega\, Q_1(\Omega) = 1$.

We then define the normalized branch conditioned on this outcome as

$$c_{\Omega_1}|\phi_{\Omega_1}\rangle = (|\Omega_1\rangle\!\langle\Omega_1| \otimes \mathbb{1}_{\mathcal{P}})\,|\psi(\Delta t)\rangle\,, \qquad |c_{\Omega_1}|^2 = Q_1(\Omega_1).$$

We evolve this branch for another period, define

$$Q_2(\Omega) = \langle\Omega|\,\mathrm{tr}_{\mathcal{P}}(|\phi_{\Omega_1}(\Delta t)\rangle\!\langle\phi_{\Omega_1}(\Delta t)|)\,|\Omega\rangle\,,$$

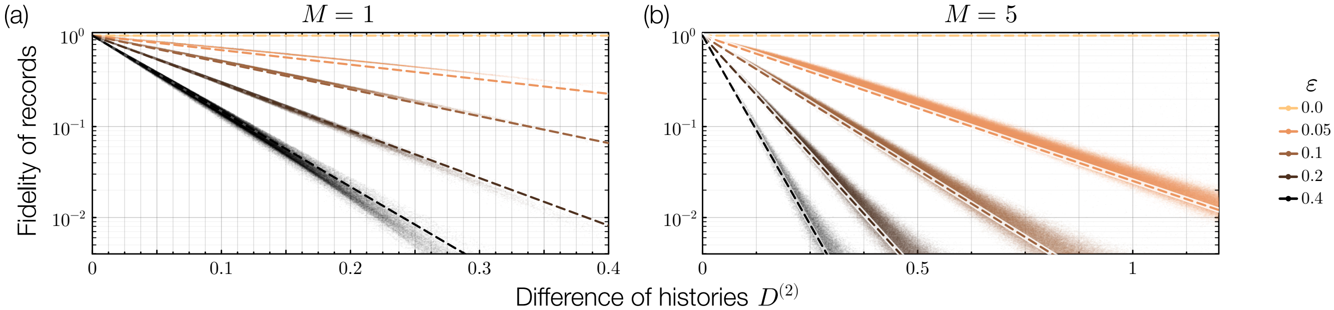

FIG. S5. Fidelity of records for couplings sampled from GOE vs cumulative squared distance between histories $D^{(2)}$. Each dot is a pair of independently sampled branches. Dashed lines mark the decay $e^{-\Gamma D^{(2)}}$. (a) $M = 1$, (b) $M = 5$ ($N = 100$, $k = 4$, $\kappa = 4.2$, $p = \pi/2$, $\theta_0 = 0.5$, $\varphi_0 = 1.1$, $\Delta t = 1$)

sample $\Omega_2 \sim Q_2$, and project again to obtain $\left|\phi_{(\Omega_1,\Omega_2)}\right\rangle$. Iterating this procedure for M steps gives a sampled branch $|\phi_{\mathbf{\Omega}}\rangle$ with probability density

$$|c_{\mathbf{\Omega}}|^2 = Q_1(\Omega_1)Q_2(\Omega_2)\cdots Q_M(\Omega_M).$$

Fig. S5 shows the fidelity of records for independently sampled pairs of branches with $\hat{K}_\mu$ drawn from the GOE. The numerical results agree well with Eq. (S134). The same procedure is shown in Fig. 3 of the main text with $\hat{K}_\mu$ taken to be random Heisenberg couplings. In that case the scatter is larger, but Eq. (S134) still tracks the lower end of the distribution.

REFERENCES

[S1] P. Zanardi, D. A. Lidar, and S. Lloyd, Quantum Tensor Product Structures are Observable Induced, Physical Review Letters **92**, 060402 (2004).
[S2] L. Li, M. J. W. Hall, and H. M. Wiseman, Concepts of quantum non-Markovianity: A hierarchy, Physics Reports **759**, 1 (2018).
[S3] S. Milz, M. S. Kim, F. A. Pollock, and K. Modi, Completely positive divisibility does not mean Markovianity, Physical Review Letters **123**, 040401 (2019).
[S4] P. Strasberg, Classicality with(out) decoherence: Concepts, relation to Markovianity, and a random matrix theory approach, SciPost Physics **15**, 024 (2023).
[S5] W. H. Zurek, Decoherence, chaos, quantum-classical correspondence, and the algorithmic arrow of time, Physica Scripta **T76**, 186 (1998).
[S6] F. Hernández, D. Ranard, and C. J. Riedel, Ehrenfest's theorem beyond the Ehrenfest time (2025), arXiv:2306.13717.
[S7] C. J. Riedel, Wavefunction branches demand a definition!, Quantum Views **9**, 85 (2025).
[S8] P. O'Donovan, P. Strasberg, K. Modi, J. Goold, and M. T. Mitchison, Quantum master equation from the eigenstate thermalization hypothesis, Phys. Rev. B **112**, 014312 (2025).
[S9] C. Nation and D. Porras, Taking snapshots of a quantum thermalization process: Emergent classicality in quantum jump trajectories, Physical Review E **102**, 042115 (2020).
[S10] P. P. Mazza, D. Zietlow, F. Carollo, S. Andergassen, G. Martius, and I. Lesanovsky, Machine learning time-local generators of open quantum dynamics, Physical Review Research **3**, 023084 (2021).
[S11] F. Carnazza, F. Carollo, D. Zietlow, S. Andergassen, G. Martius, and I. Lesanovsky, Inferring Markovian quantum master equations of few-body observables in interacting spin chains, New Journal of Physics **24**, 073033 (2022).
[S12] G. Cemin, F. Carnazza, S. Andergassen, G. Martius, F. Carollo, and I. Lesanovsky, Inferring interpretable dynamical generators of local quantum observables from projective measurements through machine learning, Physical Review Applied **21**, L041001 (2024).
[S13] C. Ates, J. P. Garrahan, and I. Lesanovsky, Thermalization of a strongly interacting closed spin system: From coherent many-body dynamics to a Fokker-Planck equation, Physical Review Letters **108**, 110603 (2012).
[S14] S. Ji, C. Ates, J. P. Garrahan, and I. Lesanovsky, Equilibration of quantum hard rods in one dimension, Journal of Statistical Mechanics: Theory and Experiment **2013**, P02005 (2013).
[S15] J. Wang and P. Strasberg, Decoherence of histories: Chaotic versus integrable systems, Phys. Rev. Lett. **134**, 220401 (2025).
[S16] D. Villaseñor, S. Pilatowsky-Cameo, M. A. Bastarrachea-Magnani, S. Lerma-Hernández, L. F. Santos, and J. G. Hirsch, Quantum vs classical dynamics in a spin-boson system: manifestations of spectral correlations and scarring, New Journal of Physics **22**, 063036 (2020).

[S17] R. E. Ingram, Some characters of the symmetric group, Proceedings of the American Mathematical Society **1**, 358–369 (1950).

[S18] D. Voiculescu, Limit laws for random matrices and free products, Inventiones mathematicae **104**, 201–220 (1991).

[S19] K. Hepp, Quantum theory of measurement and macroscopic observables, Helv. Phys. Acta **45**, 237 (1972).

[S20] L. Viola, E. Knill, and S. Lloyd, Dynamical decoupling of open quantum systems, Physical Review Letters **82**, 2417–2421 (1999).

[S21] P. Facchi, D. A. Lidar, and S. Pascazio, Unification of dynamical decoupling and the quantum Zeno effect, Physical Review A **69**, 032314 (2004).

[S22] K. E. Rönnburg, E. Mohler, H. G. Roskos, K. Ortner, C. R. Becker, and L. W. Molenkamp, Motional-narrowing-type dephasing of electron and hole spins of itinerant excitons in magnetically doped II-VI bulk semiconductors, Physical Review Letters **96**, 117203 (2006).

[S23] F. Hernández, D. Ranard, and C. J. Riedel, Classical correspondence beyond the Ehrenfest time for open quantum systems with general Lindbladians, Communications in Mathematical Physics **406**, 4 (2024).

[S24] M. Kitagawa and M. Ueda, Squeezed spin states, Phys. Rev. A **47**, 5138 (1993).

[S25] F. Hernández, D. Ranard, and C. J. Riedel, The threshold for quantum-classical correspondence is $D \sim \hbar^{4/3}$ (2025), arXiv:2512.17623 [quant-ph].

[S26] S. Friedland and L.-H. Lim, Nuclear norm of higher-order tensors, Mathematics of Computation **87**, 1255 (2018).